Landslide and debris flow warning at regional scale

A real-time system using susceptibility mapping, radar rainfall and hydrometeorological thresholds

Doctoral thesis by:
Rosa Maria Palau Berastegui

Thesis supervisors:
Marc Berenguer
Marcel Hürlimann

Landslide and debris flow warning at regional scale

A real-time system using susceptibility mapping, radar rainfall and hydrometeorological thresholds
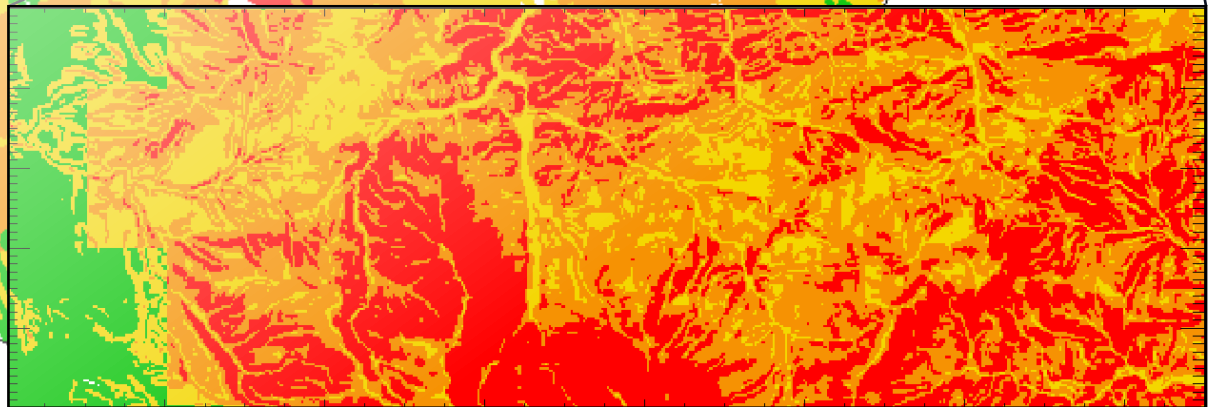
Doctoral thesis by:

Rosa Maria Palau Berastegui

Thesis supervisors:

Marc Berenguer
Marcel Hürlimann

ABSTRACT

Rainfall triggered shallow slides and debris flows constitute a significant hazard that causes substantial economic losses and fatalities worldwide. Regional-scale risk mitigation for these processes is challenging. Therefore, landslide early warning systems (LEWS) are a helpful tool to depict the time and location of possible landslide events so that the hazardous situation can be managed more effectively.

The main objective of this thesis is to set up a regional-scale LEWS that works in real-time over Catalonia (NE Spain). The developed warning system combines in real-time susceptibility information and rainfall observations to issue qualitative warnings over the region.

Susceptibility has been derived combining slope angle and land use and land cover information with a simple fuzzy logic approach. The LEWS input rainfall information consists of high-resolution radar quantitative precipitation estimates (QPEs). To assess if a rainfall situation has the potential to trigger landslides, the LEWS applies a set of intensity duration thresholds. Finally, a warning matrix combines susceptibility and rainfall hazard to obtain a qualitative warning map that classifies the terrain into four warning classes.

The evaluation of the LEWS performance has been challenging because of the lack of a systematic inventory, including the time and location of recent landslides events. Within the context of this thesis, a citizen-science initiative has been set up to gather landslide data from reports in social networks. However, some of the reports have significant spatial and temporal uncertainties.

With the aim of finding the most suitable mapping unit for real-time warning purposes, the LEWS has been set-up to work using susceptibility maps based on grid-cells of different resolutions and subbasins. 30 m grid-cells have been chosen to compute the

warnings as they offer a compromise between performance, interpretability of the results and computational costs. However, from an end users' perspective visualising 30 m resolution warnings at a regional scale might be difficult. Therefore, subbasins have been proposed as a good option to summarise the warning outputs.

A fuzzy verification method has been applied to evaluate the LEWS performance. Generally, the LEWS has been able to issue warnings in the areas where landslides were reported. The results of the fuzzy verification suggest that the LEWS effective resolution is around 1 km.

The initial version of the LEWS has been improved by including soil moisture information in the characterisation of the rainfall situation. The outputs of this new approach have been compared with the outputs of LEWS using intensity-duration thresholds. With the new rainfall-soil moisture hydrometeorological thresholds, fewer false alarms were issued in high susceptibility areas where landslides had been observed. Therefore, hydrometeorological thresholds may be useful to improve the LEWS performance.

This study provided a significant contribution to regional-scale landslide emergency management and risk mitigation in Catalonia. In addition, the modularity of the proposed LEWS makes it easy to apply in other regions.

RESUM

Els lliscaments superficials i els corrents d'arrossegalls són un fenomen perillós que causa significants perdudes econòmiques i humanes arreu del món. La seva principal causa desencadenant és la pluja. La mitigació del risc degut a aquets processos a escala regional no es senzilla. Ena quest context, els sistemes d'alerta són una eina útil per tal de predir el lloc i el moment en que es poden desencadenar possibles esllavissades en el futur, i poder fer una gestió del risc més eficient.

L'objectiu principal d'aquesta tesi és el desenvolupament d'un sistema d'alerta per esllavissades a escala regional, que treballi en temps real a Catalunya. El Sistema d'alerta que s'ha desenvolupat combina informació sobre la susceptibilitat del terreny i estimacions de la pluja d'alta resolució per donar unes alertes qualitatives arreu del territori.

La susceptibilitat s'ha obtingut a partir de la combinació d'informació del pendent del terreny, i els usos i les cobertes del sòl utilitzant un mètode de lògica difusa. Les dades de pluja són observacions del radar meteorològic. Per tal d'analitzar si un determinat episodi de pluja te el potencial per desencadenar esllavissades, el sistema d'alerta utilitza un joc de llindars intensitat-durada. Posteriorment, una matriu d'alertes combina la susceptibilitat i la magnitud del episodi de pluja. El resultat, és un mapa d'alertes que classifica el terreny en quatre nivells d'alerta.

Amb l'objectiu de definir quina unitat del terreny és la més adient pel càlcul de les alertes en temps real, el sistema d'alerta s'ha configurat per treballar utilitzant mapes de susceptibilitat basats en píxels de diverses resolucions, i en subconques. Finalment, l'opció més convenient és utilitzar píxels de 30 m, ja que ofereixen un compromís entre el funcionament, la facilitat d'interpretació dels resultats i el cost computacional. Tot i això, la visualització de les alertes a escala regional emprant píxels de 30 m pot ser difícil. Per això s'ha proposat utilitzar subconques per oferir un sumari de les alertes.

Degut a la manca d'un inventari d'esllavissades sistemàtic, que contingui informació sobre el lloc i el moment en que les esllavissades es van desencadenar, l'avaluació del funcionament del sistema d'alerta ha sigut un repte. En el context d'aquesta tesi, s'ha creat una iniciativa per tal de recol·lectar dades d'esllavissades a partir de posts en xarxes socials. Malauradament, algunes d'aquestes dades estan afectades per incerteses espacials i temporals força importants.

Per a l'avaluació el funcionament del sistema d'alerta, s'ha aplicat un mètode de verificació difusa. Generalment, els sistema d'alerta ha estat capaç de generar alertes a les zones on s'havien reportat esllavissades. Els resultats de la verificació difusa suggereixen que la resolució efectiva del sistema d'alerta età al voltant d'1 km.

Finalment, la versió inicial del sistema d'alerta s'ha millorat per tal poder incloure informació sobre l'estat d'humitat del terreny en la caracterització de la magnitud del episodi de pluja. Els resultats del sistema d'alerta utilitzant aquest nou enfoc s'han comparat amb els resultats que s'obtenen al córrer el sistema d'alerta utilitzant els llindars intensitat-durada. Mitjançant els nous llindars hidrometeorològics, el sistema emet menys falses alarmes als llocs on s'han desencadenat esllavissades. Per tant, utilitzar llindars hidrometeorològics podria ser útil per millorar el funcionament del sistema d'alerta dissenyat.

L'estudi dut a terme en aquesta tesi suposa una important contribució que pot ajudar en la gestió de les emergències degudes a esllavissades a escala regional a Catalunya. A més a més, el fet de que el sistema sigui modular permet la seva fàcil aplicació en d'altres regions en un futur.

RESUMEN

Los deslizamientos de ladera y los corrientes de derrubios son un fenómeno peligroso que causa significantes perdidas económicas y humanas alrededor del mundo. Su principal desencadenante es la lluvia. La mitigación del riesgo debido a estos procesos a escala regional no es fácil. En este contexto, los sistemas de alerta son una herramienta útil para predecir el lugar y el momento en el que se pueden desencadenar posibles deslizamientos en el futuro, y así poder hacer una gestión del riesgo más eficiente.

El principal objetivo de esta tesis es el desarrollo de un sistema de alerta para deslizamientos a escala regional, que trabaje en tiempo real en Cataluña. El sistema de alerta que se ha desarrollado combina información sobre la susceptibilidad del terreno y estimaciones de la lluvia de alta resolución para dar unas alertas cualitativas en la región.

La susceptibilidad se ha obtenido de la combinación de información sobre el pendiente del terreno y los usos y cubiertas del suelo utilizando un método de lógica difusa. Los datos de lluvia son observaciones de radar meteorológico. Para analizar si un determinado episodio de lluvias tiene el potencial de desencadenar deslizamientos, se utilizan unos umbrales de lluvia intensidad-duración. Posteriormente, una matriz de alertas combina la susceptibilidad y la magnitud del episodio de lluvias. El resultado es un mapa de alertas que cubre Cataluña y clasifica el terreno según cuatro niveles de alerta.

Con el objetivo de definir el tipo de unidad del terreno más adecuada para el cálculo de las alertas en tiempo real, el sistema se ha configurado para trabajar con mapas de susceptibilidad basados en pixeles de varias resoluciones y en subcuencas. Finalmente, la opción más conveniente resulta ser la utilización de píxeles de 30 m, ya que estos ofrecen un compromiso entre el funcionamiento, la facilidad de interpretar las alertas y el coste computacional. De todas formas, la visualización de las alertas a escala regional con una resolución de 30 m puede ser difícil. Por este motivo, se ha propuesto utilizar un mapa de subcuencas para ofrecer un sumario de las alertas.

Debido a la falta de un inventario de deslizamientos sistemático, que incluya información sobre el lugar y el momento en el que estos fueron desencadenados, la evaluación del funcionamiento del sistema de alertas ha supuesto un reto. En el contexto de esta tesis, se ha creado una iniciativa para recoger datos de deslizamientos a partir de publicaciones en redes sociales. Lamentablemente, estos datos están afectados por incertidumbres espaciales y temporales que en algunos casos pueden ser bastante importantes.

Para la evaluación del funcionamiento del sistema de alerta, se ha empleando un método de verificación difusa. Generalmente, el sistema de alerta es capaz de generar alertas en las zonas donde se habían reportado deslizamientos. Los resultados de la verificación difusa sugieren que la resolución efectiva del sistema de alerta está alrededor de 1 km.

Finalmente, la versión inicial del sistema de alerta se ha mejorada para poder incluir información sobre el estado de humedad del terreno en la caracterización de la magnitud del episodio de lluvia. Los resultados del sistema de alerta utilizando este nuevo enfoque se han comparado con los resultados del sistema utilizando los umbrales de lluvia intensidad-durada. Mediante la utilización de los nuevos umbrales hidrometeorológicos, el sistema de alerta emite menos falsas alarmas en los lugares donde se han desencadenado deslizamientos. Por lo tanto, utilizar umbrales hidrometeorológicos podría ser útil para la mejora del funcionamiento del sistema de alerta que se ha diseñado.

El estudio que se ha desarrollado supone una contribución importante que puede ayudar en la gestión de las emergencias debidas a deslizamientos en Cataluña. Además, el hecho de que el sistema sea modular, permite su fácil aplicación en otras regiones.

AGRAÏMENTS

TABLE OF CONTENTS

LIST OF FIGURES

LIST OF TABLES

Chapter 1

INTRODUCTION

1.1. Motivation

Rainfall-triggered landslides represent a major hazard that causes significant economic losses, physical asset damage, and fatalities worldwide, especially in mountainous regions (Petley 2012; Froude and Petley 2018). Although landslides are not as widely reported in Spain as in other regions, they still represent a significant hazard. Ferrer (1995) estimated the economic losses due to landslides in the period from 1986 to 2016 to be about 160 million euros per year. According to Ayala et al. (2004), the economic losses in the period spanning from 1990 to 2000 were of around 42 million euros per year. Landslides have also been the cause of several casualties. Ayala (1995) mentioned 17 deaths in the period from 1991 to1993. In the region of Catalonia, a total of 33 casualties have been reported from 1970 to 2020 (Buxó and Palau 2020). Around half were hit by landslides during transportation activities.

As a consequence of climate change the frequency and intensity of severe rainfall events that usually trigger landslides is expected to increase in some regions (Gariano and Guzzetti 2016; IEC-Generalitat de Catalunya 2016). Additionally, due to tourism development and the increased use of transportation networks in mountain and coastal areas, the exposure of communities to landslides is growing in many parts of the world, including Catalonia (Corominas et al. 2015; Buxó and Palau 2020). Active mitigation strategies cannot always be built, because of economic or environmental constraints, and the relocation of exposed settlements or infrastructures is not always possible for societal reasons (Lacasse et al. 2010). Thus, being able to predict the time and location of future landslide events is key to (i) reduce the risk by decreasing the exposure of society, and (ii) improve emergency and recovery plans (Alfieri et al. 2012).

This situation has raised the interest of different institutions to develop sustainable strategies to reduce the risk due to landslides as well as other natural hazards related with extreme weather events (Easterling 2000; Morss et al. 2011). The European Commission has developed legal frameworks such as the Water Framework Directive, and the Floods Directive to increase the prevention, preparedness, protection and response to such events and to promote research and acceptance of risk prevention measures within society (Alfieri et al. 2012). An important part of such an interdisciplinary approach for risk reduction is the establishment of early warning systems (UNISDR 2006). The Sendai framework for disaster risk reduction (UNISDR 2015) urged to increase the availability of reliable multi-hazard early warning systems. The important role that Landslide Early Warning Systems (LEWS) must play in order to reduce the landslide risk in future was highlighted by the International Strategy for Disaster Reduction (ISDR) and International Consortium of Landslides (ICL) Sendai Partnerships 2015–2025 (Sassa 2017, 2020).

Thus, in the last years, landslide early warning systems have been stablished in many regions. In the Catalonia region, a prototype landslide early warning system was developed by Berenguer et al. (2015) covering three areas in the Pyrenees.

Based on the scheme proposed by Berenguer et al. (2015), this thesis aims at developing the elements that constitute a landslide early warning system for the region of Catalonia. The approach adopted in this PhD fulfils the following conditions:

- The designed LEWS must be capable of running in real-time operationally at a regional scale.

- The outputs of the LEWS must help decision-makers to manage landslide emergencies more effectively.

Up to the date, little investigations have been conducted to asses landslide hazard at a regional scale in Catalonia. Only historical landslide inventories have been collected (Gallart and Clotet 1988; Portilla 2014; González et al. 2017), and a coarse preliminary landslide zonation proposed (RISKCAT 2008). Thus, the results of this thesis may play a significant role in regional landslide hazard assessment and risk mitigation in Catalonia.

1.2. Landslide causes, triggers and classification

Landslides consist on a mass of rock, soil, or a combination of both that moves downslope under the influence of gravity (Cruden 1991). The volume of soil and rock mobilized in a landslide can vary from small landslides involving less than 1 m^3 of material, to large landslides involving thousands or even millions of m^3.

Landslides occur when the destabilizing stresses acting down-slope exceed the resisting stresses of the materials that compose the slope. Thus, landslide causes include factors that enhance the effects of down-slope forces, and factors that contribute to reduce the strength (Iverson 2000). A trigger is defined as an external stimulus such as intense rainfall, sudden snowmelt, earthquake shacking, volcanic eruption, wave undermining or, rapid stream erosion that causes a near-immediate response in the form of a landslide by rapidly increasing stresses or by reducing the strength of the slope materials (Wieczorek 1996). Rainfall is the most important and widespread landslide trigger (e.g. Corominas 2000). As water infiltrates into the soil, pore water pressures increase and effective stresses decrease eventually leading to failure.

The term landslide includes a wide range of phenomena. For this reason, several landslide classifications can be found in literature (Stini 1941; Varnes 1958; Hutchinson 1988; Hungr et al. 2001). Possibly, one of the most widely used classification systems is the one proposed by Varnes (1958), (1978), Cruden and Varnes (1996). More recently, Hungr et al. (2014) updated the Varnes' classification to make it compatible with accepted geological and geotechnical terminology of rocks and soils. Varnes' classification is based on two main features; the material involved in the landslide, and the type of movement (Figure 1).
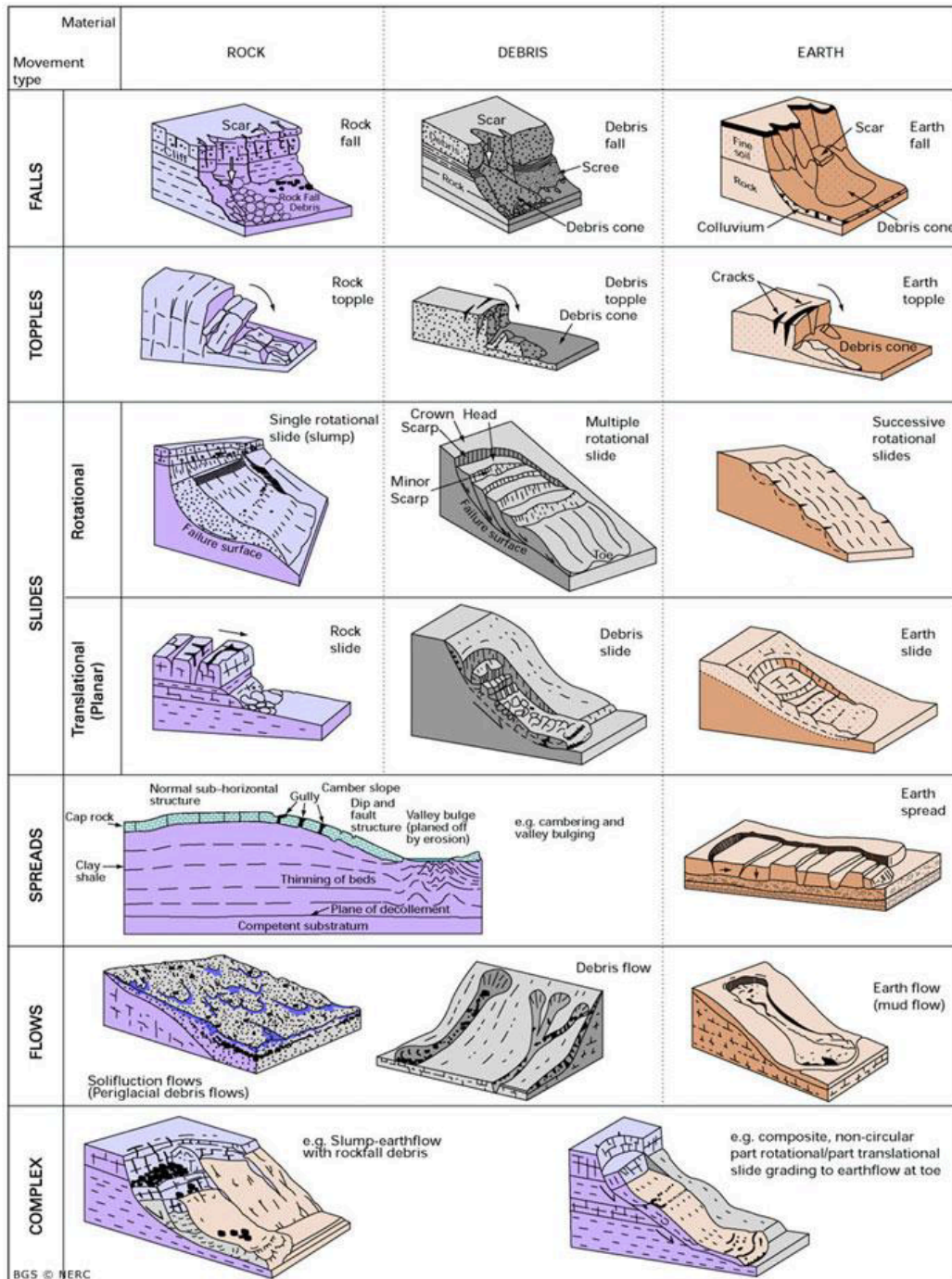
Figure 1. Types of landslide movement (Cruden and Varnes, 1996). Source: British geological survey (BGS).

The material involved in a landslide can be either soil, rock or a combination of the two. The combination of soil and rock can be described as earth if the material is mainly composed of fine-grained particles and sands, or debris if the material is composed of a mixture of finer and coarser materials. The type of movement can be a fall, topple, slide, spread or flow.

This thesis focuses on rainfall-triggered shallow slides and debris flows. Shallow slides consist on a mass of soil, that slips on a shallow surface parallel to the ground. Shallow slides usually initiate in steep slopes, with slope angles ranging from 30º-60º. The sliding surface is generally located between 0.5 and 2 m depth. The material involved in shallow slides usually consists of colluvium, weathered soils and pyroclastic deposits.

Debris flows are very rapid mass movements consisting on a high-density mixture of sand, boulders, and water. One of the characteristics of debris flows is that they move downhill through a channel in a series of surges (Jakob and Hungr 2005). Debris flows can start directly in the channel, when the water discharge is sufficient to start the erosion prosses. In addition, debris flow can also initiate as a shallow slide and transform into a flow when incorporating water and material from the channel.

1.3. Landslide early warning systems

Early Warning Systems can be defined as a set of elements needed to generate and disseminate timely and meaningful information so that individuals, communities and organizations that might be affected by a hazard can prepare and act in advance to avoid or reduce the impact (Alfieri et al. 2012; UNISDR 2015). According to the UNISDR (2009) people-centred EWS must include four elements: (i) risk knowledge, based on the collection of data and risk assessments; (ii) monitoring, analysis and forecasting of the triggering factors, the hazard, and its possible consequences; (iii) communication and dissemination of the warnings, and (iv) capabilities to respond to the warnings. Generally, LEWS are tools that integrate into a broader risk mitigation strategy.
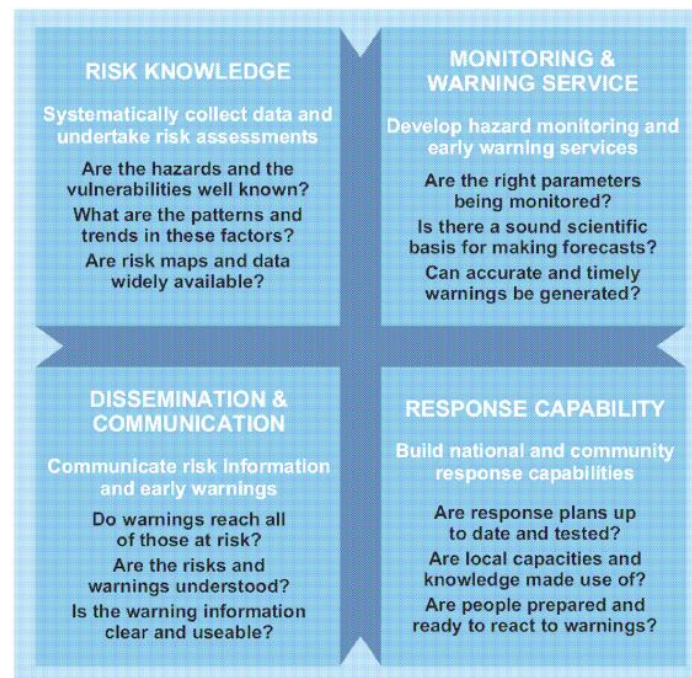
Figure 2 Components of a people centred early warning system (UNISDR - United Nations International Strategy for Disaster Reduction 2006).

The design and operation of early warning systems is a multidisciplinary challenging task that requires the combination of technical and social knowledge (Calvello et al. 2015b). Technical skills are essential to define the monitoring strategies, and asses the present and future hazard and risk. Social sciences are required to develop strategies to effectively communicate the warnings and educate communities so that early warning systems are effective tools.

EWS have been developed for different hazards. Landslide early warning systems (LEWS) are specifically designed to asses risk, and detect the conditions that may trigger or reactivate a landslide with enough time to issue a warning and mitigate its impacts. Therefore, EWS can be considered as non-structural passive risk mitigation measure (Fell et al. 2005).

Through the years, several authors have investigated the definition of the different elements that conform LEWS. Intrieri et al. (2013), based on the UNISDIR definition of people-centred EWS and the LEWS scheme proposed by Biagio and Kjekstad (2007), described LEWS as a balanced combination of four main activities: design, monitoring, forecasting, and education (Figure 3).

- The design of a LEWS consists of determining the needs and vulnerabilities of the population at risk, identifying the obstacles that may hinder the people from taking action and characterising geological and meteorological conditions that lead to landslides.

- Monitoring activities comprise the installation of instrumentation and the analysis of the collected data. Monitoring typically begins during the design phase and continues during all the LEWS life.

- Forecasting activities include the definition of thresholds, models, and all the required components to issue a warning. According to Intrieri et al. (2013), forecasting is the main element of LEWS.

- Education is key to enhance public risk perception. It is also necessary to explain the actions that should be taken given a certain warning to prevent possible damage or losses.
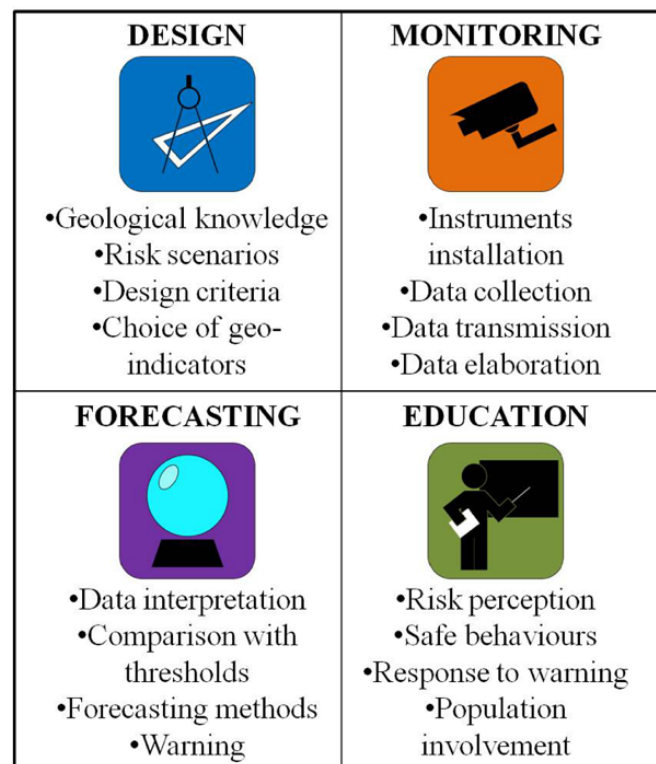
Figure 3. Components of a generic LEWS (Intrieri et al. 2013).

1.3.1. Types of landslide early warning systems depending on the scale of the domain

Focusing on the extent they cover, LEWS can be divided into two classes (Bazin 2012; Thiebes et al. 2012; Calvello 2017; Piciullo et al. 2018; Guzzetti et al. 2020): local if they focus on a single slope or basin, and geographical if they are not site-specific and cover a large area.

Local LEWS are typically implemented as alarm systems. Their objective is to temporally evacuate people from areas when the risk level at which they are exposed is intolerable. In such a case, several variables relating to the slope stability are regularly monitored to detect and issue an alarm when a landslide event is triggered. The accuracy of local LEWS is high but the lead-time is generally short (Badoux et al. 2009; Michoud et al. 2013; Pecoraro et al. 2018).

Within geographical LEWS we can distinguish between regional and global LEWS (Guzzetti et al. 2020). Regional LEWS cover a large municipality, metropolitan area, an administrative district, province, region or country. Regional LEWS are usually designed to asses weather-related landslides. Therefore, they are mainly based on the prediction and monitoring of meteorological variables. The objective of regional LEWS is to providing warnings to the governments, authorities in charge of managing the situation, or population when the probability of occurrence of landslides increases. When dealing with the possible occurrence of multiple landslides within an area, regional LEWS can be classified as territorial (Piciullo et al. 2018).

Global LEWS cover a large portion of the world (Guzzetti et al. 2020), and have a coarser resolution than regional LEWS. As regional LEWS, the existing global LEWS are intended to assess weather-induced landslides. Global LEWS aim to study long-term landslide trends, and support landslide risk assessment (Kirschbaum and Stanley 2018).

1.3.2. Components of a geographical LEWS

Geographical LEWS components can be classified as landslide models, warning models, and warning systems (Figure 4). A landslide model is one of the components of a warning

model, and in its turn, a warning model is one of the components of a warning system (Calvello 2017).

A landslide model can be defined as the empirical or physical relation between the weather characteristics, geological, geomorphological, or geotechnical features of the terrain, and landslide events (Calvello 2017; Guzzetti et al. 2020). The choice of the variables used to define a waning model depends on the size of the domain, and the type of landslide for which the LEWS is designed. Rainfall thresholds and susceptibility maps are common landslide models.
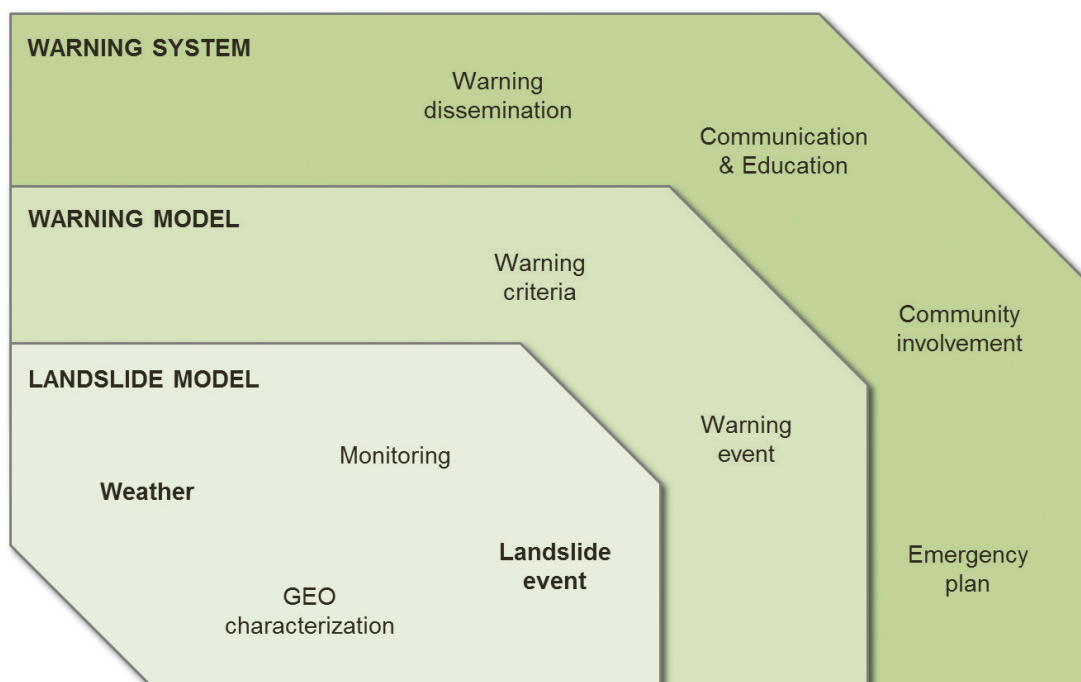
Figure 4. Components of an early warning system for weather induced landslides (Calvello 2017).

Warning models constitute the framework to issue landslide warnings. Warning models combine one or more landslide models, and define the warning criteria, warning levels, and warning zones that are used to issue warnings (Calvello 2017; Guzzetti et al. 2020). The warning criteria is the method that combines the different landslide models to decide when warnings should be issued. The warning criteria is specific for each LEWS. In the literature we can find LEWS that use warning criteria based on heuristic methods (Krøgli et al. 2018; Guzzetti et al. 2020), decision tree algorithms (Kirschbaum and Stanley 2018), and fuzzy logic (Berenguer et al. 2015), among others.

The definition of the warning levels and the warning zones are key elements of the design of a warning model (Piciullo et al. 2018). Warning levels are classes representing the possibility of having a landslide or not. Each warning level can be associated with a series of potential impacts, and therefore, depending on the warning level stakeholders will take a series of expected actions (Calvello 2017). The minimum number of warning levels required in a LEWS is two. In such case the first warning level refers to a low probability of landslides and the second level refers to a high probability of landslides. A higher amount of warning levels implies that the model is able to distinguish between different probabilities of landslide occurrence. Most of the existing LEWS use four warning levels: very low, low, moderate and high (Baum and Godt 2010; Osanai et al. 2010; Lagomarsino et al. 2013; Piciullo et al. 2017b; Kirschbaum and Stanley 2018).

Warning zones are the areas where warnings are issued. Usually they are grid-cells, slope units, catchments, or coincide with administrative areas such as municipalities or counties. In some LEWS the warning zones are fixed (Berenguer et al. 2015; Calvello et al. 2015b; Segoni et al. 2018a) while in other the warning zones change (Piciullo et al. 2017a).

Finally, warning systems include the warning models, warning dissemination and communication strategies, as well as emergency plans. The dissemination strategy must be adequate to the end-user, which could be authorities, civil protection agencies, or the general population. Risk perception is influenced by cultural and societal factors (Lacasse et al. 2010; Calvello et al. 2016). Thus, the warning message and emergency actions that must be adopted have to vary depending on whom is the LEWS target (Jacobs et al. 2005; Alcántara-Ayala et al. 2017).

A key element of a LEWS, which is not included in the components proposed by Calvello (2017) is the evaluation of its performance (Calvello and Piciullo 2016; Guzzetti et al. 2020). Yet, this task is often overlooked (Piciullo et al. 2020). In literature only few systems are described whose performance has been carefully assessed (Cheung et al. 2006; Kirschbaum et al. 2009; Calvello et al. 2015b; Calvello and Piciullo 2016; Park et al. 2020; Piciullo et al. 2020).

Herein, the most common components of the warning models and how they have been addressed by different authors are presented.

Rainfall data

Having accurate monitoring data of the variables that control landslide initiation is essential to define landslide models. Since most of the existing geographical LEWS deal with rainfall-triggered landslides, rainfall is the most common monitored variable. Usually, rainfall data is obtained from rain-gauges observations (Rossi et al. 2012; Yin et al. 2015; Segoni et al. 2018a; Park et al. 2019). However, the spatial and temporal resolution of rain-gauge networks is usually low and landslide triggering rainfalls tend to be underestimated (Marra et al. 2014, 2016, 2017; Nikolopoulos et al. 2014; Destro et al. 2017). For this reason, in some LEWS radar measurements have also been adopted. The main advantage of radar data is its high temporal and spatial resolution. However, radar data also requires careful processing to guarantee the quantitative value of rainfall products (Zawadzki 1984; Sánchez-Diezma et al. 2001; Corral et al. 2009; Borga et al. 2014; Marra et al. 2014). Global systems such as the ones proposed by Hong et al. (2006) and Kirschbaum and Stanley (2018) use rainfall estimates obtained from satellite imagery. Additionally, some landslide warning models also incorporate weather forecasts to be able to increase the lead-time of the warning. Usually these forecasts are provided by meteorological Numerical Weather Prediction (NWP) models (Krøgli et al. 2018) or by radar nowcasting (Yeung 2012).

Landslide data

Landslide inventories are fundamental to obtain landslide models and to evaluate the LEWS performance. Usually landslide inventories contain information of the time and location of past landslide events, as well as their failure mechanism, triggering factors, volumes, and damages that have caused (Corominas et al. 2014). However, landslides inventories are usually biased and include more landslides along transportation networks or in densely populated areas (Van Den Eeckhaut and Hervás 2012). Additionally, sometimes the spatial and temporal uncertainties of the landslides can be significant. Having a small number of landslide entries in the inventories, or using inaccurate or wrong landslide information, can result in large uncertainties, inaccurate landslide models, wrong warnings, and weak verifications (Kirschbaum et al. 2009, 2012; Gariano et al. 2015; Guzzetti et al. 2020).

Landslide susceptibility models

Landslide susceptibility can be understood as the spatial probability in which a certain area can be affected by a landslide (Fell et al. 2008). This depends on the topography, geology, geotechnical properties, climate, vegetation, and anthropogenic factors. Different approaches to determinate landslides susceptibility have been proposed for different types of landslides and at different scales (Guzzetti et al. 1999; Fell et al. 2008; Leopold et al. 2013; Bee et al. 2017, 2018). We can distinguish between three main methodologies to derive susceptibility: heuristic, data-driven, and physically-based (Corominas et al. 2014).

Heuristic methods determinate susceptibility qualitatively based on expert criteria. Heuristic methods can be direct, when an expert interprets the susceptibility of the terrain in the field, or indirect, when different parameters are combined based on expert knowledge on past landslides and their causal factors.

Data-driven methods make use of statistical or fuzzy logic approaches to combine the information of the factors that have resulted in landslides in the past, and make predictions in the areas that have similar conditions. Data-driven methods express susceptibility in terms of the possibility of having a landslide.

Finally, physically-based methods model slope failure processes. However, determining the required geo-mechanical parameters over large areas is not straightforward. Several assumptions, and simplifications must be made, adding uncertainties into the model (Tofani et al. 2017; Hurlimann et al. 2021).

Hydrometeorological thresholds

The majority of geographical LEWS rely on thresholds to define hydrometeorological conditions that, when exceeded, are likely to trigger landslides at the area of interest (Guzzetti et al. 2020). Hydrometeorological thresholds can be established at different scales (local, regional, global), and for distinct types of landslides. Empirical hydrometeorological thresholds are obtained from historical landslides inventories and hydrometeorological records, and can be manually drawn or derived using probability

(Brunetti et al. 2010; Nikolopoulos et al. 2014; Melillo et al. 2015; Rossi et al. 2017; Calvello and Pecoraro 2019).

Among hydrometeorological thresholds, rainfall intensity-duration (I-D) thresholds are the most popular. Caine (1980) was the first to empirically define a global rainfall I-D threshold for landslide occurrence. Since then, different authors have applied I-D thresholds (Hong et al. 2006; Guzzetti et al. 2007, 2008; Cannon et al. 2008; Brunetti et al. 2010; Segoni et al. 2014). Some authors used the total accumulated rainfall (E) and duration (D) to define rainfall thresholds (Peruccacci et al. 2012; Calvello and Pecoraro 2019). However, in reality, E-D thresholds and I-D thresholds are equivalent. E-D thresholds can be easily converted into I-D thresholds by dividing the rainfall accumulations by the duration.

One of the most critical shortcomings of I-D thresholds is that they do not account for the important role soil moisture plays in slope stability. For this reason, some authors have tried to indirectly include soil moisture information either by using antecedent rainfall measurements (Tien Bui et al. 2013; Lee et al. 2015), or by calculating an antecedent rainfall index (ARI) and computing intensity-antecedent rainfall thresholds (Glade et al. 2000; Lee et al. 2014; Ma et al. 2014; Kanjanakul et al. 2016; Kirschbaum and Stanley 2018). Still, observed soil moisture conditions do not always agree with antecedent precipitation (Longobardi et al. 2003; Brocca et al. 2008).

Another alternative consists of applying physically-based rainfall thresholds derived from soil stability models (Papa et al. 2013; Alvioli et al. 2014). However, the use of physically-based models over large areas and for early warning purposes is complex because the geo-mechanical properties of the terrain are very anisotropic and usually are obtained only for a few study sites.

To overcome empirical and physically-based rainfall thresholds limitations Bogaard and Greco (2018) proposed using hydrometeorological thresholds that, in addition to rainfall, include soil moisture information. Their main advantage over physically-based rainfall thresholds is that there is no need of determining the geo-mechanical parameters of the terrain. In the last ten years, rainfall-soil moisture thresholds have been derived using data from volumetric water content in-situ measurements, or gridded volumetric water content data from hydrological models (Posner and Georgakakos 2015; Mirus et al. 2018b; Wicki

et al. 2020; Marino et al. 2020). However the use of hydrometeorological thresholds in operational LEWS is still very limited (Krøgli et al. 2018).

Performance evaluation

LEWS need regular and systematic performance analysis to assure its reliability. The evaluation of LEWS performance consists of assessing how well the system depicts the time and location of landslide events. No clear standards exist to assess the performance of LEWS (Baum and Godt 2010; Park et al. 2020; Piciullo et al. 2020). In many cases, LEWS have operated without any type of quantitative or qualitative evaluation. (Calvello and Piciullo 2016; Piciullo et al. 2017a, 2020) proposed a method for the evaluation of territorial LEWS, the "EDuMaP". Within a warning zone, the EDuMaP accounts for the relation between the warning duration and the time landslides were reported.

Generally, contingency tables are used for the evaluation of LEWS. The components of a contingency table are:

- True positives: outcomes when the model predicts landslides, and landslides are observed.
- True negatives: outcomes when the model does not predict any landslide, and no landslides are observed.
- False positives: outcomes when the model predicts landslides, and landslides are not observed.
- False negatives: outcomes when the model does not predict landslides, and landslides are observed.

However, the lack of systematic information on landslide occurrence supposes a limitation to use the typical contingency tables. Evaluating the performance of geographical scale LEWS is often challenging. Sometimes the evaluation is done qualitatively by counting the number of days when warnings were issued, or only at specific locations where exhaustive landslide inventories are available (Berenguer et al. 2015; Krøgli et al. 2018). Another critical challenge for the evaluation of LEWS arises from the spatiotemporal uncertainty of landslides inventories. To deal with this issue, (Kirschbaum et al. 2009; Park et al. 2020) applied buffers to search for the warnings issued close in time and space from landslide reports.

1.3.3. Geographical landslide early warning systems in the world

In the last years, geographical landslide early warning systems have been developed in many parts of the world; for example, Hong Kong (Kong et al. 2020), San Francisco Bay (Cannon and Ellen 1985), Rio de Janeiro (Calvello et al. 2015a), Seattle (Baum and Godt 2010), the city of Busan in South Korea (Park et al. 2020), the Catalan Pyrenees (Berenguer et al. 2015), Southern California (NOAA-USGS Debris Flow Task Force 2005), Western Oregon (Baum and Godt 2010), Italy and different Italian regions (Rossi et al. 2012; Devoli et al. 2018; Segoni et al. 2018a), Japan (Osanai et al. 2010) Taiwan (Yin et al. 2015), Indonesia (Hidayat et al. 2019), or Norway (Krøgli et al. 2018). In this section we describe the main characteristics of some LEWS that the authors found relevant. The selected regional LEWS exist or have existed in the past.

Hong Kong

In 1977 the Geotechnical Control Office (now Geotechnical Engineering Office, GEO) set up the first regional LEWS of history in response to the two catastrophic landslide events that caused hundreds of fatalities (Brand et al. 1984; Malone 1988). Today, the "Landslip Warning System" is still operated by the GEO and the Hong Kong observatory (HKO) (Kong et al. 2020). It issues warnings for Hong Kong island, Kowloon and the New Territories (Choi and Cheung 2013; Wong et al. 2014).

The current version of the LEWS has been operational since 2004. Its input data consists of: (i) rainfall measurements from a dense rain gage network, (ii) rainfall estimates from the SWIRLS radar nowcasts (Yeung 2012), (iii) NWP rainfall forecasts. The model uses a set of four empirical relationships relating rainfall to landslide density for the most common types of engineered and natural in Hong Kong (Yu 2004; Chan et al. 2012). The LEWS is run every 6 min using a 1.5 km by 1.2 km grid that covers Hong Kong. The outputs consist on three warning levels. Each warning level is related to an expected number of landslides. Warnings are disseminated using a cell-phone app, social media, and conventional media.

The Hong Kong LEWS performance was quantitatively evaluated using 15 events during 2001-2005 period (Cheung et al. 2006). The LEWS was successful in forecasting the failure of engineered slopes, and had very few false alarms (Piciullo et al. 2018).

San Francisco Bay, California, USA

In 1982 a catastrophic storm hit the San Francisco Bay area (California), triggering thousands of shallow slides and debris flows that caused severe economic losses and casualties (KEEFER et al. 1987; Wilson 2012). The impacts of this rainfall event motivated the development a LEWS based on rainfall thresholds (Cannon and Ellen 1985; Wieczorek 1987). The San Francisco Bay LEWS was operative from 1985 to 1995.

The inputs of the San Francisco Bay LEWS consisted on 24-h quantitative precipitation forecasts (QPFs) from satellite issued twice a day by the National Weather Service (NWS) with estimates of the expected rainfall in four periods of 6h, and surface rainfall measurements from 45-60 rain gages operated by the NWS.

The warning model used two empirical rainfall I-D thresholds (Cannon and Ellen 1985; Wieczorek 1987), and one antecedent rainfall threshold (Wilson 2012) to assess rainfall event potential of triggering landslides. Depending on the magnitude of the rainfall event, four warning levels could be issued. The outputs of the warning model were examined by a team of expert forecasters who chose the most appropriate dissemination strategy. In seven occasions, advisories were given to the population through radio or TV broadcasts (Wilson 2012). Although the LEWS accurately predicted the time of major landslide events, it was less accurate in depicting the areas where landslides were triggered (KEEFER et al. 1987). In 1995 due to the lack of human and economic resources, the LEWS was shut down (Wilson 2012).

Rio de Janeiro, Brazil

The LEWS of the municipality of Rio de Janeiro was established in 1996 with the aim of warning landslides triggered by severe rainfall (Ortigao and Justi 2004). The current version of the system input data consists of rainfall measurements with a 15 min temporal resolution, rainfall estimates from two weather radars with a temporal resolution of 2 min,

and short-term weather forecasts issued twice daily by the Brazilian Centre for Weather Forecasting and Climate studies. Susceptibility is not considered.

The Alerta Rio warning model uses three rainfall thresholds that consider the 1 hour, 24 hours and 96 hours accumulated rainfall. Landslide warnings are issued by comparing the rainfall situation with the three rainfall thresholds. The municipality is divided into four warning zones. Four warning levels are used to define an expected density of landslides within the warning zone. The dissemination strategy of the Rio de Janeiro LEWS varies depending on the warning level that is issued. Moderate warnings are sent to municipality departments using a website. High warnings are communicated to the general public by TV and radio broadcasts (Calvello et al. 2015a).

The evaluation of the Rio de Janeiro LEWS performance was conducted for the period 2010-1012, applying the EDuMaP method (Calvello et al. 2015b; Calvello and Piciullo 2016). The Alerta Rio generally had a good performance, although the number of false alarms was quite significant in an area in the South East.

Italy national and regional LEWS

The national LEWS in Italy (SNAF) has been operative since 2009 (Rossi et al. 2012). Its inputs consist of: (i) 25 m resolution susceptibility map, (ii) sub-hourly rainfall measurements from the Italian rain gauge network, and (iii) 3-day lead time rainfall forecasts obtained from NWP models issued twice daily.

The warning model issues one landslide nowcast and two landslide forecasts each hour. The landslide nowcast uses rainfall observations and determines the probability of landslide occurrence using E-D thresholds (Rossi et al. 2012; Peruccacci et al. 2017). The first forecast uses rainfall forecasts and calculates the probabilities of expected rain in the following 3, 6, 12 and 34 h. The second forecast combines the susceptibility, the nowcast, and the first forecast. The results at each rain-gage are aggregated in geo-hydrological areas and interpolated using a 5 km grid. Finally, the LEWS outputs are given to civil protection.

The performance of the SNAF LEWS was analysed for the period 2014-2017 showed that landslide nowcasts were able to predict the time and location of landslides correctly. Landslide forecasts were affected by the uncertainties of the rainfall forecasts.

In addition to the national LEWS, several operational regional LEWS exist in Italy (Ponziani et al. 2013; Segoni et al. 2015, 2018a; Piciullo et al. 2017b; Brigandì et al. 2017; Devoli et al. 2018). Here, only two examples are summarised.

The SIGMA model has been operative for 20 years in the Emilia Romagna region (Segoni et al. 2018a). The SIGMA model input data consists of a susceptibility map, rainfall and temperature measurements from weather stations, and 72 h rainfall forecasts from NWP. If the temperature is below a critical value, a snowmelt module is run to add the meltwater to the measured rainfall (Martelloni et al. 2013).

The warning model employs statistical rainfall thresholds to assess if the rainfall accumulations registered in each rain-gage are sufficient to trigger landslides (Martelloni et al. 2012). Then, the rainfall triggering potential is combined with a susceptibility map using a warning matrix. The SIGMA model has three different warning outputs: The coarsest output is the expected number of landslides within polygons of thousands of squared kilometres. The mid-resolution one consists of the probability of exceedance of the rainfall thresholds and is given in territorial units of hundreds of squared kilometres. The finer resolution is specifically designed for municipalities and consists of a 100 m resolution raster map highlighting the areas where landslides are more likely to occur (Segoni et al. 2018a).

The Piedmont region has three different warning models managed by the Environmental Protection Agency: the DEFENSE, the SMART, and the TRAPS (Devoli et al. 2018). Each model has been designed to forecast a specific type of landslide. The DEFENSE (Tiranti et al. 2014) has been designed to forecast channelised debris flows in small mountain catchments. Its input data consists of a susceptibility map, radar QPEs and QPFs with 60 min lead time. Rainfall observations are updated every 5 min, and have a spatial resolution of 800 m. The susceptibility map used in the DEFENSE model classifies the basins into three classes based on their weathering capacity, their alluvial fan morphology and frequency and seasonal occurrence of debris flows. The model assesses if debris flows can be initiated using a set of intensity-duration thresholds that are different for each susceptibility class.

The SMART (Tiranti and Rabuffetti 2010; Cremonini and Tiranti 2018) is designed to forecast shallow slides in mountain and hilly areas. The SMART input data consists of

rainfall rain-gauge measurements and NWP rainfall forecasts. (Tiranti and Rabuffetti 2010). To determine if the rainfall conditions have the potential of triggering landslides, the SMART model uses empirical rainfall thresholds derived from statistical analysis of past landslide events. Recent studies have tested the performance of the SMART model using radar QPEs instead of rain-gauge data (Cremonini and Tiranti 2018). Although results were promising, radar QPEs are still not used in the operational version of the model.

Finally, the TRAPS (Tiranti et al. 2013) is used to forecast the reactivation of deep-seated landslides. Its input consists of rain-gage rainfall measurements, forecasted precipitation from NWP models, and snowmelt. The TRAPS model uses rainfall thresholds to determine if deep-seated landslides can be reactivated. The model evaluation is done quantitatively by using the data of a regional monitoring system for deep-seated landslides.

The three warning models of the Piedmont LEWS (DEFENSE, SMART, and TRAPS) are updated hourly. Additionally, a daily bulletin is automatically delivered to civil protection and local authorities.

Norway

The Norwegian LEWS is managed by the Norwegian Water Resources and Energy Directorate (NVE) (Devoli et al. 2018; Krøgli et al. 2018) and has been operational since 2013. The Norwegian LEWS input data consists of, two susceptibility maps, daily meteorological quantitative gridded forecasts of precipitation and temperature from the Norwegian Meteorological Institute (MET) and a soil water content obtained from a distributed version of the HBV hydrological model with a resolution of 1 km (Beldring et al. 2003). Additionally, in areas where groundwater stations are located a one-dimensional soil water and heat flow model is run daily.

The model uses relative water supply-relative water content hydrometeorological thresholds are applied in a 1 km grid, to assess if the hydrometeorological conditions have the potential of triggering landslides (Boje et al. 2018; Devoli et al. 2018). An expert team combines the hydrometeorological magnitude and susceptibility information to issue warnings, which are updated twice a day. Warning zones change according to the

hydrometeorological conditions. The Norwegian LEWS has four warning levels (Calvello and Piciullo 2016; Krøgli et al. 2018). Each warning level refers to an expected density of landslides. Finally, warnings are published on a website. Additionally, yellow, orange and red warnings are sent to authorities and media.

The performance of the Norwegian LEWS was assessed qualitatively for the period 2013-2017 (Krøgli et al. 2018). Additionally, over Western Norway the performance was evaluated for the period 2013-2014 using an adapted version of the EDuMaP method (Calvello and Piciullo 2016) to work with varying size warning zones (Piciullo et al. 2017a). Both assessments confirmed an overall good performance of the LEWS.

More recently, Pecoraro and Calvello (2021) designed a model to integrate pore water pressure measurements in the Norwegian national LEWS. The model was applied at specific hydrological basins where in-situ pore water pressure measurements were available and tested for January 2013-June 2017. The method was useful to improve the LEWS performance. However, in order to be applied at a territorial scale a number of measurements must be available in each of the warning zones (Pecoraro and Calvello 2021).

Busan, South Korea

The Busan LEWS input data consists of a susceptibility map, rainfall observations from a rain gauge network, and NWP rainfall forecasts. The LEWS system uses five landslide warning levels and includes two warning maps: (i) a 5-m resolution warning map and a (ii) primary administrative area warning map. Real-time warnings are updated every 10 min, warning forecasts are updated every 6 h. (Park et al. 2020).

The Busan LEWS is based on a sequential hazard evaluation method that consists of three stages (Park et al. 2019). The first phase of the sequential method is used to decide if the warning level should rise from "Null" to "Attention". In this first phase, statistical rainfall thresholds and susceptibility are combined. Next, if the warning level is increased, a physically-based rainfall threshold is used to assess if the warning level should rise to "Watch" or "Alert". Finally, the third phase is applied only if the warning level increases to "Alert". In such a case, a debris flow mobilization index is used to evaluate several

geomorphological factors and determine if the warning level should rise to "Emergency" (Kang et al. 2017).

The performance of the Busan LEWS was evaluated during the rainy seasons of 2009-2016. The landslide inventory used for the evaluation included 222 reports, some of which had significant spatial uncertainties. To deal with the spatial uncertainty of landslide reports (Park et al. 2020) applied a 50 m diameter buffer for the verification of the warnings. The LEWS was generally able to correctly issue warmings within 50 m from the locations where landslides were reported. The LEWS issued 30 warning events, from which 5 were associated to actual landslide reports.

Global LEWS

The first prototype global near real-time was proposed by Hong et al. (2006). This first global system used satellite rainfall information, and a global I-D threshold. If the rainfall threshold was exceeded, a global susceptibility map was employed to predict landslide occurrence (Hong et al. 2007). However, the first global LEWS had significant limitations due to the accuracy of the satellite rainfall products, and the resolution of the susceptibility map (Kirschbaum et al. 2009). Based on this experience, Kirschbaum and Stanley (2018) improved the components of the first global LEWS (Stanley and Kirschbaum 2017) and developed the global Landslide Hazard Assessment model for Situational Awareness (LHASA). LHASA uses satellite rainfall estimates to identify the rainfall conditions from the past seven days. If the rainfall is considered to be extreme and susceptibility values range from moderate to high a warning is issued to indicate the locations where landslides are probable. The LASHA model is intended for its use as a tool to study long-term global landslide trends, and support landslide risk assessment in near-real time.

1.4. Landslide warning in Catalonia

In Catalonia, the efforts to establish LEWS have mainly focused on the local scale. Realtime monitoring stations have been set up at sites where landslides represent a significant risk to the population (Marturià et al. 2010; Janeras et al. 2017, 2018; Peduto et al. 2021), and at three catchments at the Pyrenees where debris flows are frequent

(Hürlimann et al. 2014; Palau et al. 2017; Raïmat Quintana 2018). These monitoring stations have been designed so that they can be used to implement local LEWS in the future.

One of the main limitations for developing regional-scale LEWS in Catalonia is the shortage of landslide inventory data. Landslide inventories were only collected for historical rainfall events that triggered multiple landslides over specific regions (Gallart and Clotet 1988; Portilla 2014; González et al. 2017, 2020).

Landslide data from monitoring sites and the available inventories were used to establish preliminary rainfall thresholds for landslide initiation Catalonia in (Corominas 2000; Abancó et al. 2016). Additionally, the data was used to obtain susceptibility maps for specific areas in the Pyrenees (Santacana et al. 2003; Bregoli et al. 2015; Hürlimann et al. 2016; Shu et al. 2019), and hazard maps for areas that were of specific interest (Oller et al. 2009). Still, up to date, only a preliminary landslide zonation covering entire Catalonia was made (RISKCAT 2008).

The most relevant contribution to regional-scale LEWS in Catalonia is a prototype debris flow forecast model that was designed for two regions in the Pyrenees (Berenguer et al. 2015). The prototype LEWS used a fuzzy logic algorithm to combine susceptibility and high-resolution rainfall estimates to issue warnings at a subbasin scale.The susceptibility was derived by applying a fuzzy logic classifier to combine four morphometric parameters of the terrain (Berenguer et al. 2015). Physically-based antecedent rainfall-intensity-duration thresholds were used to determine the percentage of unstable area for each subbasin. Then a fuzzy logic rainfall classifier was applied to assess the magnitude of the rainfall situation within each subbasin. Finally, the debris flow warning level was obtained by combining the fuzzy classifications of susceptibility and the magnitude of the rainfall situation using a logic table. The output of the prototype LEWS was a map showing the warning level in each subbasin every time rainfall information was updated.

1.5. Objectives of the thesis

The present thesis aims at developing the components of a regional-scale early warning model for rainfall-induced shallow slides and debris flows. The warning model is intended to be part of a prospective operational LEWS for the Catalonia region.

The following specific objectives must be accomplished to achieve this main goal:

- Assess landslide susceptibility in the Catalonia region and derive a regional landslide susceptibility map. The susceptibility map will be used in the warning model to distinguish landslide-prone areas.

- Select the most suitable mapping unit to compute and visualize the warnings.

- Assess governing factors related to rainfall and soil moisture that led to landslides in the past.

- Define empirical thresholds that introduce soil moisture conditions in the assessment of the magnitude of the rainfall event.

- Evaluate the performance of the early warning model and its components in Catalonia.

An inventory including information on the time and location of past landslide events in Catalonia is required to fulfil the five specific objectives stated above. Therefore, the compilation of landslide inventory data is another objective of this work.

Although according to (Calvello 2017) LEWS include warning models and dissemination strategies, in this thesis, the term LEWS is often used to refer to the warning model and aspects of dissemination or communication are not treated.

1.6. Thesis structure

This document is structured in five chapters. This first chapter provides the general context and motivation of the thesis.

Chapter 2 consists of a paper that has been published in Landslides (Palau et al. 2020). It introduces the Catalonia region warning method. It focuses on the obtention of a landslide susceptibility map, and analyses the influence of the mapping units used to compute the warnings on the LEWS outputs.

Chapter 3 analyses the LEWS performance during an extraordinary rainfall event that affected Catalonia in January 2020 triggering multiple landslides over the region. The LEWS performance is analysed using a fuzzy verification framework. Additionally, the citizen science #Esllavicat inventory for the evaluation of landslide warnings in Catalonia is presented. This chapter consists of a manuscript that has been submitted to the journal Landslides (Palau et al. under review).

Chapter 4 studies the rainfall and soil moisture conditions that have led to landslides in the past. Based on this analysis, empirical thresholds relating rainfall and soil moisture are proposed for the region of Catalonia. Additionally, Chapter 4 assesses the performance of the warning model for the period April-December 2020. The text will be submitted as an article to the Journal of Hydrology (Palau et al. in prep)

Finally, Chapter 5 describes the general conclusions of this work and provides an outlook for future research.

Chapter 2

INFLUENCE OF THE MAPPING UNIT FOR REGIONAL LEWS. COMPARISON BETWEEN PIXELS AND POLYGONS IN CATALONIA (NE SPAIN)

2.1. Introduction

Rainfall-triggered shallow slides and debris flows represent an important hazard that causes major economic losses and fatalities worldwide (e.g. Jakob and Hungr 2005; Froude and Petley 2018). Although these phenomena are not as widely reported in Catalonia (NE Spain) as they are in other regions, their hazard is still significant (Gallart and Clotet 1988; Portilla et al. 2010; Hürlimann et al. 2014; Palau et al. 2017). Rainfalls that trigger shallow slides and debris flows are frequently rather short and intense (Guzzetti et al. 2008; Alfieri et al. 2012; Abancó et al. 2016) and its frequency is expected to increase due to climate change (Gariano and Guzzetti 2016). Building reliable Early Warning Systems is of key importance to reduce the risk by increasing awareness and preparedness of communities which may be exposed (Alfieri et al. 2012; UNISDR 2015; Alcántara-Ayala et al. 2017).

In the recent years, regional Landslide Early Warning Systems (LEWS) have been developed covering multiple areas worldwide; e.g. Japan (Osanai et al. 2010), Hong Kong (Lloyd et al. 2001), the Chinese Zhejiang province (Yin et al. 2008), Southern California (Baum and Godt 2010), Rio de Janeiro (Calvello et al. 2015b), the Italian regions of Emilia Romagna and Campania (Piciullo et al. 2017b; Segoni et al. 2018a), Norway (Krøgli et al. 2018) and the Catalan Pyrenees (Berenguer et al. 2015). These LEWS frequently use susceptibility maps to depict the landslide prone areas and assess whether a rainfall event might trigger a landslide by means of rainfall thresholds (Aleotti 2004; Baum and Godt 2010; Papa et al. 2013; Berti et al. 2015; Piciullo et al. 2017b; Pan et al.

2018). The quality of both the susceptibility assessment and the rainfall data (as well as the rainfall Intensity-Duration thresholds) influence significantly the accuracy of the issued warnings.

Generally, the rainfall inputs are obtained from rain-gage measurements (Piciullo et al. 2017b; Krøgli et al. 2018; Segoni et al. 2018a). But in many cases the density of rain-gage networks is low, especially in remote mountainous areas, and landslide triggering rainfalls tend to be underestimated (Marra et al. 2014). For this reason, some large scale (regional or global) LEWS use radar rainfall observations (NOAA-USGS Debris Flow Task Force 2005; Chen et al. 2007; Osanai et al. 2010; Berenguer et al. 2015) or satellite rainfall products (Rossi et al. 2017; Kirschbaum and Stanley 2018).

Susceptibility maps describe the spatial distribution of the likelihood of having a landslide (Fell et al. 2008). When implemented into a LEWS they are used to identify the locations where future events are more likely. Susceptibility maps relate landslide occurrence with a number of variables that control its initiation. However, obtaining high-resolution information of certain geotechnical variables directly related to landslide occurrence at regional scale is very difficult. As a consequence, susceptibility is usually characterized using morphological parameters obtained from digital elevation models (DEMs), and sometimes also include geological and land cover information (Leopold et al. 2013; Chevalier et al. 2013; Liu et al. 2013; Bregoli et al. 2015; Kirschbaum et al. 2016; Wilde et al. 2018).

Susceptibility zoning is based on the discretization of the study region into homogeneous mapping units (Hansen 1984). Diverse mapping units have been used to report warnings, for example polygons (municipalities, catchments…), lines (roads) or pixels (Lloyd et al. 2001; Liao et al. 2010; Huat et al. 2012; Berenguer et al. 2015; Krøgli et al. 2018; Segoni et al. 2018a). Choosing an appropriate mapping unit for LEWS is not straightforward and requires considering several factors such as the resolution, the accuracy of the warnings, end-users' interpretability of the results, and computational cost. In the past, some authors have studied the effect of using polygon or grid-cell mapping units in the performance of susceptibility assessments (Carrara et al. 2007; Calvello et al. 2013; Hürlimann et al. 2016). However, there is still no study on its influence on the performance of a LEWS.

The aim of this paper is twofold: (i) assessing the influence of the mapping unit on the outputs of a regional LEWS, and (ii) selecting the most suitable mapping unit for a regional LEWS for Catalonia adapted to real-time performance. This has required the retrieval of the susceptibility map for Catalonia, which is a secondary goal of the presented work.

2.2. Settings

2.2.1. Geographic, Geologic and Climatic Settings

The region of Catalonia is located at the NE of Spain and covers an area of around 32000 km2. Its altitude ranges from sea level to 3143 m in the Pyrenees. From a geological point of view, Catalonia is located at the Iberian Plate. Its orography is the result of (i) the collisions of the Iberian Plate, the European Plate and the African Plate during the Paleogene, forming the Pyrenees, the Catalan Coastal Range and the Iberian Range, (ii) the deposition of its sediments in the Ebro Basin depressions, and (iii) the reactivation of pre-existing faults in an extensive context during the Miocene, forming a series of horsts and grabens more or less parallel to the actual coast-line (Berastegui et al. 2010).

Catalonia's climate is varied but can be classified as Mediterranean (Mira et al. 2017). Near the coast the climate is mild and temperate. Inland, the climate is continental, with cold winters and hot summers. The Pyrenees present a high-altitude climate, with abundant snow and temperatures below 0ºC during winter. The rainiest seasons are generally spring and autumn with the exception of the Pyrenees where the rainiest season is summer. The majority of the landslides are triggered by either (i) convective rainfall events with high intensities, which are typical from mid-summer to early autumn, and (ii) long-lasting rainfalls with moderate intensities, common during spring and autumn (Corominas et al. 2002; Abancó et al. 2016).
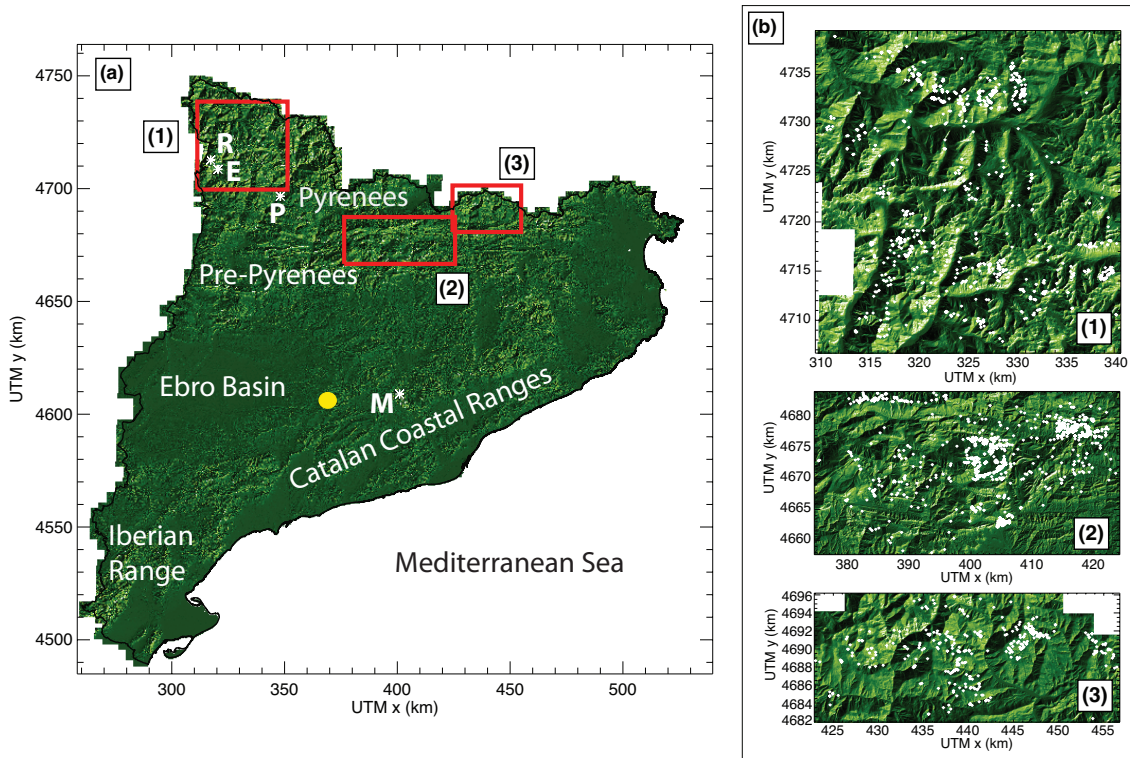
Figure 5. (a) Overview map of Catalonia. The red rectangles show the areas where landslide inventories exist in (1) NW-Catalonia, (2) NC-Catalonia and (3) NE-Catalonia. The yellow circle represents the location of the CDV C-band weather radar. R, E, P and M show, respectively, the locations of Rebaixader, Erill, Portainé and Santa Maria, where landslide events were reported during 2010 (see section 5). (b) Inventory of landslide locationsin the three areas shown with the red rectangles in panel a).

2.2.2. Datasets used

The majority of LEWS methods use susceptibility and rainfall information. Here, we describe the data that has been used to implement our prototype LEWS. A full description of the method is presented in in section 2.3.

The rainfall datasets used in this study are radar-based Quantitative Precipitation Estimates (QPE). Specifically, 30-min rainfall accumulations with a spatial resolution of 1 km. These maps have been produced with the Integrated Tool for Hydrometeorological Forecasting (EHIMI, Corral et al. 2009) from the volume scans of the Creu del Vent single-polarization C-band Doppler radar of the Meteorological Service of Catalonia (SMC). The location of the radar is shown in Figure 5. The EHIMI tool includes a chain of correction and quality control algorithms to generate the QPE products from raw radar observations.

To derive the susceptibility maps, the 5 m resolution DEM of Catalonia (ICGC 2013) has been used. Additionally, information on land use and land cover (LULC) has been obtained from the Map of Soil Coverage of Catalonia (MCSC-4, CREAF 2009).

Information of historic and recent shallow slides and debris flows contained in the inventories of three zones located in the Pyrenees and the Pre-Pyrenees (Figure 5b, Table 1) has been used for the susceptibility assessment. The NW-Catalonia inventory is the most recent and accurate and consists of 908 events. These events were principally identified by means of interpretation of aerial photos, and both 2D and 3D digital orthophotos (Chevalier 2013; Shu et al. 2019). The NC-Catalonia inventory is composed of 1249 landslide events. The majority of these events were triggered by the extraordinary rainfall episode of 7-8 November 1982 and were geolocalized on topographic maps during field surveys and photointerpretation (Gallart and Clotet 1988). The spatial accuracy of this inventory is the lowest. Finally, the NE-Catalonia inventory contains 317 landslides. Many of them were triggered by the catastrophic October 1940 rainfall event and the geolocalization of these landslides was done by analysis of the 1956-1957 aerial photographs taken by the Spanish Army Geographical Service (Portilla 2014). Further details about the three inventories and its analysis can be found in Hürlimann et al. (2016).

Table 1 Summary of the characteristics of the three inventory areas

Study Area	Main lithology	Area [km^2]	# of landslides	Average density [# of landslides per km^2]
NW-Catalonia	Igneous & Metamorphic	1018	908	0.89
NC-Catalonia	Sedimentary	1317	1249	0.95
NE-Catalonia	Igneous & Metamorphic	486	317	0.65

2.3. General methodology

The prototype LEWS applied in this study has been designed with the aim of working in real time and has the purpose of issuing warnings to the authorities in charge of managing the risk. It is based on the scheme developed by Berenguer et al. (2015), which was applied in two study areas in the Catalan Pyrenees. Its inputs are (i) susceptibility

information, and (ii) gridded rainfall observations. The output of the LEWS is a map showing a qualitative warning level ("very low", "low", "moderate" and "high") for each mapping unit every time new rainfall observations are available (in this case every 30 min, see section 2.2.2). Figure 6 shows a general scheme of the system. Its components are shown in the sections below.
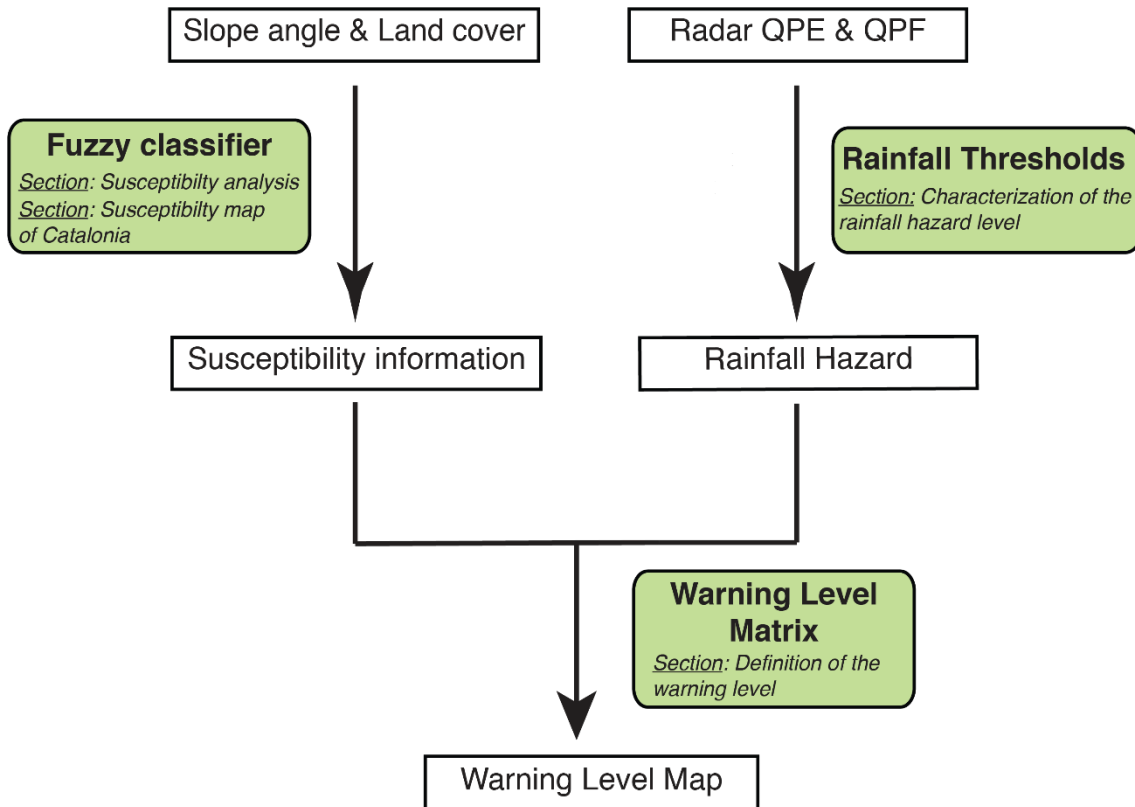
Figure 6. General flow chart of the prototype LEWS algorithm.

2.3.1. Susceptibility analysis

A static susceptibility map is used by the LEWS to distinguish landslide-prone areas. The susceptibility map for Catalonia has been derived combining the slope angle and land cover. The method used for susceptibility mapping, similar to that of Berenguer et al. (2015), is described in detail in section 2.4. It employs fuzzy logic (Mendel 1995) to classify the susceptibility in four categories: "very low", "low", "moderate" and "high".

2.3.2. Characterization of the rainfall hazard level

Rainfall intensity-Duration (I-D) relationships are widely used in LEWS to assess the hazard posed by a rainfall situation. In Catalonia no comprehensive I-D thresholds are available, only preliminary rainfall thresholds based on daily rainfall records or thresholds at catchment scale exist (e.g., Corominas 2000; Abancó et al. 2016). Thus, to assess the magnitude of rainfall situations in the analysis domain, we have used the intensity-duration-frequency (IDF) curves of the Fabra meteorological observatory in Barcelona (Casas et al. 2004) as reference. The IDF curves are the base to define four rainfall hazard levels: "very low", "low", "moderate" and "high" (Figure 7). The definition of the thresholds has been done empirically with the following criteria: for the high rainfall hazard, the I-D curve for a return period of 5 years has been used. In addition, the two other thresholds (lower limit of hazard level "moderate" and "low") were defined as parallel I-D curves that are below the two years return period. Although these thresholds do not directly relate rainfall with landslide occurrence, their slopes are very similar to the ones of local rainfall thresholds obtained for specific sites in Catalonia (e.g. Abancó et al. 2016; Hürlimann et al. 2017).
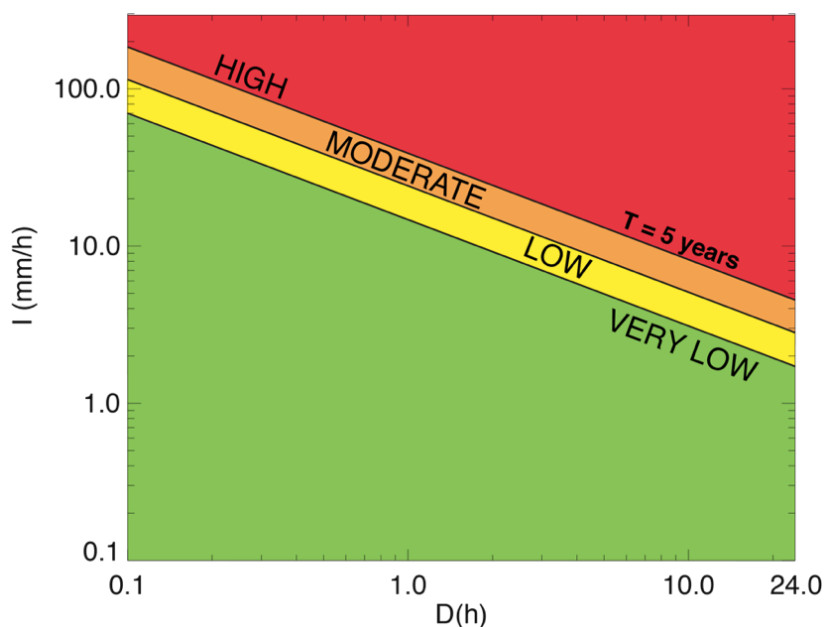
Figure 7. Rainfall intensity-duration thresholds. The background green, yellow, orange and red colours represent the four rainfall hazard level classes: "very low", "low", "moderate" and "high".

2.3.3. Definition of the warning level

Combining the susceptibility of the mapping unit and the magnitude of the rainfall event, the LEWS issues a warning. While susceptibility is considered to be static (it remains constant in time), rainfall inputs are updated every 30 minutes. The combination of the susceptibility and rainfall hazard is done according to the warning level matrix of Figure 8. The result for each timestep is a qualitative warning level for each mapping unit of one of the following four classes: "very low", "low", "moderate" and "high".

Each warning level class aims at assessing the possibility of having a shallow slide or debris flow; i.e. increasing the warning level implies increasing the probability of the expected event.

Figure 8. Warning level matrix. Rows represent the rainfall hazard level; columns represent the susceptibility degree. "VL", "L", "M" and "H" stand for "very low", "low," "moderate" and "high" warning level respectively.

2.4. Susceptibility map of Catalonia

One of the requirements to extend the LEWS to Catalonia is mapping the susceptibility over the entire region. Up to the date there is no susceptibility assessment spanning the whole region. This section first presents the methodology used to derive the susceptibility map with different mapping units, and next, the different susceptibility maps are evaluated by (i) visual inspection, and (ii) from a quantitative point of view in a validation framework.

32

2.4.1. Susceptibility mapping methodology

Chevalier et al. (2013) analysed the skill of different morphological parameters obtained from the DEM to assess shallow slides and debris flows susceptibility. Their results showed that the most significant governing factor was the terrain slope angle. Though, they did not include information associated with the soil layer in their analysis. Some authors (Nadim et al. 2006; Ciurleo et al. 2016; Wilde et al. 2018) have used information contained in geological maps to assume geotechnical properties of the soil. However, in Catalonia, the geological map mostly lacks information on surficial formations. Thus, a reasonable alternative consists in using land use and land cover (LULC) information, as proposed by several authors (e.g. Hürlimann et al. 2016; Pisano et al. 2017; Gariano et al. 2018). LULC provide indirect information of sediment availability. In addition, the vegetation plays an important role in slope stability [e.g. evapotranspiration, suction, apparent cohesion given by the plant roots (Schmidt et al. 2002; Schwarz et al. 2010)]. The removal of vegetation generally increases susceptibility (Persichillo et al. 2017; Pisano et al. 2017). For these reasons, the susceptibility map of Catalonia presented herein has been derived using slope angle and LULC, which are datasets currently available not only in Catalonia, but also in most countries.

Susceptibility maps of two main types have been derived: (i) raster grids of different resolutions (5 m, 30 m, 200 m and 1 km), and (ii) a subdivision of the analysis domain in hydrological subbasins (including 1st, 2nd and 3rd order , following the method of Strahler, 1957). The mean area and its standard deviation of these subbasins are 2.1 km^2 and 1.6 km^2 respectively. For the map based on raster grids, the 5 m DEM has been upscaled to obtain the DEMs of lower resolutions and the slope angle of each resulting cell has been computed using GIS tools.

The 241 original land cover classes of the LULC map have been reclassified into 11 classes that were significant in terms of slope stability following the Corine Land Cover Classification (EEA 1990). As the original land cover map was rasterized at a resolution of 5 m, we had to adopt a criterion to upscale the information to 30 m, 100 m, 200 m and 1 km resolutions and subbasins. Finally, we have chosen to assign the most susceptible land cover class to the larger mapping unit, on the condition that this class is representative enough (it occupies at least 15% of the (larger) terrain unit). This

methodology is quite feasible, but decreases land cover variability with decreasing resolution and biases it towards more susceptible classes as it can be seen in Figure 9.

Slope angle and land cover have been combined to retrieve the susceptibility maps using a fuzzy logic classifier (Mendel 1995). Compared to statistical methods, fuzzy logic has the following advantages: (i) it is able to model the non-linear behaviour of the susceptibility input variables, (ii) it uses expert criteria to assess the uncertainty of input parameters and landslide inventories, (iii) it is simple and can be easily adapted to different regions.
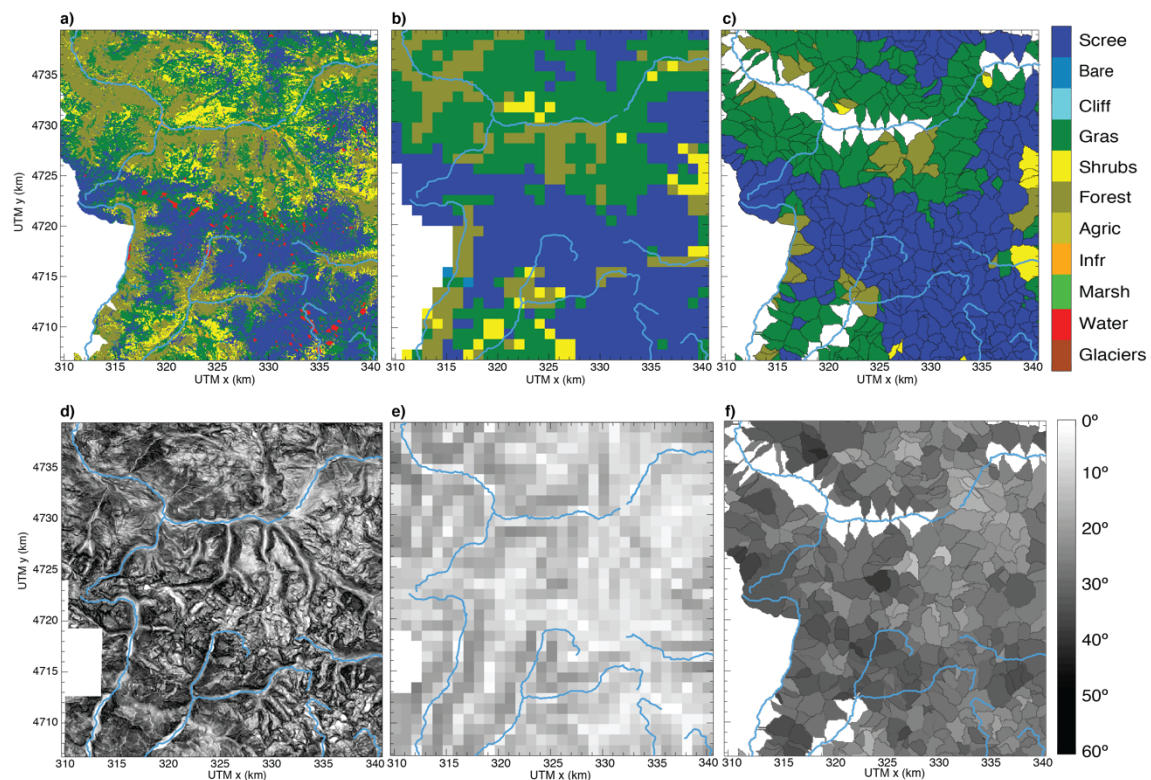
Figure 9. Maps of the NW-Catalonia study area. The upper and the bottom rows show respectively the land cover maps and the slope angle maps with pixel resolution of (a), (d) 30 m, (b), (e) 1 km, and (c), (f) hydrological subbasins respectively.

The used fuzzy logic classifier requires a weight for each input variable (slope and land cover) and membership functions for each input variable and each susceptibility class ("very low", "low", "moderate" and "high"). Membership functions measure how realistic it is that a mapping unit where one variable takes a value x belongs to a certain susceptibility class. Here, similarly as Berenguer et al. (2015), the membership functions and weights for the slope angle and the land cover have been designed by an expert using subjective criteria by taking the information of landslide frequency distributions of a

random sub-set containing half of the points of the landslide inventory as a reference (not shown). Slope angle membership functions have been adapted for all the different mapping units (Figure 10a - Figure 10c). In contrast, land cover landslide frequency distributions are very similar for all the mapping units; and thus, the same membership functions set has been adopted for all mapping units (Figure 10d).
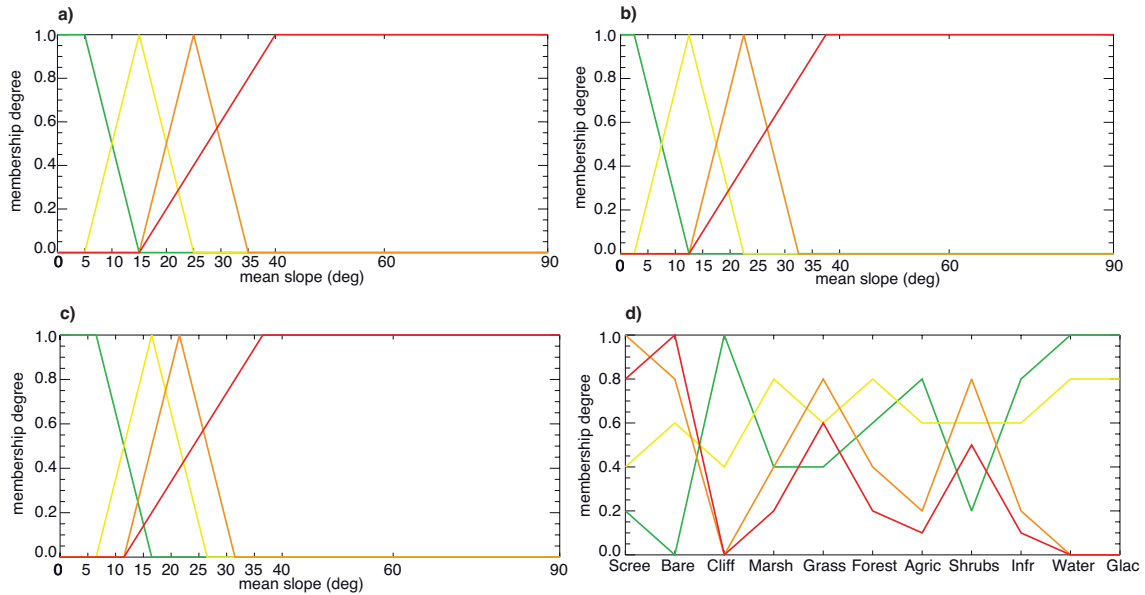
Figure 10. Slope membership functions for pixels with a resolution of (a) 30 m, (b) 200 m, and (c) hydrological catchments. (d) Land cover membership functions. Green, yellow, orange and red lines represent the membership functions of "very low", "low", "moderate" and "high" susceptibility.

From these membership functions, the membership degree to a susceptibility class (M_S) assesses the feasibility that a mapping unit belongs to it. Its value ranges from zero to one and has been computed as follows:

$$M_S = w_{sl}\, \mu_{sl,S} + w_{lc}\, \mu_{lc,S} \qquad (1)$$

where w_{sl} and w_{lc} are the weights of slope and land cover respectively, and $\mu_{sl,S}$ is the membership degree for the slope and for a susceptibility class S, $\mu_{lc,S}$ is the land cover membership degree for a susceptibility class S.

The susceptibility class having the highest membership degree (i.e. higher possibility of having landslides) has been assigned to each terrain unit. That is:

35

$$S = argmax \{M_{VL}, M_L, M_M, M_H\} \qquad (2)$$

where S states for the susceptibility class, and M_{VL}, M_L, M_M, M_H for the membership degree of the classes "very low", "low", "moderate" and "high" respectively.

2.4.2. Comparing the different susceptibility maps

The fuzzy logic classifier has been applied to create landslide susceptibility maps covering the region of Catalonia using 5 m, 30 m, 100 m, 200 m, 1 km grid-cells, and subbasins as mapping units. The susceptibility map based on 30 m grid-cells shows variability, with the areas having higher susceptibility located in the mountainous regions of the Pyrenees and the Catalan Coastal Ranges (Figure 11). The flat areas of the low Ebro Basin generally present "very low" susceptibility. The results for the other mapping units (not shown here) are relatively similar.
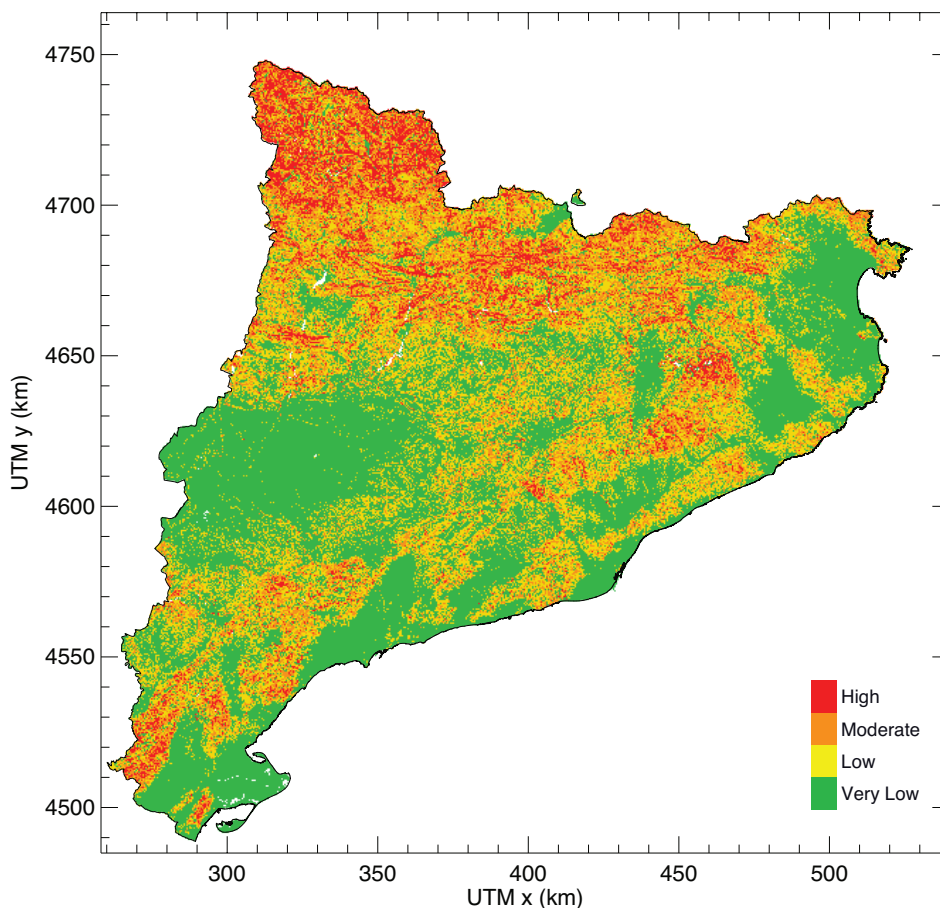
Figure 11. Susceptibility map of the Catalonia using 30 m grid-cells as mapping units.

The resulting susceptibility maps based on the different mapping units for the NW-Catalonia zone are shown in Figure 12. In this area located in the Axial Pyrenees, the 5 m, 30 m, 100 m and 200 m pixels susceptibility maps include large parts of "moderate" and "high" susceptibility.

The resulting susceptibility maps based on the different mapping units for the NW-Catalonia zone are shown in Figure 12. In this area located in the Axial Pyrenees, the 5 m, 30 m, 100 m and 200 m pixels susceptibility maps include large parts of "moderate" and "high" susceptibility.
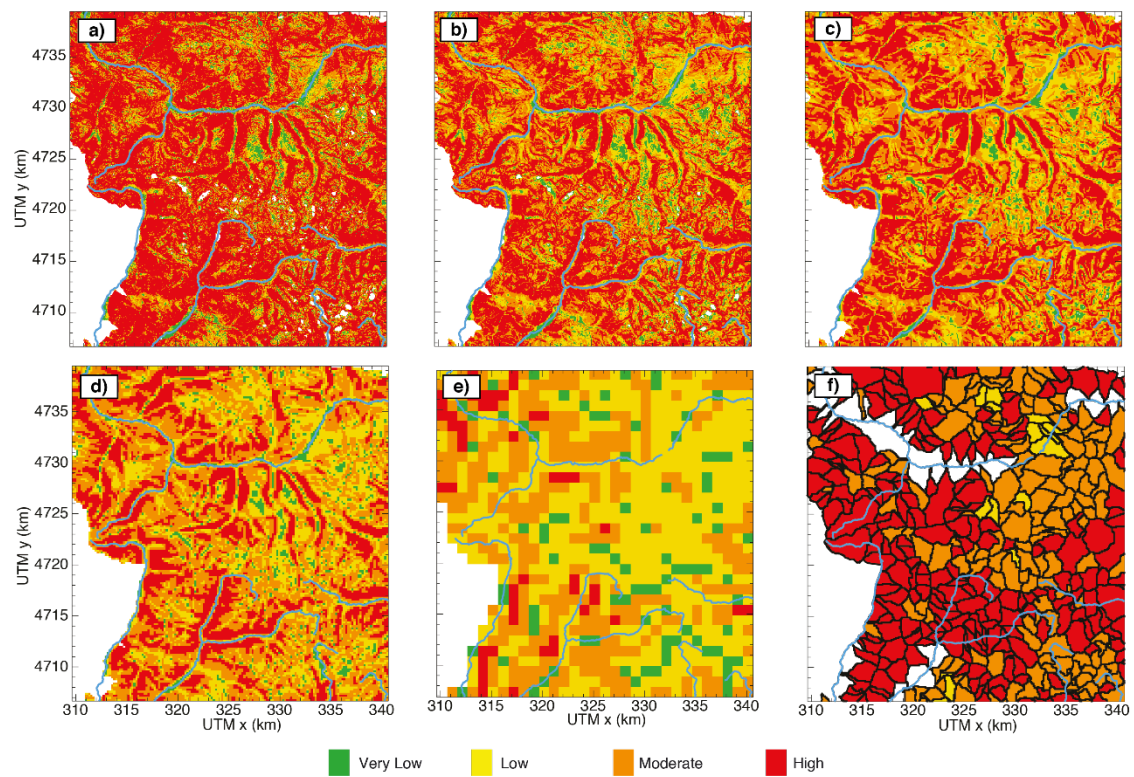
Figure 12. Susceptibility maps of the NW-Catalonia study area. (a) 5m, (b) 30 m, (c) 100 m, (d) 200 m and (e) 1 km grid-cells, and (f) hydrological subbasins.

Unlike pixel-based susceptibility maps, the susceptibility map of hydrological subbasins does not cover the entire domain and classifies almost all the mapping units in the NW-Catalonia zone as "moderate" and "high" susceptibility (Figure 12f). However, the percentage of area occupied by these two classes is similar to the area occupied by the same two classes in the map that uses pixels of 5 m resolution as mapping units (Table 2). The main difference relies on the percentage of area classified as "very low" and "low" susceptibility class which is much smaller for the map of subbasins. This can be partly

explained because the subbasin map covers mainly the upstream parts of the domain where slope is generally steeper and therefore typically it corresponds to areas that are more susceptible.

Regarding the three inventory subdomains (presented in section 2.2.2 and in Figure 5), the area occupied by moderate and high susceptibility grid cells reduces with decreasing resolution to the point that the map of 1 km pixels classifies more than half as "very low" and "low" susceptibility.

Table 2 Area (in km^2) occupied by each susceptibility class at the NW-Catalonia zone for the susceptibility maps based on the different mapping units. The percentage of the NW-Catalonia domain covered by each class is displayed in parentheses. Note that the total area occupied by hydrological subbasins is smaller than the area occupied by the rest of mapping units.

	Subbasins	Pixels 5 m	Pixels 30 m	Pixels 100 m	Pixels 200 m	Pixels 1 km
Very Low	0 (0%)	58 (6%)	64 (7%)	49 (5%)	50 (6%)	91 (10%)
Low	30 (3%)	103 (12%)	171 (18%)	187 (20%)	235 (25%)	463 (50%)
Moderate	319 (34%)	187 (20%)	292 (32%)	340 (37%)	399 (25%)	325 (35%)
High	501 (53%)	575 (62%)	402 (43%)	358 (38%)	253 (42%)	49 (5%)

2.4.3. Validation of the susceptibility maps

The resulting susceptibility maps have been evaluated using the landslide data that were not used for the calibration (i.e. retrieval of the membership functions and weights). The evaluation has been done with Receiver Operating Characteristics (ROC) curves (Fawcett 2006): For each susceptibility class, the false positive rate (fpr) and the true positive rate (tpr) have been computed, and the area under the curve (AUC) is the metric that has been used to assess the model performance. The AUC is a measure of how well a susceptibility classifier can distinguish between mapping units with and without landslide observations. The perfect discriminant is a susceptibility classifier that achieves an AUC equal to one. The larger the AUC, the better is the classification of the susceptibility map.
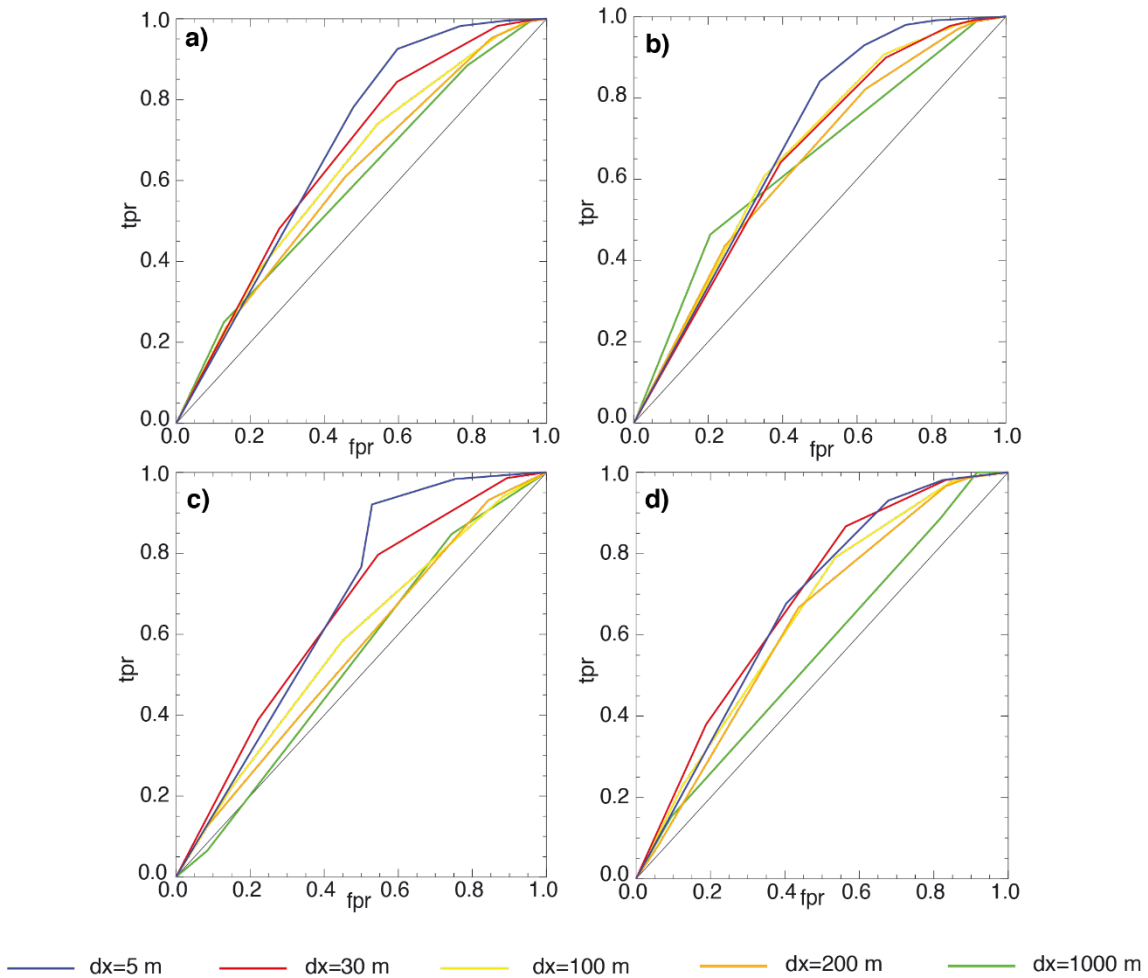
Figure 13. ROC curves of the 5 m, 30 m, 100 m, 200 m, and 1 km grid-cell based susceptibility maps at (a) NW-Catalonia, (b) NC-Catalonia zone. (c) NE-Catalonia zone and (d) all zones. The horizontal axis represents the false positive rate (fpr), the vertical axis represents the true positive rate (tpr).

Our results show that generally, the AUC of the grid-cell susceptibility maps slightly decreases with decreasing resolution. Combining the three inventory zones its AUC-values range from 0.59 to 0.67 (Figure 13 and Table 3). The smallest AUC is obtained for the susceptibility map based on 1 km grid-cells. In general, the results in the NC-Catalonia zone are the worst, with AUC values ranging from 0.52 to 0.56 (Figure 13 and Table 3). On the other hand, the region with the highest AUC values is the NW-Catalonia zone where the most complete and recent inventory is available.

Table 3 AUC values obtained from ROC analysis of the susceptibility maps based on the different mapping units. Values in bold are the highest AUC values in each inventory zone.

Pixel size [m]	AUC			
	All Zones	**NW-Catalonia**	**NC-Catalonia**	**NE-Catalonia**
Over the domain defined by grid-cells				
5	**0.67**	**0.68**	0.56	0.65
30	0.66	0.64	**0.66**	**0.67**
100	0.63	0.65	0.59	0.63
200	0.61	0.63	0.57	0.62
1000	0.59	0.65	0.52	0.55
Over the domain defined by subbasins				
5	**0.66**	**0.67**	0.59	0.67
30	0.65	0.64	**0.66**	0.67
100	0.62	0.66	0.58	0.64
200	0.61	0.63	0.55	0.62
Subbasins	0.63	0.63	0.58	**0.69**

The comparison of grid-cell based susceptibility maps that cover all the analysed domain, and subbasin-based susceptibility maps that cover only part of it is challenging. To do so, pixel-based maps have been clipped with the catchments polygons. The resulting grid-cell susceptibility maps covered the same area as the subbasin susceptibility maps and were validated using ROC analysis.

Consistently, the AUC of the clipped grid-cell susceptibility maps decreases with decreasing resolution. The smallest AUCs of the clipped grid-cell and the subbasin-based susceptibility maps are obtained in the NC-Catalonia domain (Table 3). As it can be seen in Figure 14 and Table 3 the subbasin-based map performance is slightly better than the performance of 100 m grid-cell susceptibility map and it only achieves a smaller AUC in the NW-Catalonia zone.
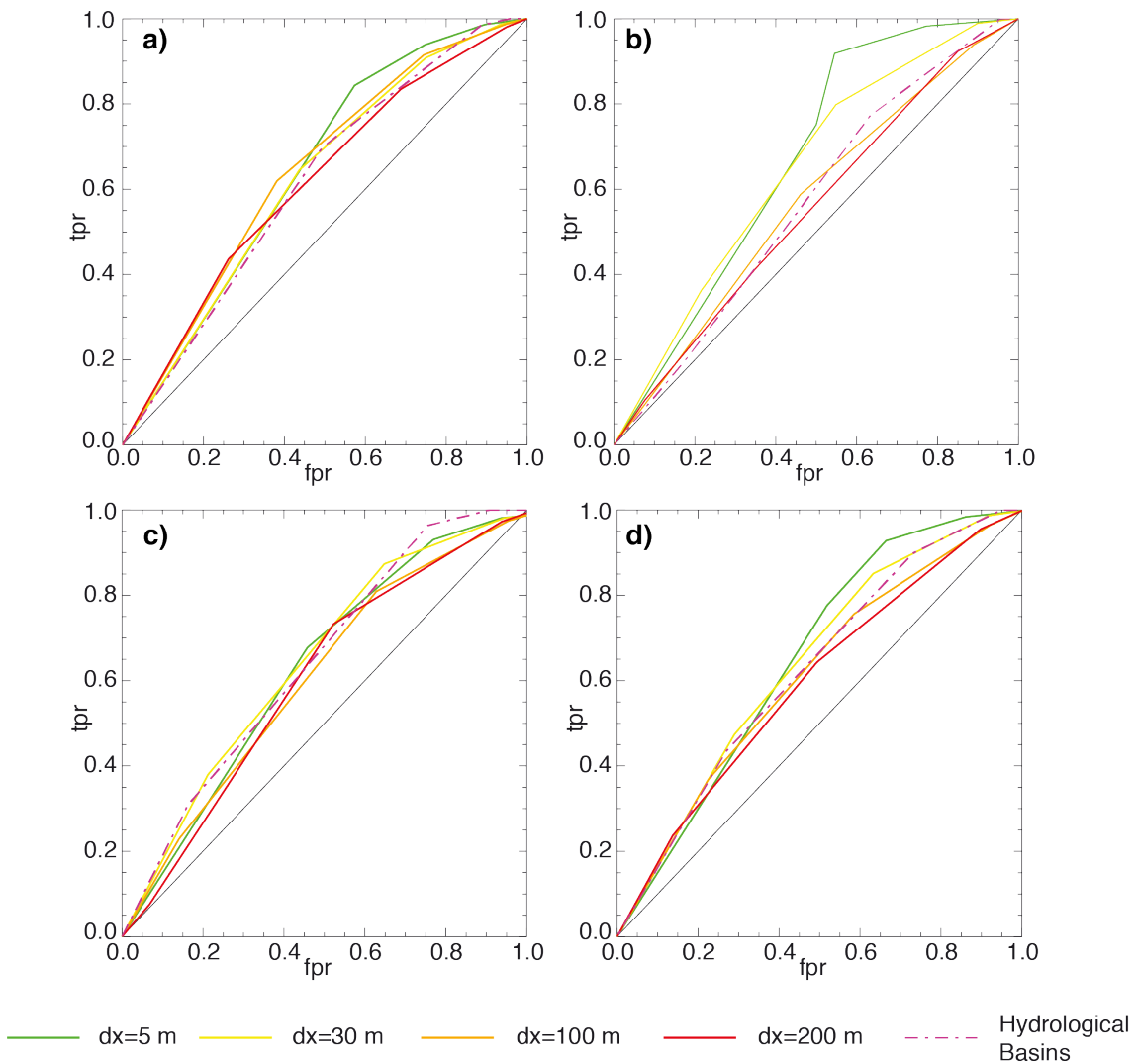
Figure 14. ROC curves comparing the performance of the susceptibility maps over the area occupied by hydrological catchments. (a) NW-Catalonia, (b) NC-Catalonia, (c) NE-Catalonia, (d) three inventory zones. The horizontal axis represents the false positive rate (fpr), the vertical axis represents the true positive rate (tpr).

Therefore, for both, the domain defined by grid-cells and the domain defined by subbasins, the best susceptibility map is the one based on 5 m resolution pixels. The poor results obtained in the NC-Catalonia zone can be, at least partly, explained by the lower quality of the landslides inventory in this domain (especially in the accuracy of the landslides location). Apart from the map based on 1 km grid-cells, the obtained susceptibility maps have an acceptable performance and could therefore be used for LEWS.

2.5. Performance of the LEWS with the different mapping units

In this section, the LEWS presented in Section 3 has been run from April to October 2010 to analyse the effect of the mapping units on the landslide warnings over Catalonia. With this aim, the LEWS has been set up using the different mapping units for which the susceptibility maps have been obtained in section 2.4. Specifically, the analysed mapping units are (i) 30 m grid-cells, (ii) 200 m grid-cells, and (iii) hydrological subbasins. Running the LEWS using 5 m grid cells is still computationally too expensive and this configuration has been discarded in this part of the analysis. The LEWS time resolution is 30 min for all the tested set-ups.

The performance of the LEWS with the different configurations has been analysed in terms of (i) the number of days with warnings for the different mapping units, (ii) its ability to identify the occurrence of specific events that took place during the studied period and for which the exact or approximate triggering time is known. Finally, some discussion about the computational cost to run the LEWS with the different mapping units is provided.

2.5.1. Number of warnings during the studied period

The total number of days during which "moderate" or "high" warning levels were issued at least once for each mapping unit is summarized in Figure 15. The results show that the areas where these warnings were issued coincide with the zones of "high" susceptibility mostly located in the Pyrenees and Pre-Pyrenees.

The 30 m grid-cells configuration issued a "moderate" or "high" warning level during more than six days in over 0.09 % of Catalonia (Table 4). This percentage of area is higher for the setup using hydrological subbasins (0.36 %). On the other hand, the 200 m resolution grid-cells configuration issues "moderate" or "high" warning level only in around 0.01 % of Catalonia.
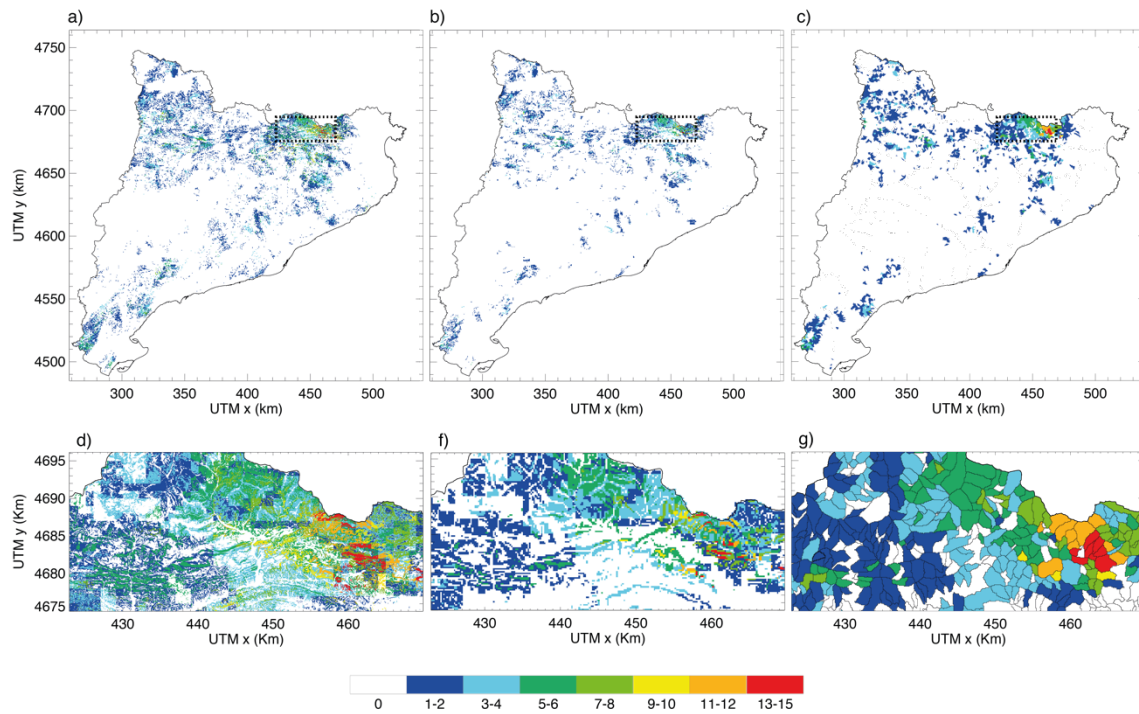
Figure 15. Number of days of the period April-October 2010 during which "moderate" and "high" warning levels where issued (at least for a 30-minutes time step of the day). (a) pixels of 30 m, (b) pixels of 200 m, and (c) subbasins. A zoom into the area enclosed by the black dashed rectangle is portrayed in (d), (e) and (f) for the 30 m, 200 m and subbasins mapping units respectively.

The validation of the results of the LEWS in Catalonia is challenging because the areas with a large number of days with warning are mainly located in highly inaccessible mountainous regions. When an event occurs, it is hardly reported because typically no infrastructures, buildings or roads are affected, and no multi-temporal landslides inventories are available.

The number of days with warnings is a qualitative result that gives an idea that the number of false positives is reasonable: warnings are generally located in the most susceptible areas that were affected by important rainfall amounts, and are issued at most 15 days of the 214 days that comprise the analysed period. Alternatively, to evaluate the LEWS results using the different mapping units, we have focused on some specific catchments where landslide reports were available during the analysed period.

Table 4 Percentage of Catalonia with 1 to 2, 3 to 5, 6 to 10 and more than 11 days with "moderate" or "high" warning level for three different mapping units.

	Domain Area [km^2]	Percentage of Catalonia area with Moderate or High warning level			
		1-2 days	3-5 days	6-10 days	11 days or more
dx = 30 m	32030	7.52	1.59	0.09	0.01
dx = 200 m	32248	2.54	0.37	0.01	0.00
Subbasins	23048	13.99	3.12	0.36	0.01

2.5.2. Validation in specific sites

The performance of the LEWS with the different setups has been analysed in two catchments where debris flows have been detected during the analysed period of 2010. These two monitored catchments (Rebaixader and Erill) are both located in the NW-part of Catalonia (Figure 5).

Although the Rebaixader catchment is relatively small (0.80 km^2), it is one of the most active torrents in the Catalan Pyrenees and has been monitored since 2009 (Hürlimann et al. 2014). The debris-flows initiation zone is located in a steep scarp in a lateral moraine. The catchment sediment supply is assumed to be almost unlimited. During the analysed period, the monitoring system recorded the second largest debris flow since 2009 (on 11 July 2010, with an estimated volume of 12500 m^3) and also two debris floods that mobilized smaller volumes (on 21 July and 9 October 2010).

The Erill catchment, with a drainage area of 3.30 km^2, is close to the Rebaixader and the outcropping material is similar. A monitoring station was installed in 2005 (Raïmat Quintana 2018) and detected one debris flow during the studied period (on 22 July 2010).

The LEWS outputs show that the events reported during the 7-month period in the two catchments mentioned above are generally associated with "moderate" or "high" warning levels (the results are summarized in Table 5 and Figure 16).

Table 5 Reported debris flows and/or debris floods at the Rebaixader and Erill catchments and maximum warning level issued by the LEWS during each of the rainfall episodes.

Subbasin	Subbasin susceptibility class	Reported events	Type of event	Maximum Warning Level		
				dx= 30 m	dx= 200 m	Subbasins
Rebaixader	High	11 July 2010	Debris flow	High	High	High
		21 July 2010	Debris flood	Low	Low	Low
		09 October 2010	Debris flood	Low	Moderate	Moderate
Erill	High	22 July 2010	Debris flow	High	High	Moderate

In the Rebaixader catchment, the three recorded events were triggered by rather intense rainfall episodes. All the LEWS configurations determine "moderate" or "high" warning levels, for the 11 July 2010 debris flow and the 9 October 2010 debris flood (Table 5 and Figure 16a, and c). However, the LEWS was not able to issue a warning for the 21 July 2010 rainfall event, when a small debris flood was detected (Table 5 and Figure 16b), because the rainfall intensities were just below the "very low"- "low" threshold.
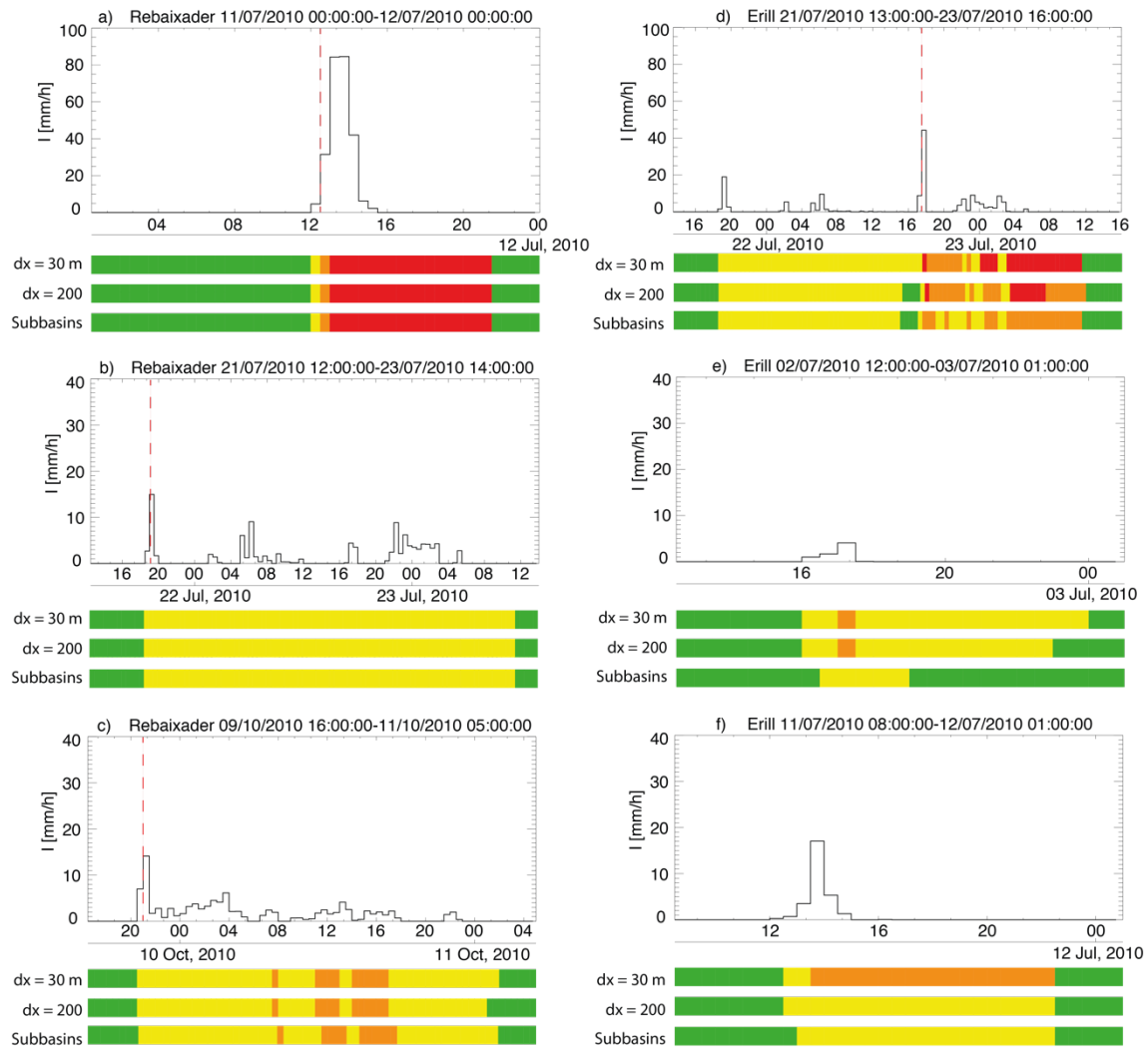
Figure 16. Site-specific validation of the LEWS. At the Rebaixader monitoring site: (a) 11July 2010 debris flow, (b) 21 July 2010 debris flood, (c) 9 October 2010 debris flood. At Erill: (d) 22 July debris flow; and the two rainfall events that did not turned on the monitoring system and (e) 2 July 2010 (f) 11 July 2010. The black line represents the 30-min rainfall intensity observed by the weather radar. The horizontal colour bars show the maximum warning level time series observed within the catchment for the analysed mapping units. Green, yellow, orange and red represent warning levels "very low", "low", "moderate" and "high", respectively. The red dashed line indicates the time when the debris flow or debris flood was detected by the monitoring station.

Similarly, in the Erill catchment the recorded debris flow was triggered by intense rainfall. The LEWS results show that both grid-cell configurations identify the event with a "high" warning level and the subbasins configuration identifies it with a "moderate" warning level (Figure 16d and Table 5).

The number of recorded events at Rebaixader and Erill have been compared with the number of days that achieved a maximum warning level of "moderate" or "high" classes (Table 6). The LEWS performance at these two specific catchments has been assessed by

calculating the true positives, false positives, and misses, using the subbasin where the sensors where installed as the mapping unit for evaluation. True positives are defined as the number of rainfall events during which the monitoring systems detect a debris flow or debris flood and the LEWS issues a "moderate" or "high" warning level within the catchment. False positives are rainfall events with a "moderate" or "high" warning within the catchment, but during which no landslide event is detected. Misses are rainfall events during which the monitoring systems record a debris flow or debris flood, but the LEWS is not switching into a moderate or high warning in any mapping unit.

Table 6 Evaluation of the performance of the LEWS for the Rebaixader and Erill monitored sites. The number of recorded debris flows and debris floods can be compared with the number of days with maximum warning level "moderate" or "high". True positives are rainfall events with correct warnings, false positives are rainfall events with "moderate" or "high" warnings but no detected landslide, debris flow or debris flood event. Misses are rainfall events with landslides, debris flows or debris floods but no "moderate" or "high" warnings.

Monitoring site	Mapping Unit	# of days with maximum warning level				#events detected	True Positives	False Positives	Misses
		Very Low	Low	Moderate	High				
Rebaixader	dx = 30 m	148	64	1	1		2	0	1
	dx = 200 m	150	62	1	1	3	2	0	1
	Subbasins	150	62	1	1		2	0	1
Erill	dx = 30 m	146	66	2	2		1	2	0
	dx = 200 m	146	66	1	2	1	1	1	0
	Subbasins	152	60	2	0		1	0	0

In the analysed catchments all the tested configurations have the same number of true positives and misses. However, the number of false positives seems to increase with the resolution of the mapping unit, particularly in Erill (Table 6). The difference in the number of false positives between both 30 m and 200 m grid-cell mapping units are due to the larger area classified as "highly" susceptible in the 30 m grid-cell map at the Erill catchment (Figure 17a and Figure 17b).

The false positives at Erill have been further examined. Our analysis shows that the significance of the false positives depends on the area (number of pixels) of the subbasin where a "moderate" or "high" warning level is issued and its location. Since the monitoring station is located at the catchment outlet, small landslides or debris flows happening near the headwaters and traveling short distances are perhaps not detected. Therefore, false positives due to a few headwaters' pixels with "moderate" or "high" warnings are not very significant. In contrast, a false positive is more relevant if pixels with "moderate" or "high" warnings are located close to the outlet or affect a large portion of the catchment.

During the analysed period, a false positive with low significance was issued for the 11 July 2010 event by the 30 m grid-cell configuration at the Erill (Figure 16 f), when a moderate warning was released. However, the moderate warning was caused by a very small area (4 % of the entire basin) located in the highest part of the catchment, where the radar recorded larger amounts of rain (Figure 17 g). In addition, the grid-cell configurations issued another false positive that affected a portion of the Erill catchment near the outlet (Figure 17 d and e) during the event of the 2 July 2010. However, the area over which both configurations issued the warning was different. On the one hand, the 200 m grid-cell set-up issued "moderate" warnings over only a 1.3 % of the catchment area, therefore its significance was low. On the other hand, the 30 m grid-cell set-up issued "moderate" warnings over a larger area (4.8 % of the subbasin), therefore its significance was larger.
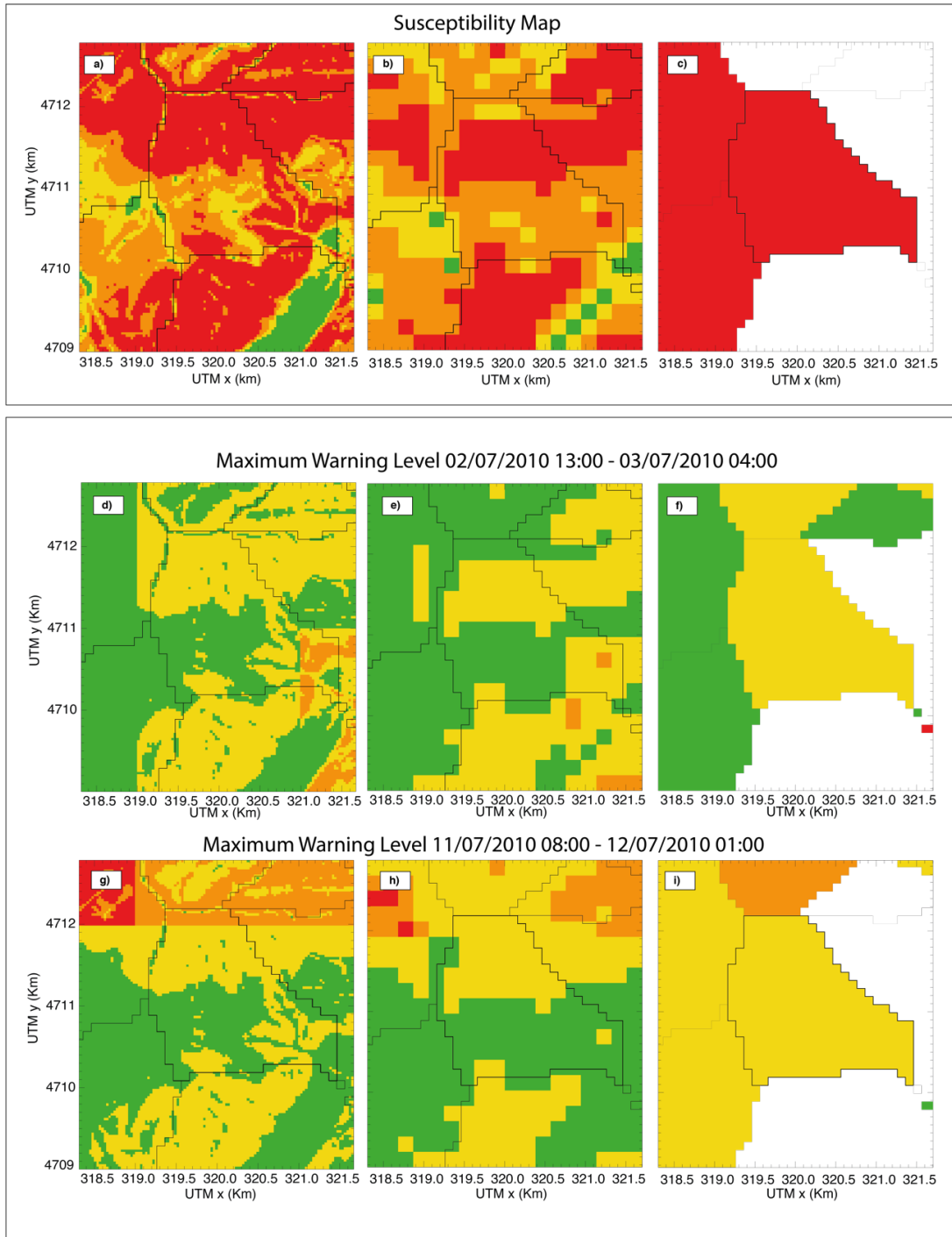
Figure 17. Analysis of false positive warning issues at Erill. The top panel displays the susceptibility map based on (a) 30 m, (b) 200 m grid-cells, and (c) subbasin mapping units. Middle panel shows the maximum warning level for the three mapping units at Erill during the 2 July 2010 rainfall event. Bottom panel presents the maximum warning level for the three configurations during the July 11 July2010 rainfall. See text for detailed explanations.

Additionally, the outputs of the three LEWS configurations have also been checked for the reported events in two supplementary unmonitored catchments, where three events were reported: Portainé and Santa Maria (Figure 5). The Portainé catchment has an area of 2.50 km². Two debris flow events affected a secondary road and a small dam located

49

downstream, one occurred on the 22 of July 2010 with a mobilized volume of 25000 m^3, and a smaller one on 12 August 2010 (Palau et al. 2017). The Santa Maria is a 1.70 km^2 catchment located in the mountain of Montserrat. Shallow slides and debris flows were reported there by road and railway managing authorities during the night of 10 October 2010.

The 30 m gridded setup was able to correctly issue a "moderate" or "high" warning level coinciding with the approximate time of the events in Portainé and Santa Maria (Table 7). On the other hand, the 200 m setup failed to issue a warning for the Portainé 22 July 2010 debris flow, and the subbasin setup missed both events at Portainé. The computation of the total number of true positives, false positives and misses has not been possible for these two sites because only the events that affected important infrastructures were reported.

Table 7 Reported debris flows, debris floods and/or shallow slides at the Portainé and Santa Maria catchments and maximum warning level issued by the LEWS during each of the rainfall episodes.

Subbasin	Subbasin susceptibility class	Reported events	Type of event	Maximum Warning Level		
				dx= 30 m	dx= 200 m	Subbasins
Portainé	Moderate	22 July 2010	Debris flow	Moderate	Low	Low
		12 August 2010	Debris flow	High	Moderate	Very Low
Santa Maria	High	10 October 2010	Debris flow & shallow slides	High	Moderate	Moderate

In summary, the results obtained with the different configurations of the LEWS are quite similar and show coherence. The main difference is the lower number of false positives obtained with the subbasin setup. However, the 200 m grid-cell and the subbasin configurations also present additional misses at Portainé (Table 7). It is worth noticing though, that one of the 30 m grid-cell configuration false positives is issued over a very small area at the catchments headwaters and therefore its significance is low.

2.5.3. Computational requirements

One of the criteria that strongly influences the feasibility to apply the LEWS in real time at regional scale is the computational cost, which should allow us to update the warning level every time new rainfall observations are available within a short time. Herein, we have analysed the computational cost to run one time step over Catalonia with the different configurations analysed in this section 2.5.

To fulfil the computations, we have used a server with two 12-cores 3.5 GHz CPUs and 48 GB of RAM. With the current version of the code, the time needed to fulfil one time step over the entire Catalonia is around 1.5 min, 2.9 s, and 0.7 s for the case of 30 m, 200 m grid-cells and subbasins respectively. The computational cost increases with the area of the domain covered by rain. In either case, the three mapping units could be used to compute warnings operationally. In section 2.4 we have decided that it is not yet feasible to run the 5 m grid over Catalonia because with the current version of the codes completing the calculation of one time-step through Catalonia requires around 50 min, still far from real-time requirements.

2.6. Discussion and conclusions

This study assesses the influence of the mapping unit into the outputs of a regional scale LEWS with the aim of selecting the most suitable mapping unit for a real-time LEWS for Catalonia. Susceptibility maps covering Catalonia have been obtained combining the maps of slope and land cover with a fuzzy logic approach. This simple methodology has been applied to obtain and compare susceptibility maps based on different mapping units (pixels of several resolutions and hydrological subbasins), which have been applied to run a LEWS method in the region of Catalonia during seven months of 2010.

The evaluation of the susceptibility maps has been done using part of the inventory available in three subdomains in the Catalan Pyrenees and Pre-Pyrenees. The results show that for the gridded susceptibility maps, its quality decreases with resolution, whereas the one obtained on a subbasin division performs slightly better than the map based on pixels of 100 m resolution.

The analysis of the performance of the LEWS with the studied mapping units shows that landslide warnings were generally located at susceptible areas affected by large rainfall amounts. Results show that the area where the warnings were issued increases with the mapping unit resolution for the grid-cell set-ups but is higher for the subbasins configuration. Due to the lack of systematic landslide reports, the evaluation of the performance remains a challenge and has been done for specific locations with reported shallow slides and debris flow events. The subbasin setup has failed to issue a warning for three landslides that were recorded at the selected sites. The number of misses decreases with the resolution. While the 200 m grid-cell configuration misses two landslide events, the30 m grid-cell setup misses only a debris flood but has an additional false positive. However, its significance is rather low.

Regarding the computational cost, as expected, the high resolution configurations are more demanding than the coarser configurations. Regardless of that, with the exception of 5 m grid-cells, all the studied configurations could be applied in real time.

Choosing the most appropriate mapping unit for operational LEWS purposes is not trivial. It must include a compromise between performance, resolution and computational cost, whereas it must also consider the end-users' interpretability of the warnings. In this sense, at a regional scale the interpretation of the warnings is much easier for the subbasins configuration. However, grid-cell configurations have a higher resolution and display the possible landslide initiation zones with more detail.

Based on the results obtained for the analysed period and monitored sites (a more extensive evaluation over longer periods of time and with a larger number of landslide reports would be required to make the results more conclusive), the best option may be working with 30-m grid cells to compute the warnings and present them in subbasins displaying the maximum warning level of the enclosed pixels. This approach simplifies the assessment at regional scale without losing the extra information contained in the pixel data. If a warning is issued for a given catchment, detailed information on the possible landslide triggering areas can be displayed when zooming into it. Thus, this solution enhances the understanding of the situation and enables to allocate the available resources in the most problematic places. A similar solution has been adopted in the SIGMA model (Segoni et al. 2018a) where three types of mapping units are used (alert zones, municipalities and 100 m grid-cells).

One aspect that is fundamental to guarantee the performance of the LEWS is the quality of the rainfall inputs. In this regard, the use of radar QPE has clear advantages (i.e. good depiction of the variability of the rainfall field at high spatio-temporal resolutions), but it also needs careful processing of radar observations to guarantee the quantitative value of the rainfall products (e.g. Zawadzki 1984; Corral et al. 2009; Borga et al. 2014), since global or local biases of the rainfall field have a direct effect on the performance of the LEWS (it may lead to false positives and misses). It is also worth noting that the spatial resolution of the rainfall inputs (1 km) is much coarser than that of the LEWS (which matches the resolution of the susceptibility map). This difference, which can be seen in Figure 17, implies that the small-scale variability of the rainfall field cannot be resolved and an adds uncertainty in the performance of the LEWS.

A limitation of the current LEWS methodology is the lack of well-established rainfall thresholds in Catalonia. Therefore, IDF-curves of a meteorological station were used to determine the rainfall hazard level. However, future advances on critical rainfall conditions in Catalonia would certainly improve the performance of the LEWS. An additional drawback is that the current thresholds account for neither the antecedent rainfall nor soil moisture conditions. Using regional rainfall thresholds for landslides, as well as including antecedent rainfall or soil moisture information could help reducing the number of false positives and therefore improve the performance of the LEWS (Bogaard and Greco 2018; Mirus et al. 2018b).

Another important factor that could help improve the performance of the LEWS would be the distinction between weathering limited and sediment unlimited catchments. Weathering limited catchments require a certain period between debris-flow events to recharge the available sediment. Currently the input susceptibility maps are static, and therefore, this condition is not considered by the LEWS

Additionally, since most shallow slides and debris flows happen during or shortly after the triggering rainfall event to issue effective early warnings the presented methodology should be implemented in real-time using rainfall forecasts (Alfieri et al. 2012), for instance based on radar nowcasts (e.g. Berenguer et al. 2011) or high-resolution numerical weather prediction.

Chapter 3

EVALUATION OF A REGIONAL-SCALE LANDSLIDE EARLY WARNING SYSTEM DURING THE JANUARY 2020 GLORIA STORM IN CATALONIA (NE SPAIN)

3.1. Introduction

Multiple-occurrence regional landslide events (MORLEs) are defined as hundreds of individual landslides occurring almost simultaneously over large areas (Crozier 2005). Usually, MORLEs are constituted by shallow slides or flows that are triggered in steep slopes by intense rainstorms or earthquakes. MORLEs have been described in different regions around the globe, such as New Zealand (Crozier 2005), Taiwan (Yu et al. 2006), China (Yang et al. 2020), USA (Campbell 1975; Whittaker and McShane 2012), Switzerland (Nicolet et al. 2013), or Italy (Crosta and Frattini 2003; Lombardo et al. 2018).

Several MORLEs also happened in the region of Catalonia (NE Spain) in the past: October 1940 (Portilla 2014), August 1963 (Portilla 2014), November 1982 (Gallart and Clotet 1988; Corominas and Alonso 1990), June 2008 (Portilla et al. 2010)or June 2013 (Shu et al. 2019). These MORLEs mainly affected the Pyrenees and Pre-Pyrenees and were associated with severe rainfall events and flooding. Most recently, from 20 to 23 January 2020, an extraordinary E-NE cyclonic storm (named Gloria) affected the region of Catalonia. The significant and widespread Gloria storm rainfalls triggered multiple landslides, especially in the Montseny (Fig. 1).

The high number of landslides and the large area affected by MORLEs normally suppose a challenge to the authorities in charge of managing the risk and the maintenance of roads

and railways. In this context, regional landslide early warning systems (LEWS) may help to identify the time and location where landslides are most likely to occur and increase their preparedness (Alfieri et al. 2012; UNISDR 2015).

In the last 20 years, regional landslide early warning systems have been developed covering multiple regions, e.g., Southern California (Baum and Godt 2010), Rio de Janeiro (Calvello et al. 2015b), Indonesia (Hidayat et al. 2019), Hong Kong (Lloyd et al. 2001), Japan (Osanai et al. 2010), the province of Zhenjiang province in China (Yin et al. 2008), Norway (Krøgli et al. 2018), the Emiglia-Romagna and Campania regions in Italy (Piciullo et al. 2017b; Segoni et al. 2018a), and Catalonia in Spain (Berenguer et al. 2015; Palau et al. 2020). Usually, LEWS determine the areas that are prone to landslides employing susceptibility maps and assess whether a rainfall event might trigger a landslide using rainfall thresholds (Aleotti 2004; Guzzetti et al. 2007; Papa et al. 2013; Rossi et al. 2017; Pan et al. 2018). The majority of LEWS use rain gauge data to assess the rainfall hazard. However, in many cases, the density of rain gauge networks is low, and landslide triggering rainfalls tend to be underestimated (Nikolopoulos et al. 2014). Other LEWS use remote sensing data such as satellite or ground-based radar rainfall products (Berenguer et al. 2015; Rossi et al. 2017; Kirschbaum and Stanley 2018).

LEWS need regular and systematic performance analysis to assure the reliability of the models. Up to the date, research has mainly focused on the validation and improvement of rainfall thresholds (Gariano et al. 2015; Brunetti et al. 2018) and susceptibility maps (Kirschbaum et al. 2016). Only a few studies have put their attention in back-analysing the output warnings and its correspondence with reported landslides. Calvello and Piciullo (2016) and Piciullo et al. (2020) proposed the EDUMAP method for the evaluation of regional-scale LEWS. This methodology considers the possible occurrence of multiple landslides within a warning zone and takes into account the relation between the duration of the warning and the landslide reporting time. However, applying this methodology when the landslide inventory is incomplete and the location and triggering time of the landslides are uncertain, is not straightforward. Especially if warning zones are small. Kirschbaum et al. (2009) and Park et al. (2020) proposed using a neighbouring window to determine the performance of regional-scale LEWS. In this line, fuzzy verification methods have long been employed to assess the performance of mesoscale high-resolution precipitation forecasts (Brooks et al. 1998; Atger 2001; Damrath 2004; Roberts and Lean 2008; Ebert 2008) and could be applied for the evaluation of LEWS

performance. Fuzzy verification methods analyse how do the evaluation results change when relaxing the condition of co-localization between simulations and observations (i.e. warnings and landslide inventory points).

Having landslide inventories that are complete in space and time is crucial to establish reliable LEWS and to evaluate their performance. Historically, landslide inventories were collected focusing on small areas from the interpretation of aerial photographs, remote sensing data, field surveys and local reports (Galli et al. 2008; Guzzetti et al. 2012). Alternatively, inventory data can be obtained from data sources such as newspapers reports, and crowdsourcing (Guzzetti et al. 1994; Kirschbaum et al. 2010; Ekker et al. 2013; Juang et al. 2019). However, these inventories are often incomplete and usually biased to landslides that affected urban areas or infrastructures (Ardizzone et al. 2002).

The large number of landslides that were reported during the Gloria storm gives us a unique opportunity to analyse the performance of the existing landslide early warning system for the region of Catalonia. To do so, we propose to apply a fuzzy verification method using several neighbouring window sizes. The objectives of the study are: (i) to analyse the Gloria storm rainfall event and the landslides that were triggered, (ii) to assess the performance of the LEWS during the Gloria storm.

3.2. General settings

Catalonia is located in the NE of the Iberian Peninsula and covers an area of around 32000 km^2. From a geological point of view, Catalonia is part of the Iberian Plate. Its orography (Figure 18) is the result of (i) the collision between the Iberian Plate, the European plate and the African Plate that formed the Pyrenees with peaks over 3000 m asl., the Catalan Coastal Range and the Iberian Range during the Paleogene; (ii) the later deposition of sediments in the Ebro Basin; and (iii) the reactivation of the pre-existing Paleogene faults in an extensive context during the Miocene forming a series of horst and grabens more or less parallel to the actual coastline (Berastegui et al. 2010).
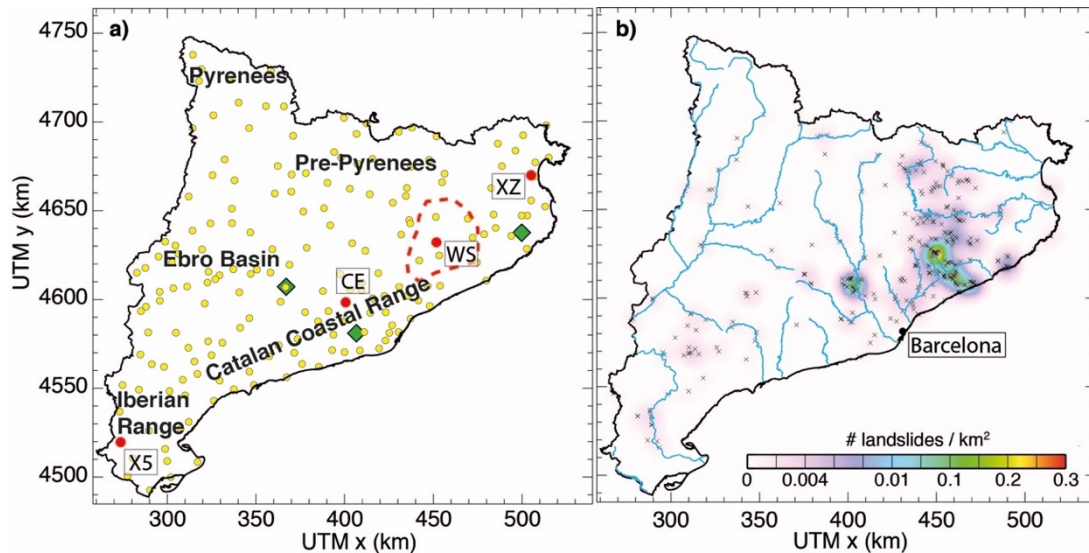
Figure 18. (a) General overview map of Catalonia. The green diamonds show the location of the weather radars and yellow circles the 183 rain gauges. The four red circles show the location of the Viladrau (WS), PN dels Ports (X5), Torroela de Fluvià (XZ), and Els Hostalets de Pierola (CE) rain gauges. The red dashed polygon portrays the location of the Montseny area. (b) Density map of the landslides triggered by the Gloria storm and gathered in the inventory. The black crosses represent the landslide points of the ICGC and the #Esllavicat inventories. The main rivers are represented as blue lines. The location of Barcelona is indicated with a black circle.

Catalonia's climate is varied, but can be classified as Mediterranean (Emberger 1952). Near the coast, the weather is mild and temperate, with a mean annual temperature of 17 °C. Inland, the climate is continental with cold winters, hot summers and less abundant precipitation. The Pyrenees present a high-altitude climate with abundant snow and temperatures below 0 °C during winter. The rainiest seasons are generally spring and autumn, except for the Pyrenees, where the rainiest season is summer. The mean annual rainfall ranges from less than 400 mm in some parts of the Ebro Basin to over 1200 mm in the Pyrenees. In Catalonia, the 10-year return period 24 h rainfall accumulation commonly exceeds 100 mm (Clavero et al. 1996). Daily accumulations of over 200 mm can be regularly seen at least once a year in the coastal area (Martín Vide and Olcina Cantos 2001). The Gloria storm was a rather unusual event of heavy rains during the driest months of the year.

Landslides are generally triggered by either (i) convective rainfall events with high intensities, typical from mid-summer to early autumn, and (ii) long-lasting rainfalls with moderate intensities, common during spring, and autumn (Corominas et al. 2002; Abancó et al. 2016). The Gloria storm rainfalls happened during winter, but still triggered a significant number of landslides.

58

3.3. Description of the Gloria storm

From 20 to 23 January 2020 the Gloria storm affected the region of Catalonia, causing several different hazards such as storm surges, erosion of beaches in coastal areas, floods and landslides. According to the OCCC (Canals and Miranda 2020), the economic losses due to these impacts exceeded 500 million euros. The Gloria storm was exceptional, because it took place during winter, an unusual season for torrential rainfalls in this area, and also because of its long duration.

This section presents the meteorological situation and analyses the rainfall accumulations and the landslides triggered by the Gloria storm.

3.3.1. Meteorological situation

On 18 January 2020, a cold front coming from the North Atlantic entered through the North West of the Iberian Peninsula and moved South towards the Mediterranean Sea. On the British Isles, an unusual anticyclonic situation recorded pressures up to 1050 hPa, the highest pressure since 1957 (Servei Meteorològic de Catalunya 2020a). This high had an elongated shape from East to West and covered a large part of central Europe.

The Gloria storm was the result of the combination of the unusual high pressures on the British Isles and the low located on the south of the Iberian Peninsula. The gradient of pressures between these two centres caused strong East-Northeast winds, and provided a high humidity and abundant and widespread precipitation (Servei Meteorològic de Catalunya 2020b). The duration of the Gloria storm was long because the North Atlantic cold-air mass was stationary over Catalonia for several days.

3.3.2. Rainfall analysis

The rainfall datasets used in this study consist of the measurements of 187 tipping bucket rain gauges from the Meteorological Service of Catalonia (SMC), and the quantitative precipitation estimates (QPEs) from the composite of the observations of the SMC radar network (XRAD). The location of the rain gauges and the radars is portrayed in Figure 18 a.

Radar QPEs have been produced from the volume-scans of Creu del Vent, La Panadella, and Puig d'Arques C-band single-polarisation Doppler radars of the SMC with the Integrated tool for Hydrometeorological forecasting (EHIMI, Corral et al. 2009). The EHIMI tool includes a chain of quality control, correction, mosaicking and accumulation algorithms to generate QPE products from raw radar observations. The product used here is the 30-min precipitation accumulation field with a spatial resolution of 1 km.

Rain gauge measurements and radar observations have been combined to obtain an improved QPE applying the method proposed by Velasco-Forero et al. (2009) and Cassiraga et al. (2020). This method employs a geostatistics technique known as kriging with an external drift (KED) to interpolate the rain gauges observations using radar rainfall as a secondary variable that provides the drift to the rainfall field between rain gauges. As shown by Velasco-Forero et al. (2009) this method benefits from the direct surface rainfall observations of the rain gauges located within the study area, and the radar description of the spatiotemporal variability of the rainfall field.

Figure 19 presents the daily precipitation accumulations from 20 to 23 January 2020. The evolution of the Gloria storm and the spatiotemporal variability of the rainfall field can be observed in these plots. It also shows the locations of landslide reports in relation to the rainfall.

The storm began on 20 January 2020 when snow and rain were observed in the Northeast and the South (Figure 19 a). On 21 January 2020, precipitations fell over the entire region. Still, they were more abundant parallel to the coastline, where the 24 h rainfall accumulations exceeded 200 mm at the Montseny area and the Iberian range (Figure 19 b). During 22 January 2020 rainfall fell intermittently over most of Catalonia. More than 140 mm were accumulated in the Montseny area (Figure 19 c). Additionally, important rainfall accumulations were recorded at the southwest of Catalonia, the Pyrenees, and the Pre-Pyrenees. The main precipitation system moved towards the North during the morning of 23 January 2020. Rainfall fell intermittently with moderate and low intensities. Although rainfall accumulations were not as relevant as the previous days (Figure 19 d), they were still significant in the Montseny area, where over 100 mm were recorded in some areas, and in the Pre-Pyrenees.
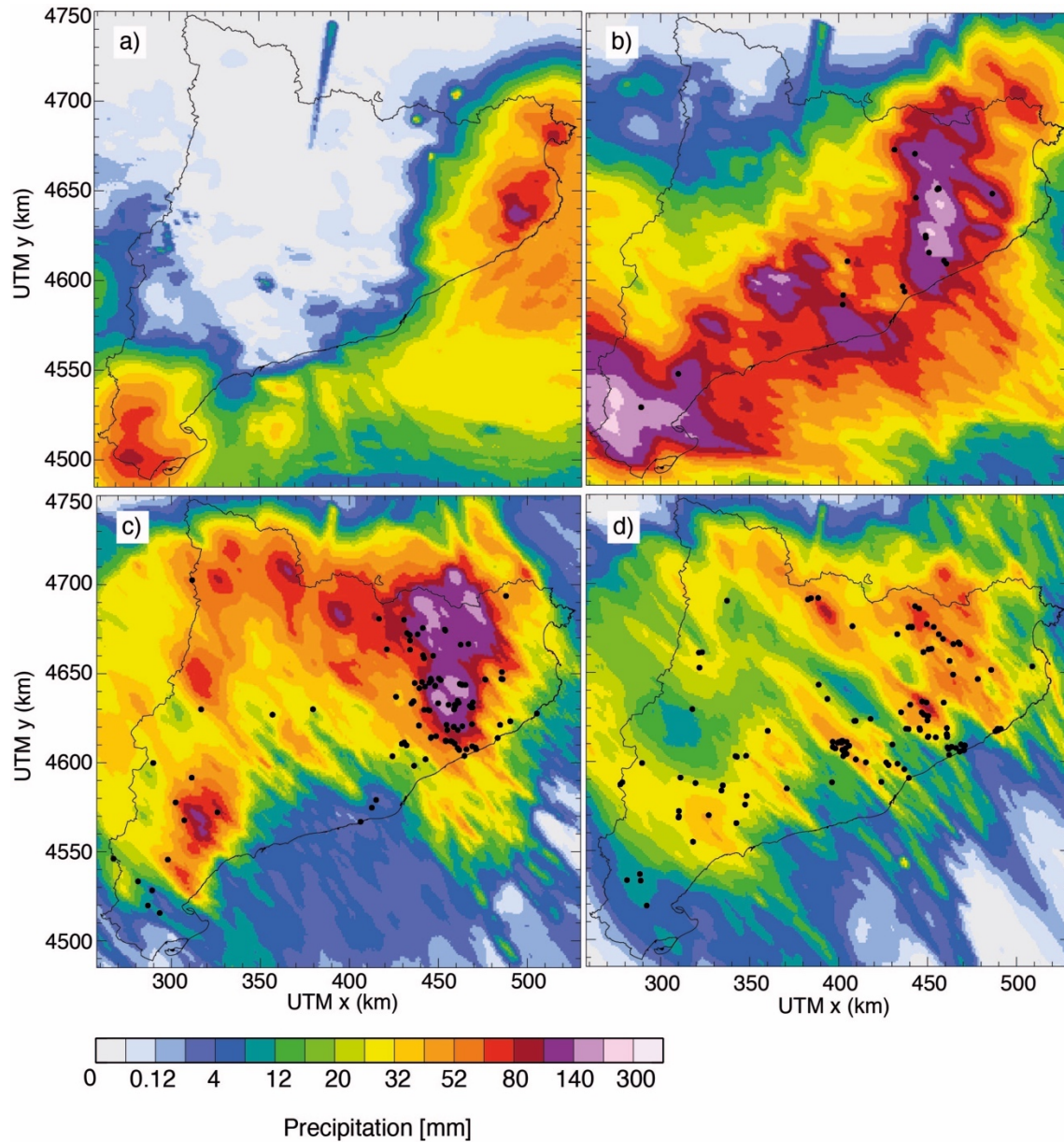
Figure 19. Daily rainfall accumulations during the Gloria storm: (a) 20 January 20202, (b) 21 January 2020, (c) 22 January 2020, (d) 23 January 2020. Black circles represent the landslides included in the inventory each day. In the following sections, more details.

The total accumulated rainfall during the four days was significant over most of Catalonia (Fig. 3 a). The largest rainfall amounts fell over the North-East, with around 480 mm in the Montseny area.

During the first day of the Gloria storm, no landslides were reported. In the following days, the areas that recorded the highest rainfall accumulations coincide rather well with the places where landslides were reported (black circles in Figure 19 and Figure 20).
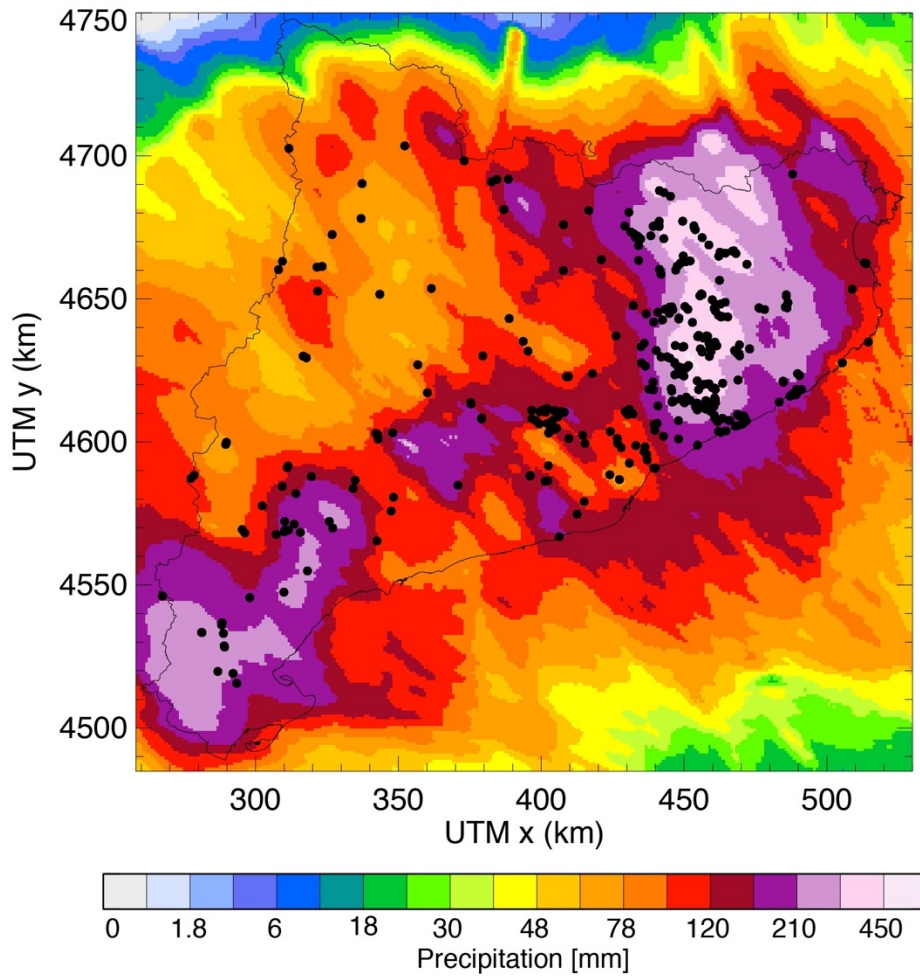
Figure 20. Accumulated rainfall from the 20 January 2020 00:00 to the 23 January 2020 24:00. The black circles represent the landslides included in the ICGC and the #Esllavicat inventories.

3.3.3. Analysis of the quality of the precipitation estimates

This section presents an analysis of the quality of the precipitation estimates obtained applying the KED method. The performance has been evaluated by leave-one-out cross-validation using the observations at the rain gauges as the reference. To do so, we have applied the KED method removing one of the rain gauges from the calculation to estimate the rainfall at the location of the removed rain gauge. Then, we have compared the estimated value with the observed rainfall. This process has been repeated for every 30 minutes and each of the 187 considered rain gauges.

Figure 21 shows the comparison between the event precipitation accumulations obtained from cross-validation and the event accumulations observed at each of the rain gauges. Additionally, four statistics have been added to the scatter plot; the bias, the standard

deviation of the error (SD error), the root mean squared error (RMSE) and the root mean squared relative error (RMSR). The event KED estimates generally show a good agreement with the event accumulations recorded at rain gauges. The SD of the error and the RMSE are similar, around 31 mm, therefore, the bias is rather low. And the event RMSR of 22 %.
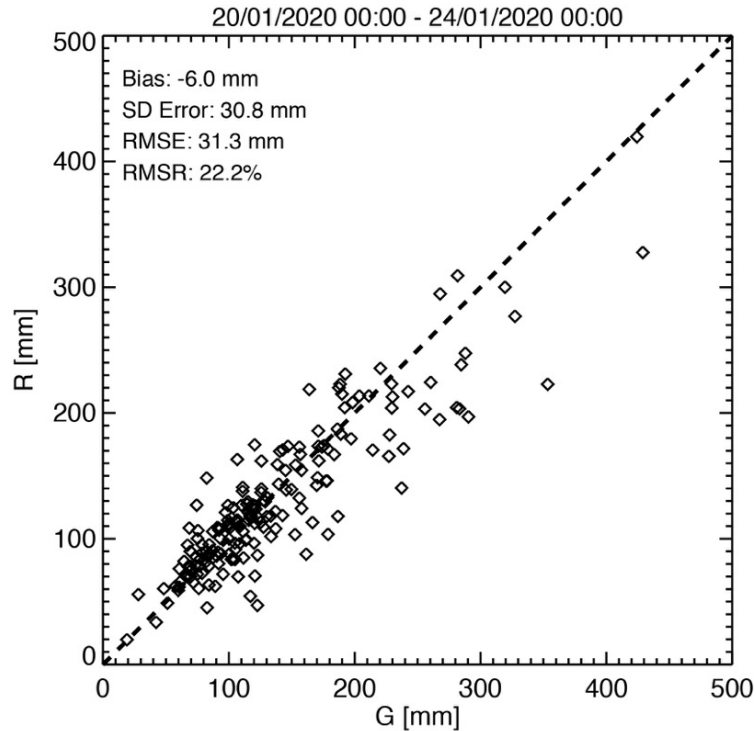
Figure 21. Cross-validation scatter plot comparing the observed total accumulated rainfall at each of the 187 rain gauges (R) and the KED estimated value from the radar observations (G).

The results from the comparison of the hyetographs obtained by cross validation and the hyetographs from rain gauge observations for four selected rain gauges distributed over the Catalan territory (see Figure 18) are presented in Figure 22 The evolution of 30-min accumulations reproduces the observations satisfactorily at the majority of the rain gauges. However, in some locations (e.g. Viladrau and PN dels Ports), the KED underestimates the measured intensities. In other sites, such as Torroella de Fluvià, the KED slightly overestimates the observed rainfall. The results for the 30-min accumulations obtained at all the available rain gauges show that the RMSE ranges between 0.15 mm and 1.72 mm. In the calculation of the RMSR, we have imposed a threshold of 1mm/30 min, and the results for RMSR range between 21.7 % and 107.4 %, with a median value of 42.8 %. The errors in small accumulations have a significant

effect in the calculation of RMSR, and the larger values are obtained in areas with event accumulations between 100 and 150 mm.
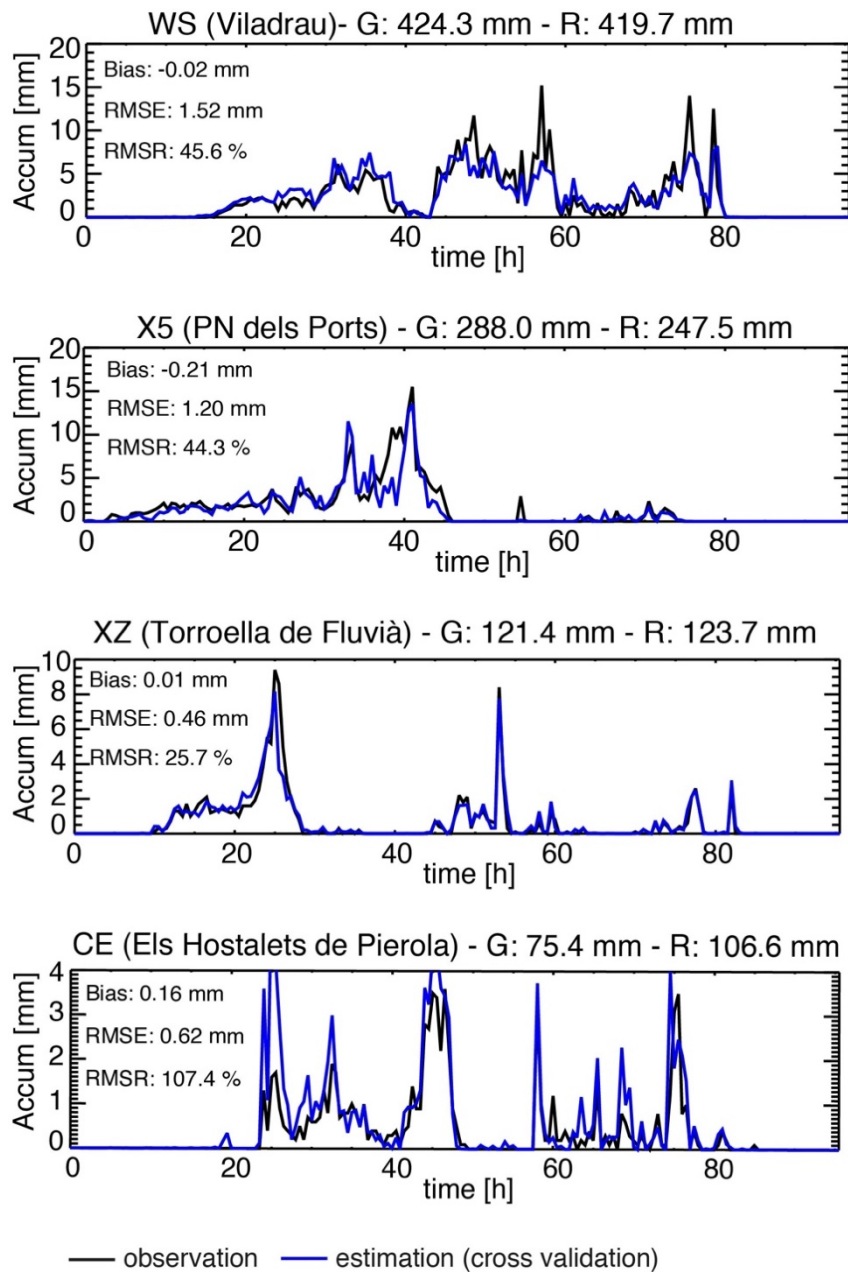
Figure 22. Observed (black line), and estimated (blue line) hyetographs from cross-validation for four rain gauges from the 20 January 2020 00:00 to the 23 January 2020 24:00. The location of the rain gauges can be observed in Fig. 1. The time step is 30 minutes.

The results presented in this section quantitatively describe the uncertainty in the QPEs obtained by KED during the Gloria storm. These QPEs are the precipitation inputs to the Catalonia region LEWS, and therefore, their uncertainty will affect the performance of the LEWS and the quality of the issued warnings during this event (see Section 3.4).

3.3.4. Landslide inventory and impacts

The significant rainfall accumulations and high intensities registered during the Gloria storm triggered a large number of landslides over different areas in Catalonia. One of the main challenges for the evaluation of the performance of LEWS is the availability of a complete landslide inventory. In Catalonia no systematic and official landslide inventory exists. Therefore, in this study we have used information contained in two different landslide inventories; the inventory of the Cartographic and Geological Institute of Catalonia (ICGC inventory - González et al. 2020), and the #Esllavicat inventory.

The ICGC inventory gathers landslide information from several sources such as reports from different administrations (municipalities, county councils, civil protection, mountain rangers, and other institutions), interpretation of aerial photographs taken after the Gloria storm along some river banks, and media reports. It includes a total of 348 entries. However, information of these 348 landslides is not complete and many times lacks of details. For example, the ICGC inventory does not include volume information. The majority of landslides are classified according to the Varnes (1978) classifications. Yet, some reports may be due to accumulation of sediment on roads associated with other processes such as water erosion. All the entries of the ICGC inventory include information on the timing. However, some entries have no clear date and the day of occurrence during the Gloria storm is therefore uncertain. Additionally, the location of around 25% of the reports is uncertain, and 23 landslides are located in urban areas in flatlands, where no slope or talus could be observed in their vicinity. Therefore, these points have not been used for our analysis since we considered their spatial uncertainty was too large.

The #Esllavicat inventory collects data from social network posts of local observers. A total of 108 geolocated landslides were reported through social networks and have been included in the #Esllavicat inventory. The majority of #Esllavicat landslide reports included a photograph or video of the initiation or deposit area (see examples of Figure 23). Most of the landslide locations have been checked by pre-storm Google Street View. Using this information, together with the descriptions provided in some posts, the landslides have been classified into different types according to the classifications proposed by Varnes (1978) and Hungr et al. (2014). Additionally, a measure of the event size has been assigned to each inventory entry to differentiate between three volume

ranges: less than 1 m^3, between 1 and 10 m^3, and more than 10 m^3. Some of the #Esllavicat reports were made once the storm had ceased; thus, the precise triggering date is uncertain.

Figure 23. Examples of landslides triggered by the Gloria storm in the Montseny area. a) Rotational slide in a colluvium slope (photo courtesy of Clàudia Abancó). b) Rotational slide that affected a road embankment and parts of natural slopes (photo courtesy of Roger Ruiz)

For this study, the ICGC and the #Esllavicat inventories have been merged, and duplicated points have been removed. The final landslide data set contains 58 points from the #Esllavicat inventory, 275 from the ICGC inventory and 50 that are included in both, resulting in a total 383 landslide points.

The Montseny is the area where the largest density of landslides was observed, 0.28 landslide/km^2 (Figure 18 b). This density is rather low, compared with the density of landslides observed for historical MORLEs in Catalonia (e.g. 1.5 landslides/km^2 in the Pyrenees 1982; Corominas and Alonso (1990), and 1.16 landslides/km^2 in Val d'Aran 2008, Shu et al. (2019)). The differences may be partly due to the completeness of historical inventories, which fully covered smaller regions inside Catalonia with field surveys and the interpretation of aerial photographs. This was not possible for the Gloria storm inventory due to the much larger extension and because no post-event flight surveillances were made over the most affected areas.

The characteristics of the landslides triggered by the Gloria storm and contained in the final inventory are described hereunder. The accumulated rainfall at the location of the reported landslides has been checked (Figure 20). From the 383 landslides used for this study, more than 100 were reported in places that registered event rainfall accumulations over 300 mm in 96 hours (Figure 24a).
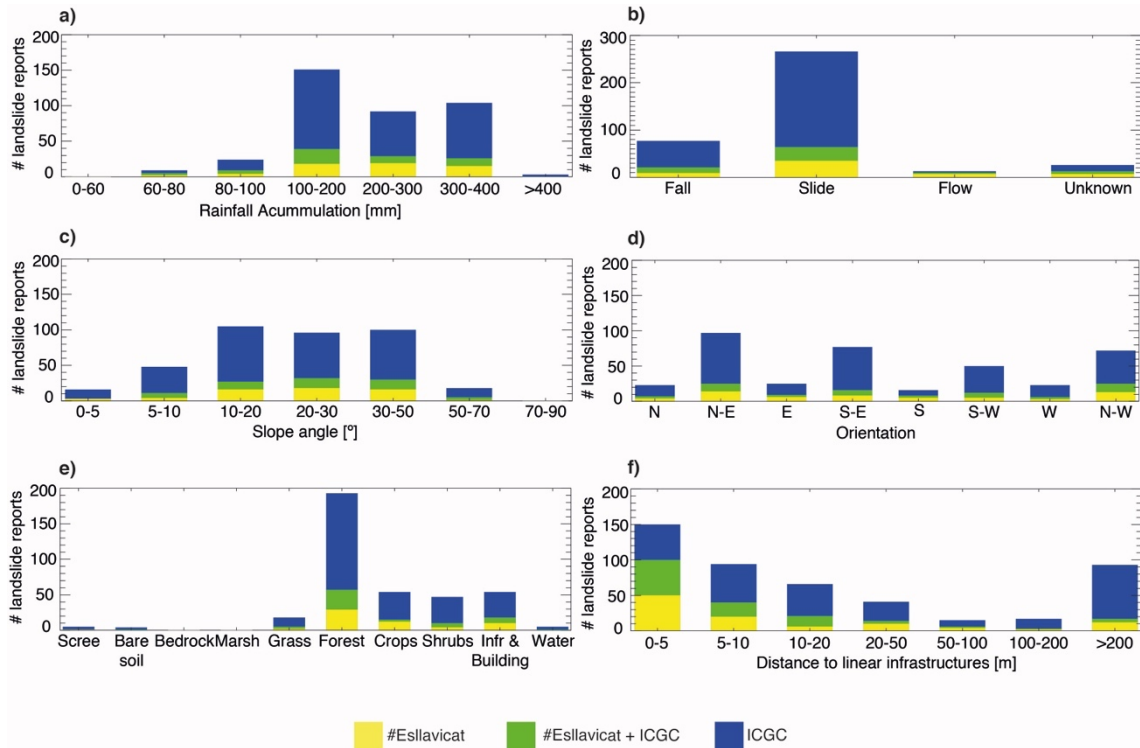
Figure 24. Histograms showing the distribution of Gloria storm landslide reports contained in the ICGC and the #Esllavicat inventories according to (a) rainfall accumulation, (b) landslide type, (c) slope angle, (d) orientation, (e) land use and land cover, and (f) distance to the closest road or railway axis.

According to its type, 69 % of the inventoried landslides were slides, 20 % falls, and 3 % flows (Figure 24b). The type of the remaining 8 % of events triggered by the Gloria storm is unclear. Regarding the landslide volume, only information from the #Esllavicat reports is available. Most of the landslides contained in the #Esllavicat inventory were relatively small, with a volume between 1 and 10 m3.

The 5 m resolution DEM has been used to estimate the slope angles, and the 30 m resolution DEM has been employed to obtain the orientation (ICGC 2013). Similarly, land use and land cover with a resolution of 30 m (MCSC-4, CREAF 2009) and the graph of the Catalonia infrastructures network (DGMT 2019) have been applied to analyse the

most common land use and land cover classes at the landslide locations and the proximity to roads and railway lines.

The majority of landslides were located at steep slopes of over 20 º (Fig. 7c). Around 27 % of the events were reported in slopes with angles between 10-20 º, and about 16 % in gentle slopes with slope angles less than 10 º. Such low slope angles are rather difficult to justify from a geotechnical point of view and may be related to spatial uncertainty. No clear trend can be observed in the orientation of the slopes where landslides were reported. However, the total number of events triggered in East, North-East, and South-East facing slopes is slightly larger than the sum of the events at South, South-West, and West facing slopes (Figure 24d). The main wind direction of the Gloria storm was towards West-North West; thus, East and South-East facing slopes would be the most exposed.

Landslides most frequently occurred in forest areas (Figure 24e) and 55 events were reported in areas with infrastructures or buildings. Two of the landslides contained in the inventory were located in water bodies, which might be related to the scouring in river banks Most of the reported landslides were spotted close to linear infrastructures (Figure 24f). Around 64 % were triggered between 0 and 10 m away from the road or railway axis. The number of landslides reports diminishes with the distance from linear infrastructures. Only 38 % of the reported landslides were located further than 200 m. These results provide two conclusions: (i) more than the half of the reports were related to slope failures of road cuts and embankments in linear infrastructures, and (ii) landslides happening in remote inhabited areas may generally be unreported.

3.4. Landslide warnings during the Gloria storm

In the following section, we briefly present the regional-scale early warning system (LEWS) for rainfall triggered landslides in Catalonia (Berenguer et al. 2015; Palau et al. 2020). Then, we analyse the LEWS outputs during the Gloria storm.

3.4.1. Description of the LEWS

Herein we briefly describe the LEWS for the region of Catalonia. More details can be found in Berenguer et al. (2015) and Palau et al. (2020). The LEWS has the aim of issuing real time warnings to the authorities in charge of managing landslide risk in Catalonia. It

combines two input parameters (i) a 30-m resolution susceptibility map (Figure 25a) and (ii) high-resolution rainfall observations. The output of the LEWS is updated every time new rainfall observations are available and consists on a map showing a qualitative warning level.
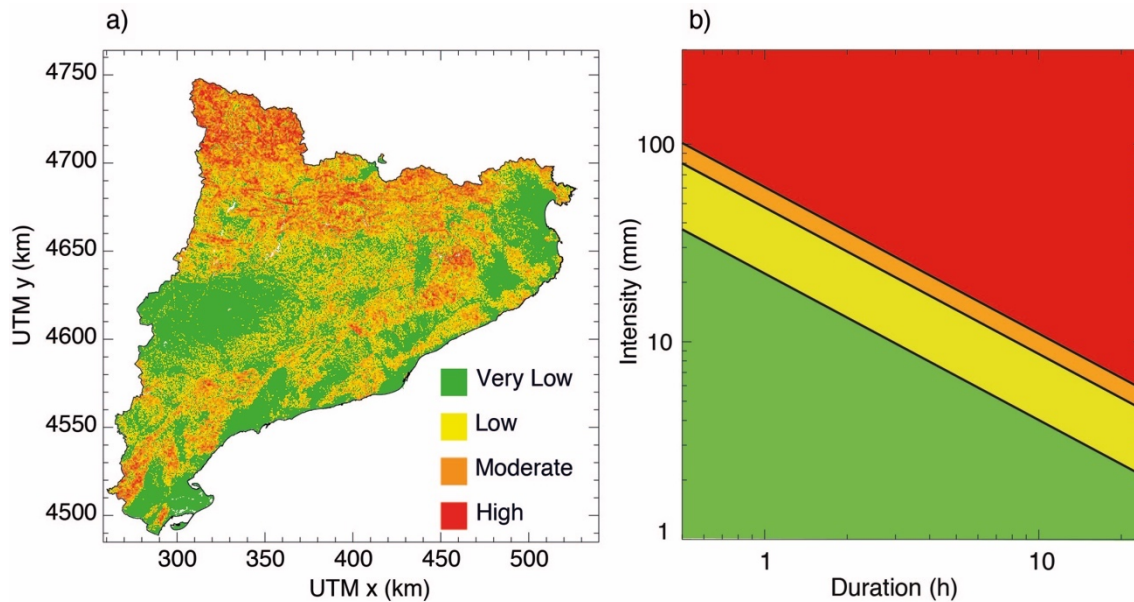
Figure 25. Susceptibility map (a) and rainfall intensity-duration thresholds (b) employed by the LEWS.

The susceptibility map (Figure 25a) is used to depict the locations where landslides may occur. It was derived by Palau et al. (2020) applying a fuzzy logic methodology to combine slope angle and land use and land cover information.

To asses if a rainfall event has the potential of triggering a landslide the intensity-duration-frequency IDF curves of the Fabra meteorological observatory in Barcelona (Casas et al. 2004) are used to define four rainfall hazard levels (Figure 25b).

Finally, the rainfall hazard and the susceptibility, are combined through a warning matrix. The result is a 30 m gridded warning level map. Each warning level ("very low", "low", "moderate" and "high") indicates the possibility that a landslide is triggered at a specific location. Additionally, a summary showing the maximum warning level issued within the first second and third order hydrological subbasins as defined by Strahler (1957) is provided.

Additional analysis of recent rainfall events that triggered landslides in Catalonia showed that the rainfall intensity – duration (I-D) thresholds initially applied to determine the

"Moderate" and "High" warning levels were too low. Therefore, here we have adapted the I-D thresholds employed in (Palau et al. 2020). The five years and 20 years return period I-D curves have been used to define the "Moderate" and "High" rainfall hazards respectively

3.4.2. Landslide warnings during the Gloria storm

The LEWS has been run from 20 to 23 January 2020 using the KED 30 min rainfall accumulation estimates as inputs to analyse the quality of the warnings issued each day of the Gloria storm.

Figure 26 shows the subbasin maximum warning level summary of each of the days of the Gloria storm and the positions of inventory reports. From the comparison of the warning maps of Figure 26 and the 24 h rainfall accumulations of Figure 19, it can be observed that generally, "Moderate" and "High" warnings were issued in the areas that recorded the most significant rainfall accumulations during the corresponding day.

Generally, landslides (displayed as black circles in Figure 26) were reported in places where the subbasin daily warning summary is "Moderate" or "High". At the eastern half of Catalonia, "High" warnings were issued over the area where the inventory has the highest density of landslides (Figure 18 b). "Moderate" and "High" warnings were given over the South-West of Catalonia on 21 January and over the North-West of Catalonia on 22 January 2020, but few landslides were reported in these areas (Figure 26 b and c). The Pyrenees, Pre-Pyrenees, Iberian Range, and the western Catalan Coastal Ranges have a low population density. Therefore, it may be the case that some landslides might have been unreported.
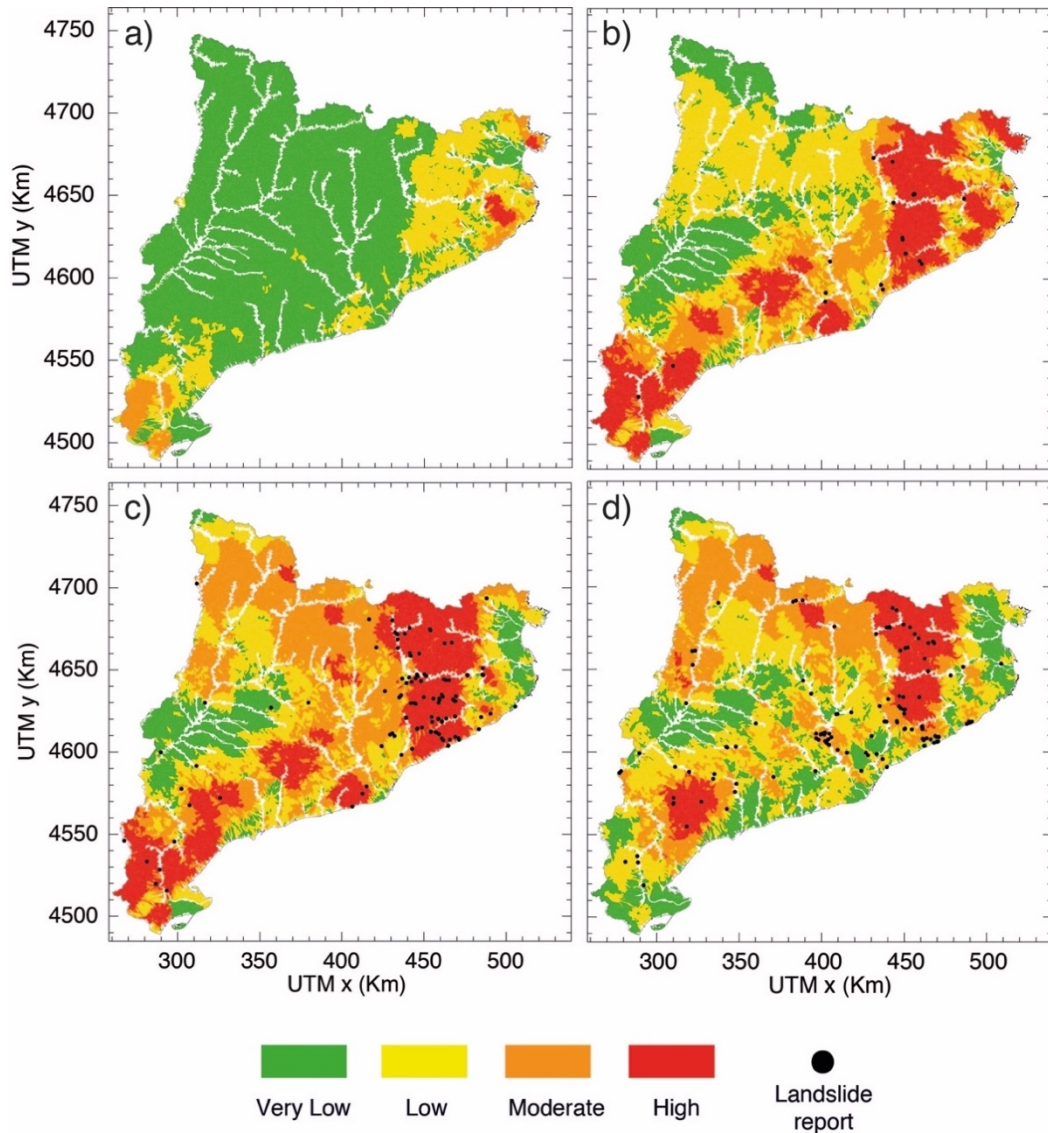
Figure 26. Daily maximum warning level subbasin summary. (a) 20/01/2020, (b) 21/01/2020, (c) 22/01/2020 and (d) 23/01/2020. The black circles represent the landslides contained in the inventory.

3.5. Evaluation of the performance of the LEWS during the Gloria storm

Evaluating the performance of a high-resolution LEWS over entire Catalonia is challenging because of the spatial and temporal uncertainties of the landslide inventory as well as its incompleteness (see Section 3.3.4).

Traditional verification methods match the location and time of the warnings to the precise location and time of the reported landslides to analyse the performance of a

LEWS. Consequently, the uncertainties and incompleteness of landslide inventories have an effect on the results of traditional verification methods.

To deal with the uncertainties of the landslide inventory, fuzzy verification methods are an alternative that does not require the exact coincidence between warnings and observations. Instead, such methods assume that the location and time of warnings can be slightly different from the location and time of landslide observations but still be useful. To do so, fuzzy verification methods look in a space-time neighbouring window around each observed event for the evaluation of the performance of the model (e.g. Ebert 2008, 2009) enabling some flexibility in the matching between the prediction and the observation. This makes this approach interesting to evaluate the performance of the LEWS employing a landslide inventory which is not complete and has temporal and spatial uncertainties.

3.5.1. Description of the verification method

The fuzzy verification method that has been applied for the evaluation of the warnings during the Gloria storm is known as the "minimum coverage criterion" (Damrath 2004; Ebert 2008). This method considers a neighbouring window to search for warnings that have been issued around each observation used as reference. The minimum coverage method assumes that events are equally likely to occur anywhere within the neighbouring window. Then, categorical scores based on the contingency table are employed for the verification (Fawcett 2006) and applied considering different neighbouring window sizes, which provide additional information on the quality, and space and time representativeness of the issued warnings.

For the verification purposes we have considered that a warning was issued when the LEWS warning level was either "Moderate" or "High", and no warning was issued when the warning level was either "Low" or "Very Low". The landslides contained in the inventory have been used as reference. Following the minimum coverage criterion, a true positive is an outcome where the LEWS correctly issues at least one warning within the neighbouring window of a landslide observation. In contrast, a false negative is an outcome where the LEWS incorrectly issues no warning within the neighbouring window of a landslide observation. Similarly, a true negative is an outcome where the LEWS correctly issues no warning outside the neighbouring windows of landslide observations.

And a false positive is an outcome when the LEWS incorrectly issues a warning outside the neighbouring windows of landslide observations.

To study the performance of the LEWS, we have selected three different metrics:

- the true positive rate (TPR),

$$TPR = \frac{TP}{TP+FN} \tag{3}$$

- the false positive rate (FPR)

$$FPR = \frac{FP}{FP+TN} \tag{4}$$

- and the true skill statistic (TSS)

$$TSS = TPR - FPR = \frac{TP}{TP+FN} - \frac{FP}{FP+TN} \tag{5}$$

where TP, FP and TN are, respectively, the number of true positives, false positives and true negatives. TPR and FPR values range from 0 to 1. Ideally, a LEWS should issue no false negatives and no false positives, therefore the perfect TPR and FPR should be 1 and 0 respectively. The TSS combines the TPR and the FPR. It measures how well the warning map can separate points with landslides observations from points where landslides have not been observed. Its scores range from -1 to 1, 0 indicates no skill. The TSS perfect score is 1.

Here, the minimum coverage method has been applied using 30 m, 500 m, 1 km, 2 km, and 10 km squared neighbouring windows around each landslide observation. Additionally, we have included two types of polygon neighbouring windows that we considered of special interest: hydrological subbasins and municipalities. As explained in Sect. 4.1, hydrological subbasins are the LEWS reporting units. Its mean area and standard deviation are 2.1 km² and 1.6 km², respectively. Municipalities have been chosen since they are relevant from an emergency management point of view. The area of municipalities is very variable. Its mean area is 26.9 km², and the standard deviation is 30 km². Indeed, the largest municipality has an area of 303 km².

Finally, two different time windows have been applied to deal with the uncertainty of the reporting date. First, a time window of 48 h comprising the day of the landslide report and the day before has been used for the daily verification of the LEWS outputs. Second, a time window of the entire duration of the Gloria storm has been employed for the event verification of the warnings.

3.5.2. Daily verification

First, the minimum coverage criterion has been implemented using as a reference the 245 inventory entries that had a specific triggering date. For every landslide observation, each of the different space neighbouring windows have been jointly applied with the time window of 48-h. Table 8 shows the results for the fuzzy verification of the warnings issued with the LEWS for the Gloria event. Since it is easier to find warnings within a larger domain, the number of true positives increases with the size of the neighbouring window employed for the LEWS verification. In contrast, the number of false negatives decreases when the neighbouring window size increases (Table 8). As a consequence, the TPR increases with the neighbouring window size (Figure 27 a). The worst TPR value is 0.37 for 30 m neighbouring windows on 23 January 2020. Whereas its highest score is 1.00 for the 10 km neighbouring window during 21 and 23 January 2020, and for the municipalities neighbouring window during 21 January 2020. In fact, for the verifications applying large neighbouring windows (1 km, 2 km and 10 km, subbasins and municipalities) the TPR scores are generally high (> 0.83). This indicates that when using such neighbouring windows, a warning could be found at the surroundings of 83 % of the landslide observations.

Because of the incompleteness of the landslide inventory, especially in the less densely populated areas, the number of false positives is expected to be large. However, the area where false positives are issued, is an order of magnitude smaller than the area where true negatives are issued (Table 8). Therefore, the FPR values are rather low and range from 0.00 to 0.16 for all the neighbouring windows used (Figure 27 b). Regarding the TSS, the highest score, 0.92, is achieved employing 10 km neighbouring windows for the 21 January 2020 (Table 8 and Figure 27). Both, the 30 m, and 500 m neighbouring windows verifications have relatively low TSS values, especially for 22 and 23 January 2020. In contrast, TSS values are always above 0.68 when using the larger neighbouring windows.

Table 8 Daily skill scores for different neighbouring window scales. True positives (TP), false negatives (FN), false positives (FP) area, true negatives (TN) area, true positive rate (TPR), false positive rate (FPR), and true skill statistic (TSS) for the different neighbouring window types.

Neighbouring window size	Date [dd/mm/yyyy]	Number of events	TP	FN	FP-area [km²]	TN-area [km²]	TPR	FPR	TSS
30 m	20/01/2020	0	0	0	200	39344	-	0.00	-
	21/01/2020	20	10	10	3176	36367	0.50	0.08	0.41
	22/01/2020	103	48	55	6119	33424	0.46	0.15	0.31
	23/01/2020	122	46	76	6392	33151	0.37	0.16	0.21
500 m	20/01/2020	0	0	0	200	39344	-	0.00	-
	21/01/2020	20	12	8	3176	36367	0.60	0.08	0.51
	22/01/2020	103	56	47	6119	33424	0.54	0.15	0.38
	23/01/2020	122	54	68	6392	33151	0.44	0.16	0.28
1 km	20/01/2020	0	0	0	200	39344	-	0.00	-
	21/01/2020	20	17	3	3168	36351	0.85	0.08	0.76
	22/01/2020	103	86	17	6075	33347	0.83	0.15	0.68
	23/01/2020	122	108	14	6348	33054	0.88	0.16	0.72
2 km	20/01/2020	0	0	0	200	39344	-	0.00	-
	21/01/2020	20	19	1	3151	36304	0.94	0.07	0.87
	22/01/2020	103	91	12	5960	33149	0.88	0.15	0.73
	23/01/2020	122	113	9	6240	32813	0.92	0.15	0.76
10 km	20/01/2020	0	0	0	200	39344	-	0.00	-
	21/01/2020	20	20	0	2681	35110	1.00	0.07	0.92
	22/01/2020	103	102	1	4149	29198	0.99	0.12	0.86
	23/01/2020	122	122	0	4380	28263	1.00	0.13	0.86
Subbasins	20/01/2020	0	0	0	200	39344	-	0.00	-
	21/01/2020	20	18	2	3149	36329	0.89	0.07	0.82
	22/01/2020	103	89	14	5995	33249	0.86	0.15	0.71
	23/01/2020	122	112	10	6273	32930	0.91	0.16	0.75
Municipalities	20/01/2020	0	0	0	200	39344	-	0.00	-
	21/01/2020	20	20	0	2972	35773	1.00	0.07	0.92
	22/01/2020	103	100	3	4974	31684	0.97	0.13	0.83
	23/01/2020	122	118	4	5143	30467	0.96	0.14	0.82

Additionally, Table 8 and Figure 27 a and b show that TPR and TSS scores are very similar for the verifications applying squared 1 km, 2 km, and subbasin neighbouring windows. They are also resemblant for 10 km and municipalities neighbouring windows. These results are reasonable because the area of most subbasins ranges between the area of 1 km and 2 km neighbouring windows. The area of the largest municipalities is also

similar to the area of 10 km neighbouring windows. A significant improvement has been observed in the skill scores when increasing the neighbouring window size from 500 m to 1 km.
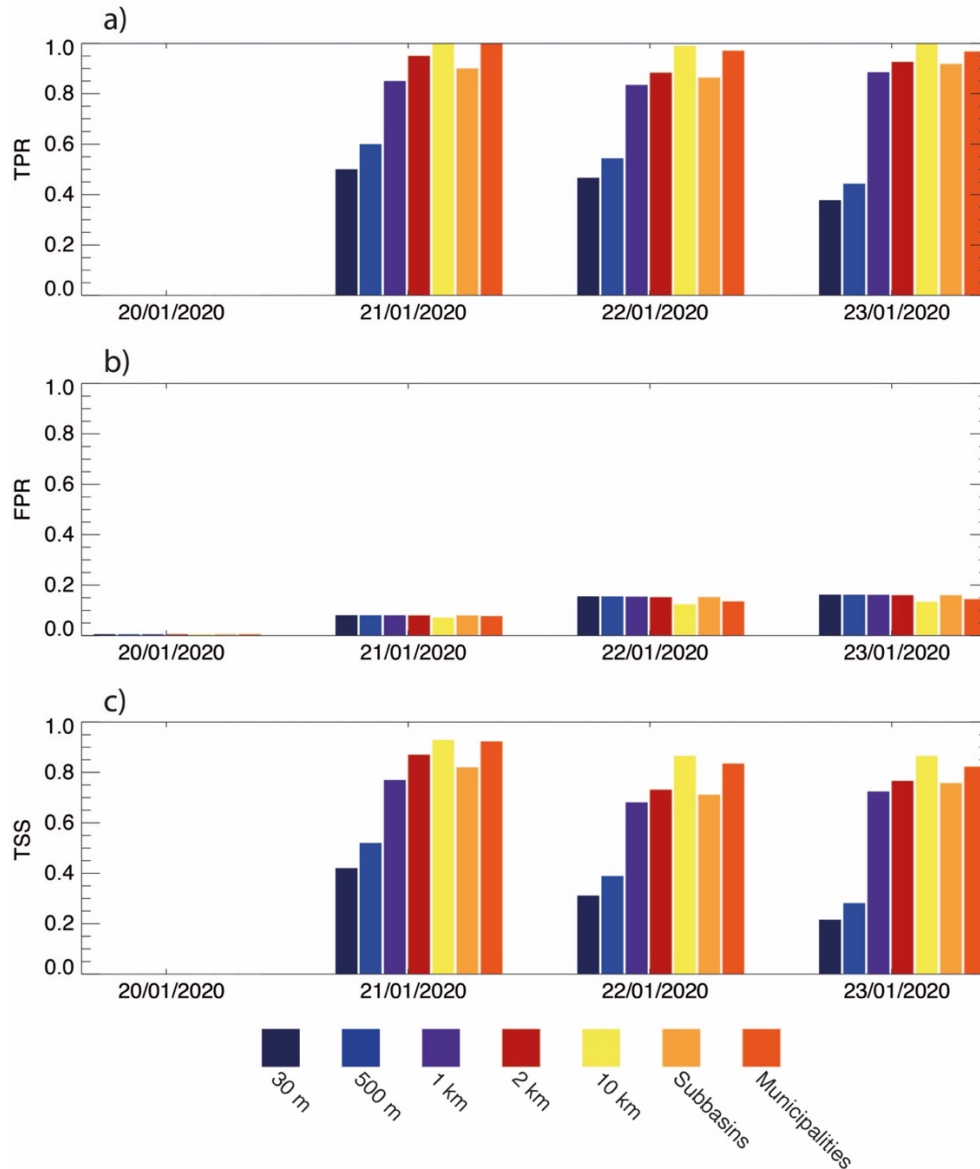
Figure 27. Daily verification skill scores using different spatial neighbouring windows. (a) True positive rate, (b) false positive rate, and (c) true skill statistic

3.5.3. Event verification

Some landslide reports were made after the end of the storm. Thus, an event verification allows us to include the additional 138 landslides that have an unclear triggering date. Here, all the 383 landslide events included in the landslide inventory have been used. The

TPR, FPR and TSS skill scores have been computed with the different spatial windows mentioned in Section 3.5.1, and with a time window including the entire event.

As expected, the number of TP is larger than the obtained for the daily verification, and the number of FP is lower. As a consequence, the scores obtained when applying an event neighbouring window for the LEWS verification improve. This is partly because the inventory employed for the event verification includes a larger amount of landslide reports. Additionally, the uncertainties on the triggering time are less significant when using a longer time window.

As in the daily verification, the larger the neighbouring windows, the higher the TPR and TSS are. Except for the 30 m and 500 m neighbouring windows verifications, the TPR and TSS are relatively good with values above 0.87, and 0.71, respectively (Figure 28 a and c). FPR values are rather low, around 0.15 for the evaluations using the different neighbouring windows (Figure 28 b).

The subbasin neighbouring windows verification achieves slightly higher TPR and TSS scores than the 1 km neighbouring windows verification. Both TPR and TSS are also very similar for the verifications using 10 km and municipalities neighbouring windows.

As observed in the daily verification, the results of the event verification show a significant improvement in the LEWS skill when increasing the size of the neighbouring window from 500 m to 1 km. The verification results do not change significantly for the larger neighbouring windows (2km, 10 km, subbasins and municipalities). Hence, if a warning is issued, we will probably be able to find a landslide within a surrounding area of 1 km^2. We could interpret this result as an effective resolution of the LEWS, at which the warnings are more reliable.
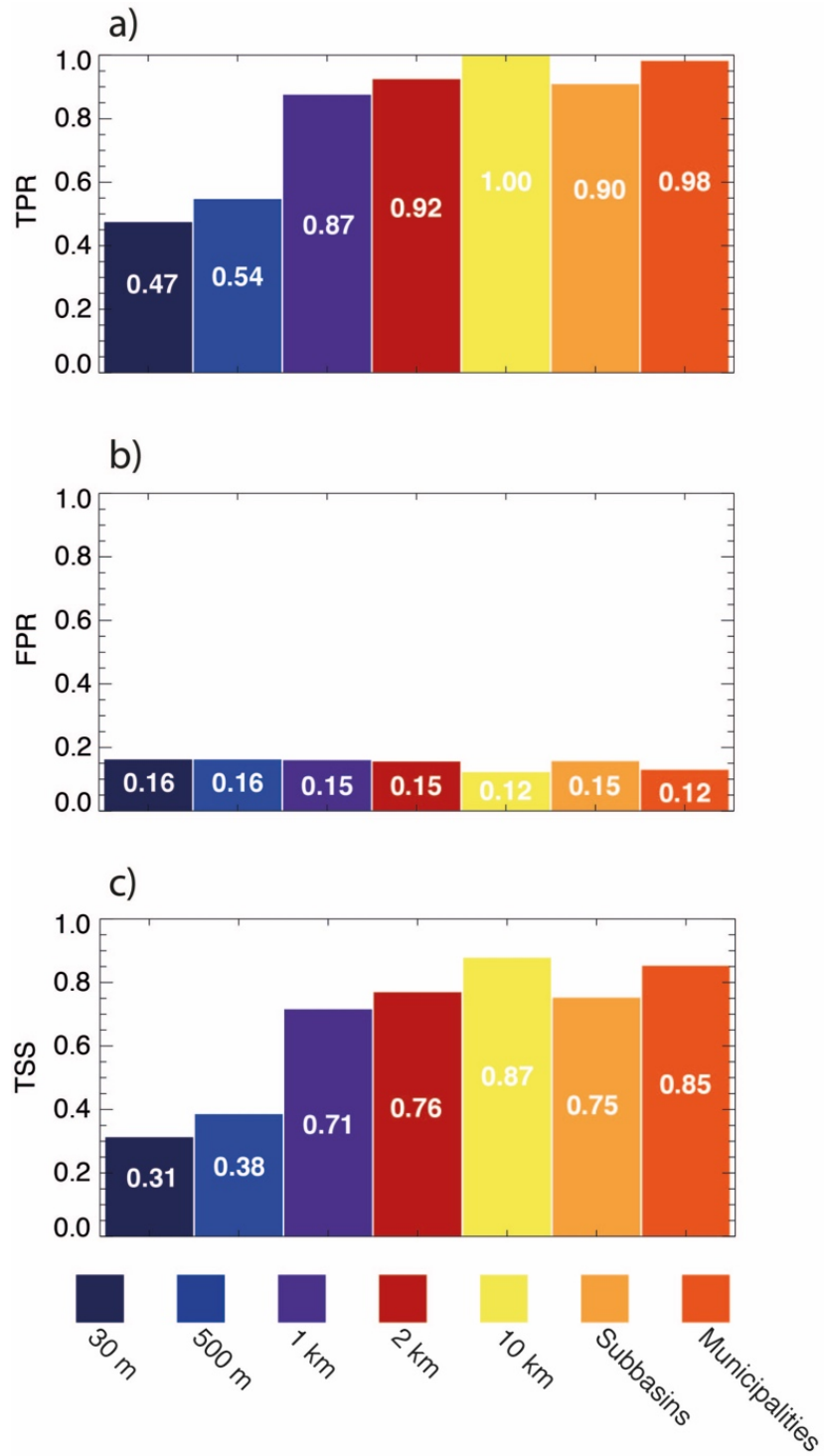
Figure 28. Event verification skill scores applying different spatial neighbouring windows. (a) True positive rate (b) false positive rate, and (c) true skill statistic

3.6. Conclusions

From the 20 to the 23 January 2020, the extraordinary storm Gloria hit the region of Catalonia. Its significant precipitations triggered multiple landslides at a regional scale. In this study, the Gloria storm rainfalls and landslides that were triggered have been analysed. Then, we have taken the opportunity of this unique event to evaluate the performance of the regional scale LEWS applying a fuzzy verification method.

To analyse the Gloria storm rainfalls, KED estimates combining radar and rain gauges surface measurements have been obtained. Additionally, the uncertainties of the Gloria storm estimated QPEs have been quantified by cross-validation. These QPEs constitute the precipitation input of the Catalonia region LEWS. Therefore, although rainfall estimates generally show a good agreement with the rainfall observations, its errors are a source of uncertainty of the LEWS and influence its performance.

The available Gloria storm landslide inventory data is affected by reporting biases: The majority of landslides included in the inventory were triggered in forests, adjacent to railway lines and roads, and some affected buildings. However, landslides that occurred in remote uninhabited areas have probably been unreported. In addition, many events were reported in gentle slopes. Such events can be attributed to the spatial uncertainty of the landslide inventories.

Because of the limitations of the inventory, the evaluation of the LEWS performance was challenging. For this reason, a fuzzy verification method has been applied using different neighbouring windows. Kirschbaum et al. (2009) and Park et al. (2020) used a similar approach for the evaluation of LEWS performance. However, they employed a single neighbouring window size. The main advantage of fuzzy verification methods is determining at which scales the warnings have a useful skill (Ebert 2009). Our results show that the LEWS has little predictability at small scales (30 m and 500 m), yet a significant improvement of the LEWS performance can be observed when increasing the neighbouring window size from 500 m to 1 km. Hence, from these results, it can be reasoned that the LEWS effective resolution is 1 km.

It is interesting to notice that the LEWS effective resolution is similar to the resolution of the rainfall data that has been employed to compute the warnings, which is 1 km.

Although these results seem to indicate that the rainfall resolution might affect the scale at which warnings have a useful skill, the effective resolution could also depend on other factors such as the resolution of the susceptibility map. Further research needs to be conducted in order to determine in which extent both factors influence the effective resolution of the warnings.

Additionally, the landslide inventory that has been employed for the verification is not complete. If an exhaustive landslide inventory had been available, we could possibly find a landslide within an area of less than 1 km^2 from a warning. Thus, the results of the fuzzy verification for smaller neighbouring windows would have probably been better. For this reason, it could be hypothesised that the actual LEWS effective resolution might be better than 1 km, between 500 m and 1 km.

Finally, it has been observed that the LEWS skill from the verification using subbasin neighbouring windows is somewhat better than the skill obtained from the 1 km neighbouring windows verification. Therefore, our results confirm that subbasins are indeed a suitable mapping unit to summarise the LEWS outputs, as proposed by Palau et al. (2020).

Chapter 4

IMPLEMENTATION OF HYDROMETEOROLOGICAL THRESHOLDS FOR REGIONAL LANDSLIDE WARNING IN CATALONIA

4.1. Introduction

Rainfall triggered landslides constitute a significant hazard in mountainous regions, causing major economic losses, physical asset damages and fatalities (Froude and Petley 2018). Landslide Early Warning Systems (LEWS) are a suitable option to reduce landslide risk by decreasing the exposure and increasing the preparedness of communities that might be affected (Alfieri et al. 2012; Calvello 2017).

The majority of regional-scale LEWS determine if rainfall events have the potential of triggering a landslide by employing empirical rainfall thresholds that relate landslide occurrence with certain rainfall conditions (NOAA-USGS Debris Flow Task Force 2005; Tiranti and Rabuffetti 2010; Jakob et al. 2012; Rossi et al. 2012; Yeung 2012; Segoni et al. 2018a). Rainfall thresholds have been derived applying heuristic and probabilistic approaches, for different geographical settings and spatial scales (Caine 1980; Guzzetti et al. 2007, 2008; Brunetti et al. 2010; Abancó et al. 2016; Calvello and Pecoraro 2019). However, rainfall thresholds usually do not take into account the important role that soil moisture plays in slope stability.

As water infiltrates into the soil during a rainfall event, pore water pressure increases, and soil shear strength decreases, eventually leading to failure (Terzaghi 1943; Bogaard and Greco 2016). Therefore, if the initial soil conditions are wet, less rainfall will be required

to trigger a landslide. Conversely, if the initial soil conditions are dry, more rainfall will be needed.

For this reason, some authors have tried to indirectly include soil moisture information to rainfall thresholds by incorporating cumulative rainfall amounts preceding the triggering of the landslide event, or by using antecedent precipitation indexes (Crozier 1999; Glade et al. 2000; Aleotti 2004; Godt et al. 2009; Frattini et al. 2009; Martelloni et al. 2013). Still, observed soil moisture conditions do not always correspond well to antecedent precipitation (Longobardi et al. 2003; Brocca et al. 2008). Consequently, the predictive value of rainfall thresholds is often low, and the number of false positives may be high.

With the aim of improving the predictive skill of "rainfall-only thresholds", Bogaard and Greco (2018) have proposed identifying the conditions leading to landslides combining rainfall information (trigger), and soil moisture information (cause). The so called "hydrometeorological thresholds".

Most of the proposed hydrometeorological thresholds have been derived using soil moisture from direct in-situ sensor measurements (Chitu et al. 2017; Mirus et al. 2018a, b; Zhao et al. 2019; Wicki et al. 2020; Oorthuis et al. in prep). The majority of these studies concluded that hydrometeorological thresholds slightly improved the performance of "rainfall-only thresholds" and helped reduce the number of false positives. However, using instrumentation soil moisture data for regional-scale warning is not always possible. The representativeness of the soil moisture measurements significantly decreases with the distance from the monitoring site (Wicki et al. 2020). In many regions, soil moisture sensor networks have a low density or are not available at all. Satellite soil moisture data can also be used (Thomas et al. 2019; Abancó et al. 2021). However, satellite products spatial and temporal resolution is coarse, and the sensing depth is shallow. A feasible alternative consists of using information from lumped or distributed hydrological models (Ponziani et al. 2012; Posner and Georgakakos 2015; Ciavolella et al. 2016; Chitu et al. 2017; Marino et al. 2020), which might also be useful to improve regional-scale landslide warning (Bogaard and Greco 2018; Wicki et al. 2021 under review).

Still, up to date, the use of hydrometeorological thresholds in operational regional-scale LEWS is very scarce. A good example is the Norwegian LEWS (Devoli et al. 2018;

Krøgli et al. 2018), which uses a set of relative water supply-soil saturation degree thresholds obtained from a spatially distributed version of the HBV hydrological model (Beldring et al. 2003). Segoni et al. (2018b, a) tested two different approaches to upgrade the early warning system of the Emilia Romagna region (Italy) by including daily soil moisture data from a distributed rainfall-runoff model (Ciarapica and Todini 2002). However, the operational version has not yet been implemented.

The LEWS running in real-time over the region of Catalonia (NE Spain) combines information on the terrain susceptibility and the triggering rainfall to depict when and where landslides might occur (Palau et al. 2020, under review). Still, from the analysis of recent rainfall events, it has been seen that warnings were issued over relatively large areas where landslides had not been reported. Some of these warnings may be false positives. This study aims to explore the potential of using modelled soil moisture data to improve the performance of the Catalonia region LEWS. This has required to fulfil a secondary goal; obtain a set of empirical hydrometeorological thresholds for the Catalonia region.

4.2. The early warning system for the region of Catalonia

4.2.1. Description of study area

Catalonia is a region of around 32000 km^2 located at the NE of Spain. The climate in Catalonia is varied but can be classified as Mediterranean (Emberger 1952). Near the coast, the weather is mild and temperate. Inland, the climate is continental with hot summers, cold winters. The Pyrenees present a high-altitude climate, with abundant snow and temperatures below 0°C during winter. Generally, in Catalonia, the rainiest seasons are spring and autumn, except for the Pyrenees, where the rainiest season is summer. Landslides are usually triggered by either convective rainfall events with high intensities or long-lasting rainfalls with moderate intensities (Corominas et al. 2002; Abancó et al. 2016).

From a geological point of view, Catalonia is part of the Iberian Plate. The bedrock lithology is very diverse and includes igneous, sedimentary and metamorphic materials. In many locations, the bedrock is covered by surficial formations of varied thickness.

While in some areas, these deposits merely consist of a few centimetres, in others, the surficial formations can be very thick, of the order of meters.

4.2.2. Warning System

The Catalonia region LEWS (Palau et al. 2020) combines in real-time two types of information: (i) the terrain susceptibility, and (ii) data describing the rainfall situation. The output is a 30 m-resolution qualitative warning map, updated every time new rainfall information is available (Figure 29).
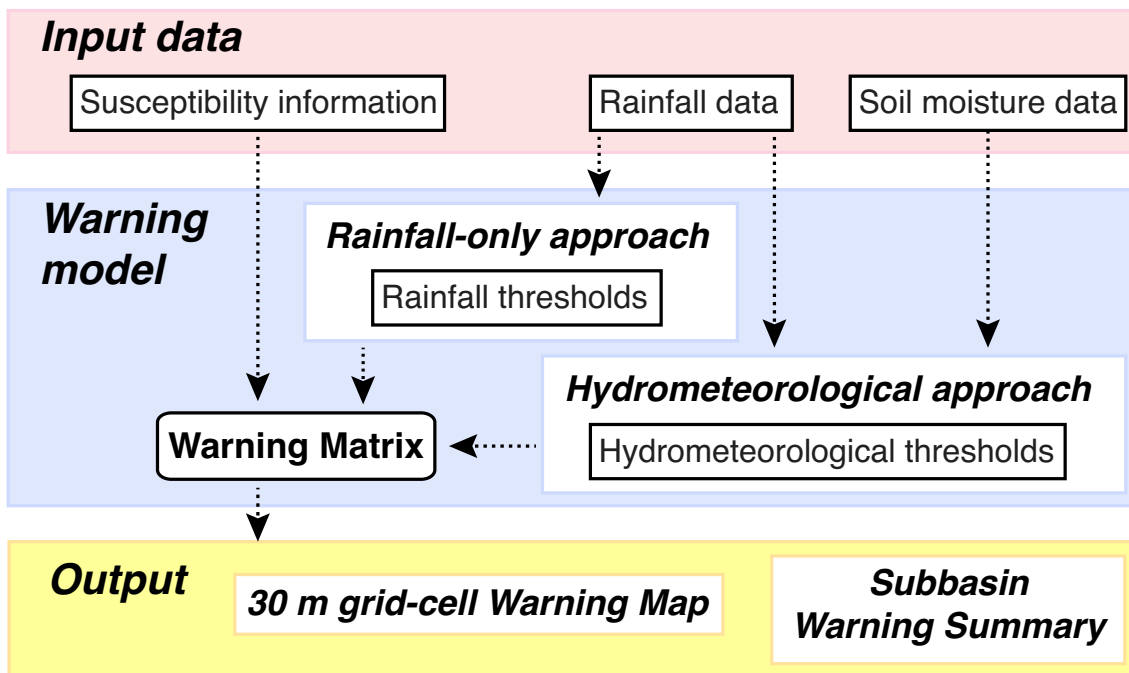
Figure 29. Scheme of the Landslide Early Warning System of Catalonia. The warning module which can either be run using the rainfall-only approach or the hydrometeorological approach.

The susceptibility map (Figure 30) is applied to distinguish the locations where landslides may occur. It was obtained by Palau et al. (2020) applying a fuzzy logic methodology combining slope angle and land use and land cover information.

To determine if the rainfall situation has the potential to trigger a landslide, the original version of the warning model described in Palau et al. (2020) uses only high-resolution rainfall data (Figure 29). In this study, the warning model has been set up to work with a hydrometeorological approach and employs both high-resolution rainfall information, and modelled soil moisture data (Figure 29).
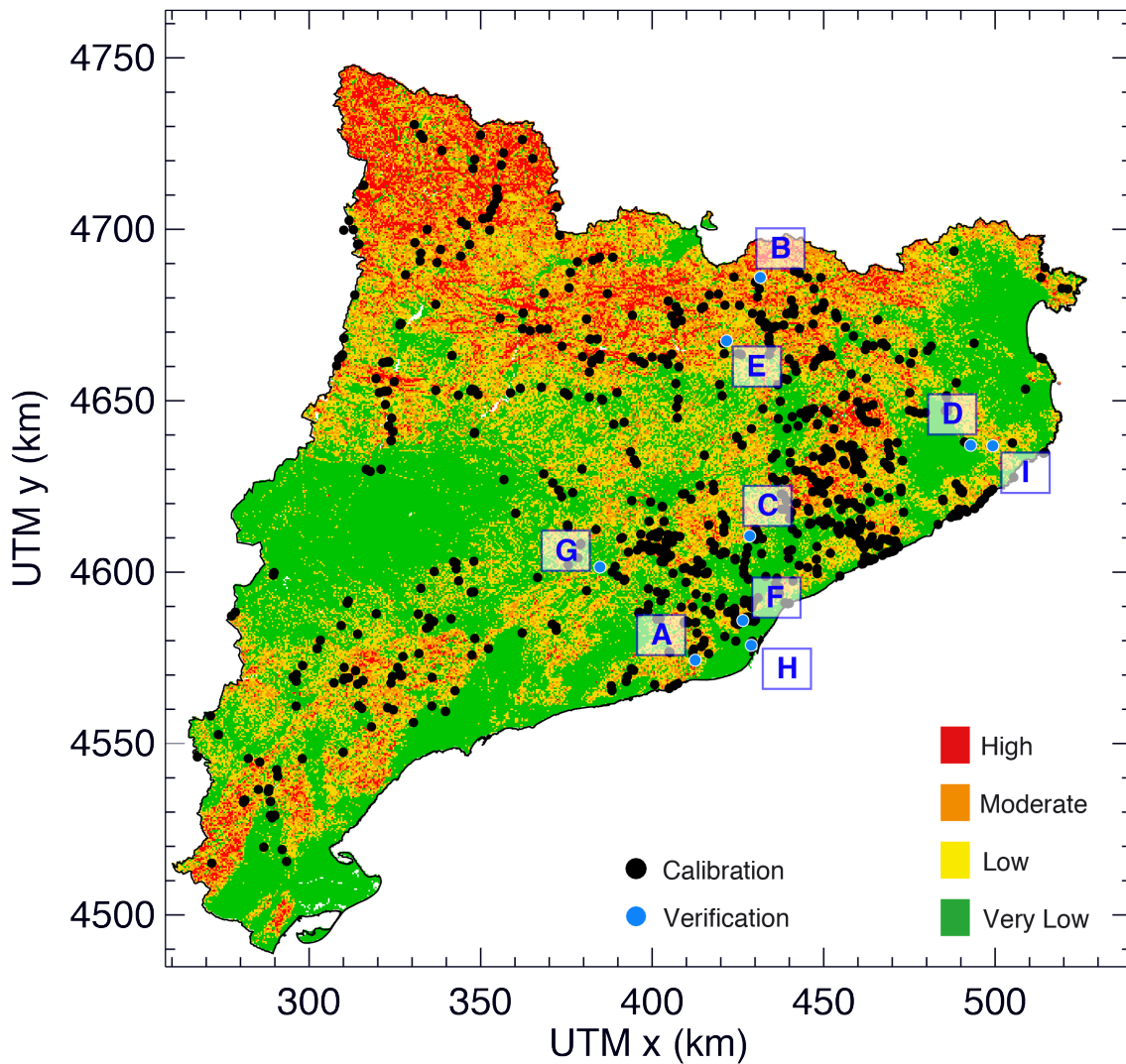
Figure 30. The susceptibility map that has been used as LEWS input data. The landslides included in the database that has been used to obtain the hydrometeorological thresholds are represented as black circles. The blue circles are the landslides that have been used to analyse the LEWS performance.

The rainfall-only approach employs intensity (I) – duration (D) thresholds to define four rainfall hazard classes (Figure 31 a). Then a warning matrix combines susceptibility and the rainfall hazard to obtain a qualitative warning level map (Figure 29). Similarly, the hydrometeorological approach applies the thresholds derived in Section 4.4 to characterise the hydrometeorological hazard (Figure 29). Then, the warning matrix is used in the same way to combine susceptibility and the hydrometeorological hazard and obtain a qualitative warning map.

Increasing the warning level implies increasing the possibility that a landslide is triggered at a specific location. Additionally, 30 min and daily warning summaries showing the

maximum warning level issued in 1st, 2nd, and 3rd order subbasins are provided to simplify the visualisation of the warnings.
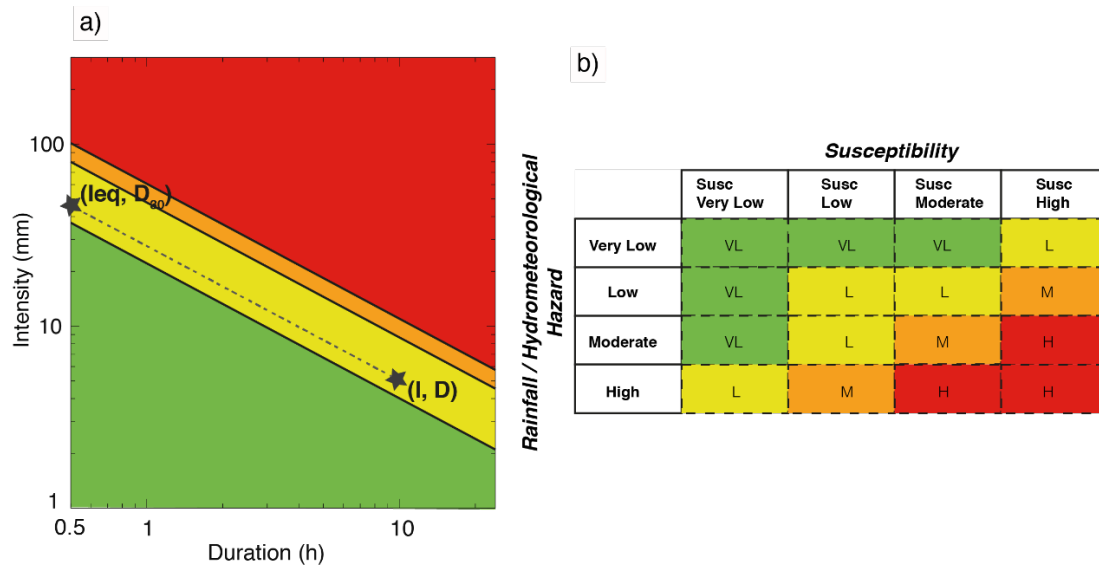
Figure 31. (a) Rainfall intensity- duration thresholds employed in the original version of the LEWS as described by (Palau et al. 2020). The two stars show the rainfall intensity-duration (I-D) conditions and their equivalent intensity for a 30 minutes duration (Ieq, D₃₀). (b) Warning matrix used in the LEWS to combine susceptibility and the rainfall or the hydrometeorological hazard.

4.3. Data

In this Section, details of the rainfall data, soil moisture data and landslide inventories that have been used in this study are given.

4.3.1. Rainfall data

Herein, we have used a rainfall data set consisting of a radar-rain gauge blended product. Rain gauge data has been obtained from the measurements of 187 tipping bucket rain gauges from the Meteorological Service of Catalonia (SMC). Radar QPEs consist on the composite of the observations of the SMC radar network (XRAD).

Radar QPEs have been produced from the volume scans of the C-band single polarisation Doppler radars of the XRAD with the Integrated Tool for Hydrological Forecasting (EHIMI, Corral et al. 2009). This tool includes a chain of quality control, correction, mosaicking and accumulation algorithms to generate QPE products from raw radar observations. The QPEs have a spatial resolution of 1 km.

Radar QPEs and Rain gauge observations have been combined to obtain an improved rainfall field using kriging with an external drift (KED), as proposed by Velasco-Forero et al. (2009) and Cassiraga et al. (2020). This method interpolates the rain gauges observations using radar rainfall as a secondary variable that provides the drift. KED rainfall estimates benefit from the direct surface observations of the rain gauges and the high-resolution description of the spatiotemporal variability of the rainfall field as observed by radar QPE. As shown by Velasco-Forero et al. (2009), KED estimates provide a high correlation with radar data and a small bias in comparison to rain gauge data.

4.3.2. Soil moisture data

This study aims to use soil moisture data to improve the performance of the regional-scale LEWS for Catalonia. In Catalonia, soil-moisture readings from monitoring data are only available for few specific sites such as those in the Pyrenees and pre-Pyrenees (Hürlimann et al. 2014; Oorthuis et al. 2017). Soil moisture is very variable and the representativeness of sensor data decreases with the distance (Wicki et al. 2021). Thus, using soil moisture monitoring data for regional early warning in Catalonia is not feasible.

Consequently, the approach implemented here relies on the simulations of soil moisture generated by a hydrological model at a regional scale. For this study, the LISFLOOD hydrological simulations (Van Der Knijff et al. 2010; Burek et al. 2013) in the European Flood Awareness System-EFAS (Thielen et al. 2009; Cloke et al. 2013) have been used. The main advantage of the LISFLOOD model is that it is run in real-time at a Pan-European scale, thus it could be employed in an operational version of the LEWS.

Over the EFAS domain, LISFLOOD is set up on a 5 km grid, and computes a complete water balance for each grid-cell at a 6 hourly time-step (Van Der Knijff et al. 2010). LISFLOOD was calibrated using streamflow data from river gauges, and temperature and rainfall information from meteorological stations.

Soil moisture water balance is computed at three different soil layers on a daily time step. The results are then used to initiate LISFLOOD simulations of the following day. In the top layer, LISFLOOD accounts for infiltration of precipitation, soil evaporation, and plant transpiration. At the bottom soil layer, the model accounts for deep percolation and

groundwater storage in the subsoil. The description of soil moisture fluxes between the three soil layers and the subsoil is based on the assumption that the flow of soil moisture is entirely gravity-driven, and always in a downward direction (Van Der Knijff et al. 2010). Since we are mainly interested in shallow processes, only the volumetric water content information of the top layer has been used in this study.
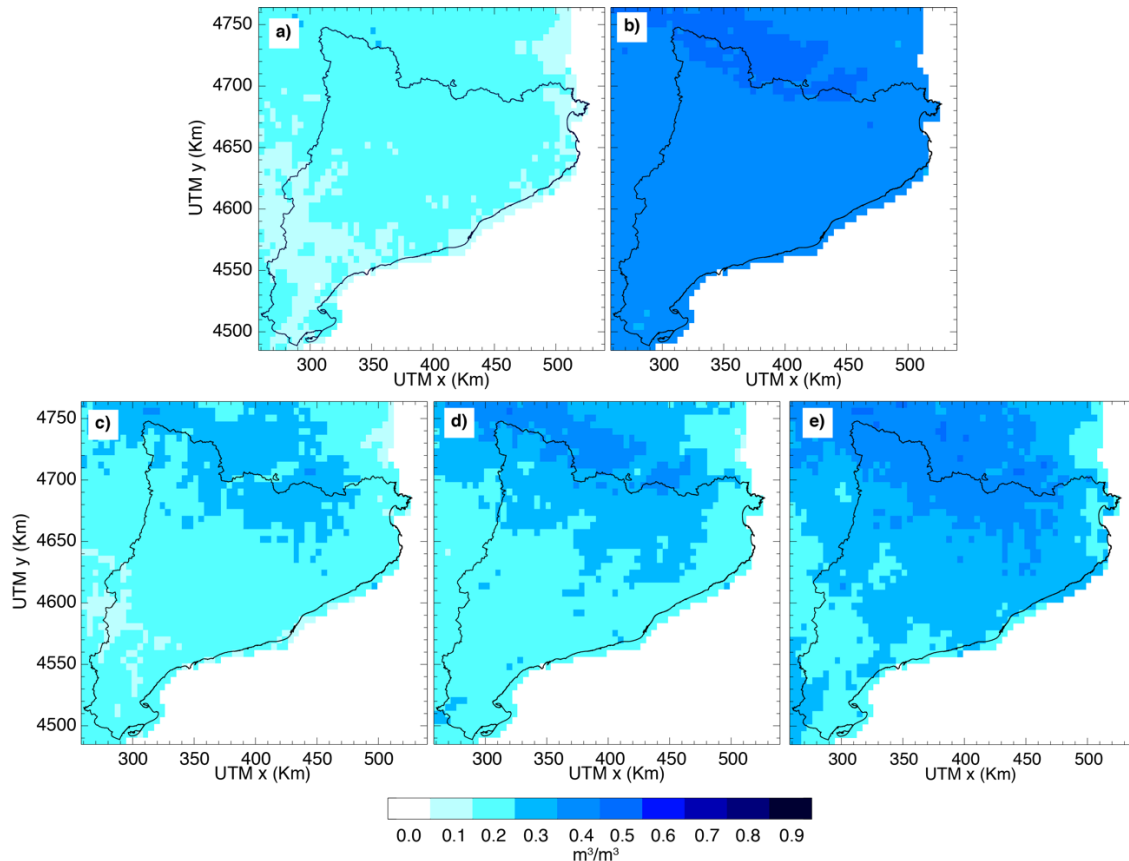
Figure 32. Analysis of the VWC conditions simulated by the LISFLOOD model during the period 2018-209. (a) minimum VWC, (b) maximum VWC, (c) 25th, (e) 50th and (d) 75th percentiles of VWC.

The LISFLOOD volumetric water content (VWC) over Catalonia has been analysed for the period 2018-2020. The minimum and maximum volumetric water content (VWC) simulated by the LISFLOOD over this period together with the 25, 50 and 75 percentiles are shown in (Figure 32). The minimum modelled VWC ranges between 0.1 m^3/m^3 and 0.2 m^3/m^3 and the maximum between 0.4 m^3/m^3 and 0.5 m^3/m^3. The driest soil conditions have been exhibited at the southwest and at the north-eastern coast, where the VWC is equal or lower than 0.2 m^3/m^3 for 75 % of the days in the analysed period. The most humid conditions have been observed in the Pyrenees, where the modelled VWC is over 0.4 m^3/m^3 during 25% of the days Figure 32 c, d, and e).

4.3.3. Landslide inventories

Landslide inventories are a vital element to correctly characterise the rainfall and soil moisture conditions that have led to landslides in the past, obtain hydrometeorological thresholds, and evaluate the LEWS performance. Having complete landslide inventories that include temporal information is often challenging (Kirschbaum et al. 2010; Van Den Eeckhaut and Hervás 2012; Gariano et al. 2015; Peres et al. 2018). In this study, we have combined landslide reports from (i) Catalan Civil Protection (CECAT), (ii) road maintenance and management authorities, and (iii) the #Esllavicat initiative for the period 2018-2020. Additionally, for the exceptional event of 20-23 January 2020, the Cartographical and Geological Institute of Catalonia (ICGC) Gloria storm inventory (González et al. 2020) has been used to obtain the most comprehensive landslide database possible (Table 9). This database has been used to derive the hydrometeorological thresholds (see Section 4.4).

Table 9. Used inventory data.

Inventory Name	Period	Number of rainfall-triggered entries
#Esllavicat + CECAT + roads	2018-2020	328
ICGC Gloria storm inventory	20-23 January 2020	275

The #Esllavicat inventory has been compiled from landslide posts of local observers on social networks. The reports specify the approximate time and location of the landslides. Additionally, some include pictures or videos of the landslides' initiation or deposit areas and a brief description of the deposits and impacts. The #Esllavicat initiative began in 2018. Since then, 336 landslide reports on social networks have been included. Additionally, data from the Catalan civil protection (CECAT) and the road network managing authorities has been provided by the ICGC and used to complete the #Esllavicat inventory for the year 2018 and the month of October 2019. Finally, the inventory contains 530 landslides. After a detailed analysis regarding the type of process, triggering factor, and temporal and spatial uncertainties, 328 entries corresponding to rainfall-triggered landslides were selected for the current analysis (see Table 9)

The ICGC Gloria storm inventory contains 275 landslides triggered during the extraordinary 19-23 January 2020 rainfall event (González et al. 2020). The data was gathered from different administrations, and interpretation of post-storm aerial photographs along river banks. Further details on this inventory can be found in Palau et al. (under review).

The final database includes 603 landslide entries in the periods April-December 2018, October 2019 and April-December 2020. It is important to state that the available landslide inventories are biased towards areas with a high population density or close to linear infrastructures (Figure 30). For example, a large number of landslide entries are located in the vicinities of Barcelona, where the majority of the population live. However, only a few landslides can be found in areas with a low population density, like the northwest and southwest of Catalonia.

4.4. Hydrometeorological thresholds for Catalonia

4.4.1. Assessment of the hydrometeorological conditions

This Section aims to obtain hydrometeorological thresholds that include VWC information and allow a better characterisation of the landslide triggering conditions in Catalonia. These thresholds will be applied into the Catalonia region real-time LEWS described in Section 4.2.2.

The hydrometeorological thresholds have been obtained using information of the landslide database described in Section 4.3.3 and hydrometeorological information of the periods (i) April-December 2018, (ii) October 2019, 20-23 January 2020, and (iii) April-December 2020, for which landslide inventories were available.

To study the hydrometeorological conditions that have led to landslides, the VWC has been included as a new variable to the formerly used rainfall intensity-duration space (see Section 4.2.2). To ease the data interpretation, we have defined the 30 min equivalent intensity (I_{eq}) as the intensity for an event duration of 30 min that has the same rainfall hazard as the actual rainfall event of intensity I, and duration D (see Figure 31 a). Applying this concept, any point in the volumetric water content-intensity-duration 3-D

space can be represented in a 2-D space defined by the equivalent intensity and volumetric water content.

Since landslide inventory data mostly includes only information on the triggering date and the volumetric water content has a daily resolution, the daily maximum equivalent intensity has been selected for the analysis. Thus, each landslide entry have been related to the maximum daily equivalent intensity and the daily volumetric water content.

The hydrometeorological conditions at the location of 603 landslide reports during the analysed periods are shown in Figure 33. Although rainfall intensities over the lowest I-D threshold triggered most landslides, some rainfall events with lower intensities also triggered landslides.
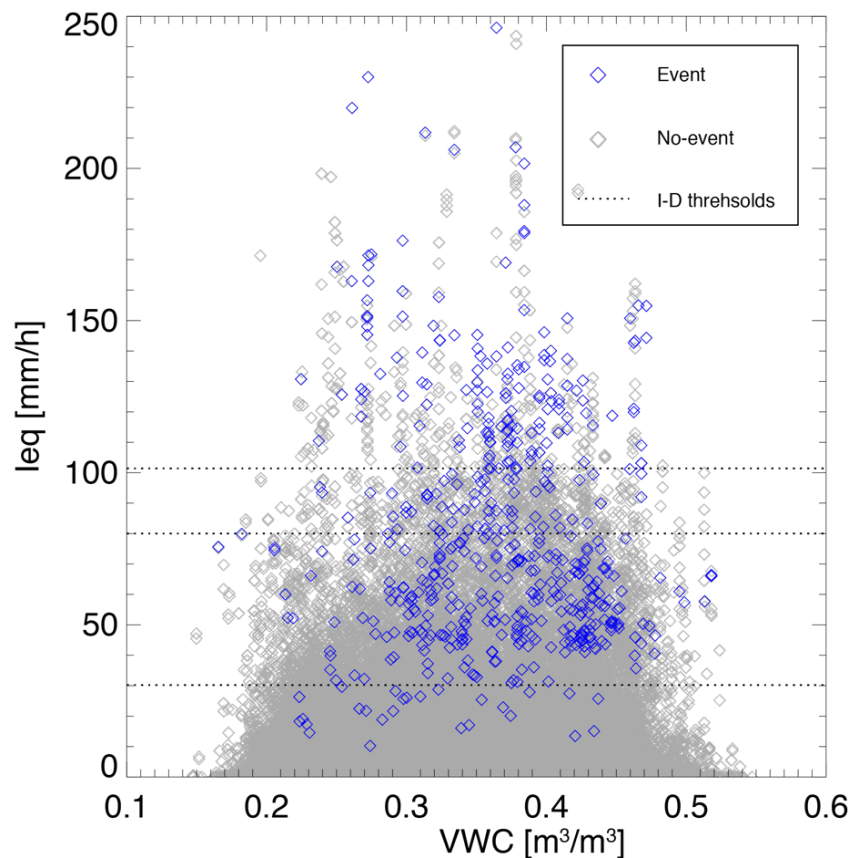
Figure 33. Daily maximum equivalent rainfall intensity (Ieq) and volumetric water content (VWC) for the period April-December 2018, October 2019, 20-23 January 2020, and April-December 2020, at the location of the 603 landslides contained in the inventory. The blue diamonds represent the days with landslide events. The grey diamonds show the days without landslide events at these 603 points. The horizontal black dotted lines represent the rainfall I-D thresholds.

The density distributions of landslide events and no-events are shown in Figure 34. The majority of landslide events were triggered when the VWC was higher than 0.30 m³/m³ and the equivalent intensity above 40 mm/h (Figure 33 and Figure 34 a). Fewer landslide events have been triggered by rainfalls with equivalent intensities higher than 140 mm/h. This fact can be explained because rainfall events with such high intensities are less frequent. Similarly, only few landslide events have been triggered with VWC over 0.45 m³/m³. As seen in Section 4.3.2, such VWC are not frequent in Catalonia (Figure 32). The number of days without landslides is a few orders of magnitude higher than the number of days when landslides were reported (Figure 34 b). The density of no-events is very high for volumetric water contents ranging from 0.15 m³/m³ to 0.55 m³/m³ and equivalent intensities below 100 mm/h.
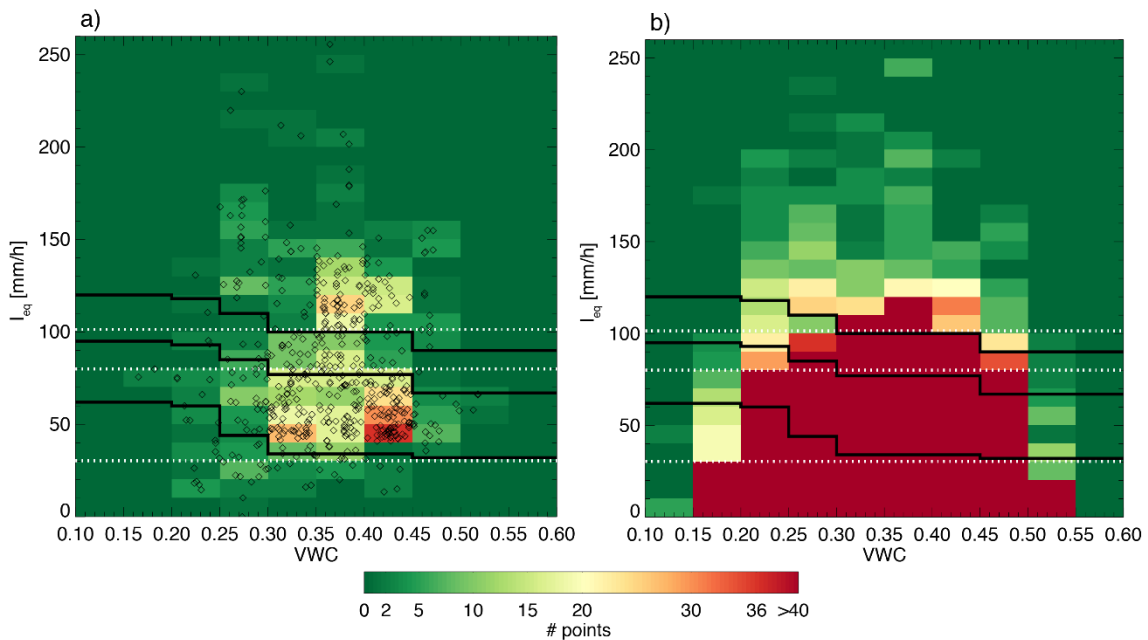
Figure 34. Density distribution of (a) landslide events, and (b) no-events of the inventory during the period April-December 2018, October 2019 and April-December 2020. *The white dotted line indicates the rainfall intensity duration thresholds. The black lines are the proposed Hydrometeorological thresholds. The black diamonds in (a) represent the 603 landslide events.*

4.4.2. Definition and skill of hydrometeorological thresholds

This Section first presents the approach used to obtain the set of hydrometeorological thresholds (i.e., in the space of VWC-I_{eq}) to be applied in the landslide model (see Section 4.2.2). Then, the hydrometeorological thresholds are compared with the rainfall-only thresholds in terms of their skill scores.

A hydrometeorological threshold is a dichotomous classifier that separates the I_{eq}-VWC conditions that can lead to landslides and the ones that cannot not. From the results presented in Section 4.4.1, no clear separation between landslide events and no events can be drawn at first sight. To objectively draw a hydrometeorological threshold we have employed a categorical statistic that allows to determine how well a threshold can separate landslide events and no-events, the true skill statistic (TSS). TSS values range from -1 to 1. Its perfect score is 1; 0 indicates no skill. The TSS can be defined as:

$$TSS = \frac{TP}{TP+FN} - \frac{FP}{FP+TN} = TPR - FPR \qquad (6)$$

Where TP, FN, FP, and TN are the number of true positives, false negatives, false positives, and true negatives. TPR is the true positive rate, and FPR is the false positive rate.

True positives are outcomes when landslides have been observed and the I_{eq}-VWC conditions are above the hydrometeorological threshold. False negatives are outcomes when landslides have been triggered but the I_{eq}-VWC are below the threshold. True negative are outcomes when the I_{eq}-VWC conditions are below the threshold and no landslide are observed. False positives are outcomes when the I_{eq}-VWC conditions are above the threshold but do not correspond to any landslide observation.

An optimal I_{eq}-VWC threshold has been obtained by maximising the TSS for each 0.05 m^3/m^3 VWC interval. Using the optimal threshold as a benchmark, we have proposed the three I_{eq}-VWC thresholds shown as black dashed lines Figure 34 to define four hydrometeorological hazard classes (very low, low, moderate, and high). These thresholds have been heuristically obtained considering the expected warnings when combining the hydrometeorological hazard and susceptibility (see Section 4.2.2 and Figure 31 b).

Table 10 presents the skill that can be achieved to separate landslide events from no events with the proposed hydrometeorological thresholds compared to the skill the rainfall thresholds achieve. The I_{eq}-VWC thresholds TSS scores are slightly higher than the TSS scores obtained with the rainfall I-D thresholds.

Landslide warnings are obtained combining susceptibility and the hydrometeorological thresholds (Section 4.2.2 and Figure 31 b). Thus, the very low - low threshold is key to discriminate between the hydrometeorological conditions that can trigger a landslide in areas where the terrain susceptibility is high. The number of false positives of the very low -low I_{eq}-VWC threshold is smaller than the number of false positives of the I-D threshold (Table 10). Therefore, we expect that if the LEWS runs with the hydrometeorological thresholds, fewer false alarms in high susceptibility terrain will be issued.

Table 10. Comparison of the skill scores obtained for the rainfall I-D thresholds and the hydrometeorological thresholds. TP states for the true positives, FN false negatives, FP false positives, and TN true negatives. TPR and FPR are the true positive rate and the false positive rate, respectively.

		TP	FN	FP	TN	TPR	FPR	TSS
	V low - low	576	27	11671	25525	0.96	0.31	0.64
I-D thresholds	Low - Mod	255	348	1582	35614	0.42	0.04	0.38
	Mod - High	185	418	489	36707	0.31	0.01	0.29
	V low - low	557	46	8718	28478	0.92	0.23	0.69
Hydrometeorological thresholds	Low - Mod	264	339	1756	35440	0.44	0.05	0.39
	Mod - High	190	413	534	36662	0.32	0.01	0.30

The low-moderate threshold determines when moderate or high warnings are issued in areas where the susceptibility is moderate. In low susceptibility terrain, the moderate-high threshold is critical to distinguish the hydrological conditions required to trigger a landslide (Section 4.2.2 and Figure 31 b). The results in Table 10 show that in both cases,

the number of true positives and false positives is slightly higher for the hydrometeorological threshold. Thus, we can expect that when applying the proposed thresholds into the LEWS, the number of hits will slightly increase in moderate and low susceptibility terrain at the expenses of also having a somewhat higher number of false alarms.

4.5. Performance demonstration of the LEWS during 2020

The analysis of the LEWS performance at a regional scale was challenging. Firstly, it required independent landslide inventory data that wasn't already applied to obtain the hydrometeorological thresholds. The inventories described in Section 4.3.3 were already employed to derive the hydrometeorological thresholds in Section 4.4. Thus, for the analysis of the LEWS performance, we used an additional landslide database that the ICGC provided; the landslide impact inventory.

This inventory includes 71 landslide points in the period from April to October 2020. Each entry contains information on the date and approximate time of the day when the landslide was reported and its spatial and temporal uncertainties. It also specifies the landslide type, triggering factor and nature of the affected slope (natural or embankment). Additionally, information on the damages, economic losses, injuries, and fatalities is provided.

The ICGC impact inventory has been filtered to remove those landslides that had already been included in the inventories described in Section 4.3.3 or that had a significant uncertainty. Finally, nine entries corresponding to rainfall triggered slides or flows that affected natural slopes have been selected to study the LEWS performance. The location of this points is portrayed in Figure 30.

Since the available inventory is fairly incomplete, a detailed evaluation of the LEWS performance was not possible. In this Section the performance of the LEWS has been qualitatively analysed in terms of (i) the number of days with warnings and (ii) its ability to identify the occurrence of the nine landslide events of the ICGC impact inventory.

4.5.1. Performance demonstration of the LEWS during 2020

The warning model has been run for 9 months (April-December 2020). As it has been explained in Section 4.2.2, landslide warnings have been obtained combining susceptibility and the magnitude of the rainfall situation, which has been quantified using the rainfall-only and the hydrometeorological thresholds.
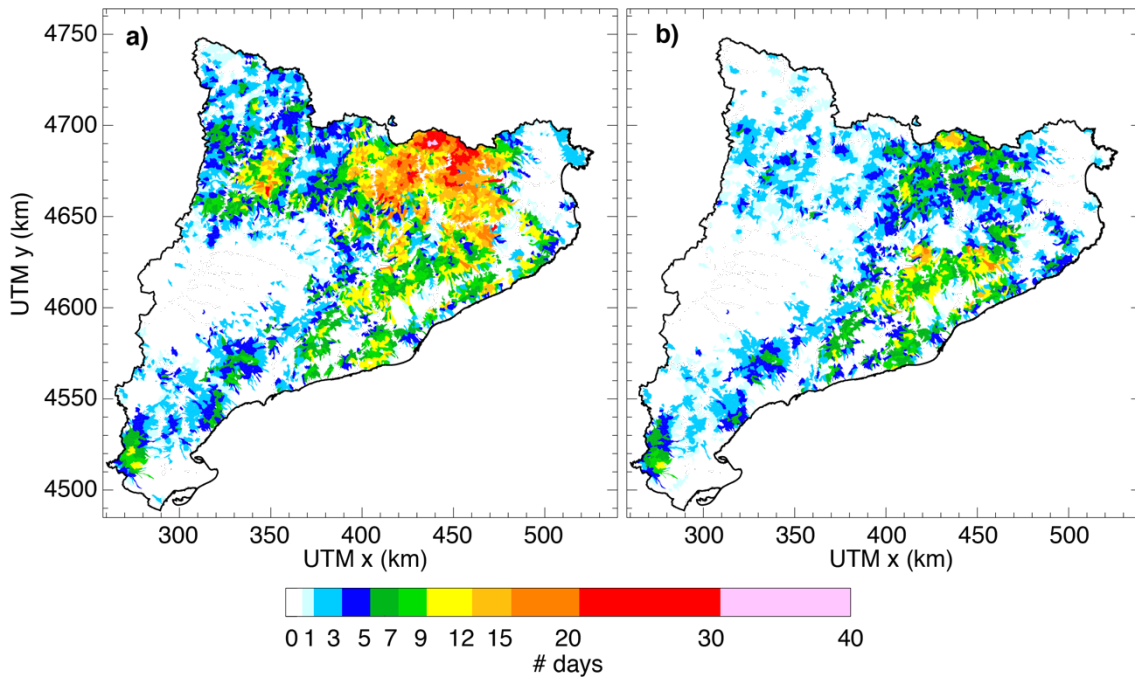
Figure 35. Number of days with moderate or high warning obtained using the LEWS (a) rainfall threshold set-up and (b) hydrometeorological threshold set-up.

The number of days during which moderate or high warnings were issued has been counted for the rainfall and the hydrometeorological thresholds configurations. Results show that the areas where most of these warnings were issued coincide with high susceptibility areas, mainly located at the Pyrenees and the Catalan Coastal Ranges (Figure 35 and Figure 30).

When applying the rainfall intensity-duration thresholds, moderate or high warnings have been issued up to 34 days in two subbasins and more than 12 days in many others (Figure 35 a). Having such a large number of landslides in nine months is not realistic. Most of these warnings are probably false alarms. As we expected from the findings in Section 4.4.2, the number of days with moderate or high warning significantly decreases when running the LEWS with the hydrometeorological thresholds (Figure 35 b). Therefore,

probably fewer false alarms are issued when employing the hydrometeorological thresholds.
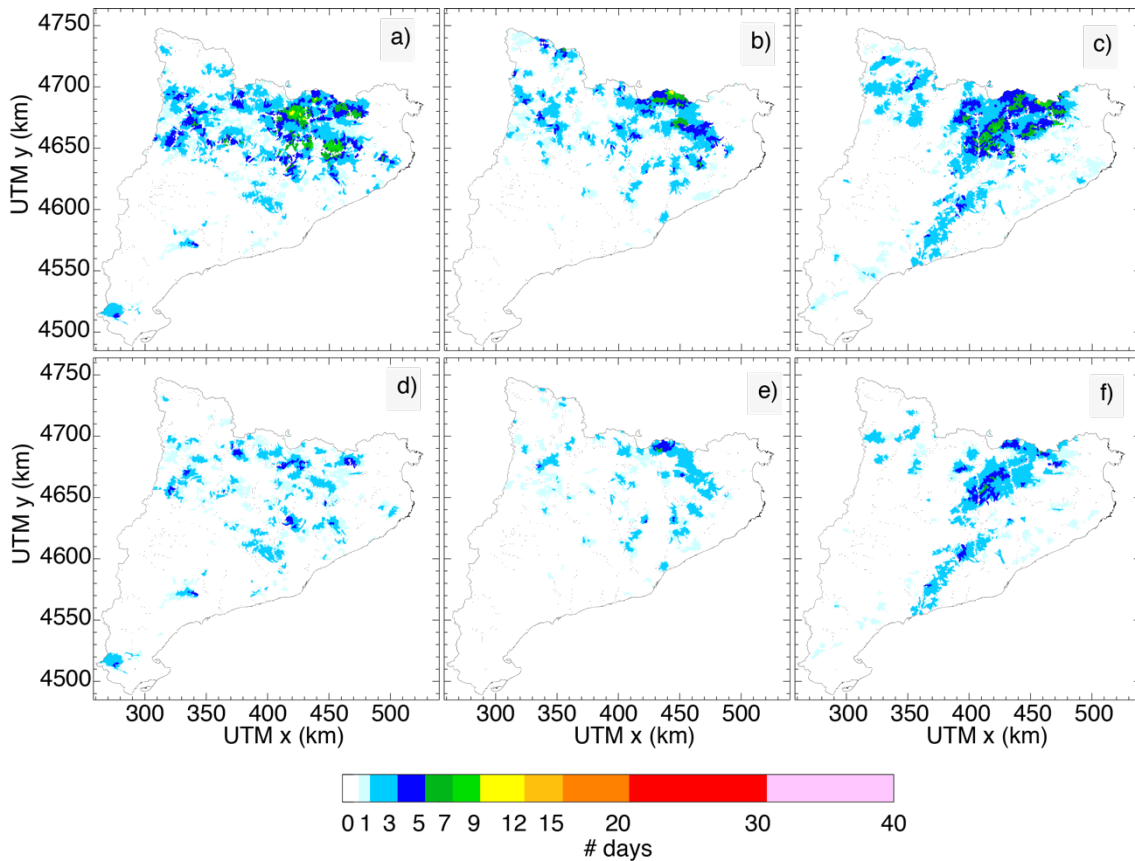
Figure 36. Number of days during which a moderate or high warning has been issued using the I-D thresholds during the months of (a) June, (b) July, and (c) August 2020. Number of days during which a moderate or high warning has been issued using the I_{eq}-VWC thresholds during the months of (d) June, (e) July, and (f) August 2020.

The majority of these moderate or high warnings were issued during June, July, and August 2020 (Figure 36 a, b, and c) at the Pyrenees, where the susceptibility is generally moderate or high (Figure 30). During these three months, the rainfall accumulations in this area were significant (see Figure 37 a, b and c). Therefore, the required conditions to issue a warning by combining rainfall-only thresholds and susceptibility were met. However, the monthly mean VWC conditions in the area were equal to 0.3 m^3/m^3 (Figure 37 d, e, and f). With such VWC conditions, the I_{eq} required to exceed the hydrometeorological thresholds is higher than the I_{eq} required to exceed rainfall-only thresholds (Figure 34). Some rainfall events didn't achieve these higher I_{eq}. Additionally, it is interesting to notice that the June, July and August 2020 monthly mean VWC in the Pyrenees (Figure 37 d, e and f) is relatively frequent and correspond to the 50th percentile of VWC of the area (Figure 32 d).

97
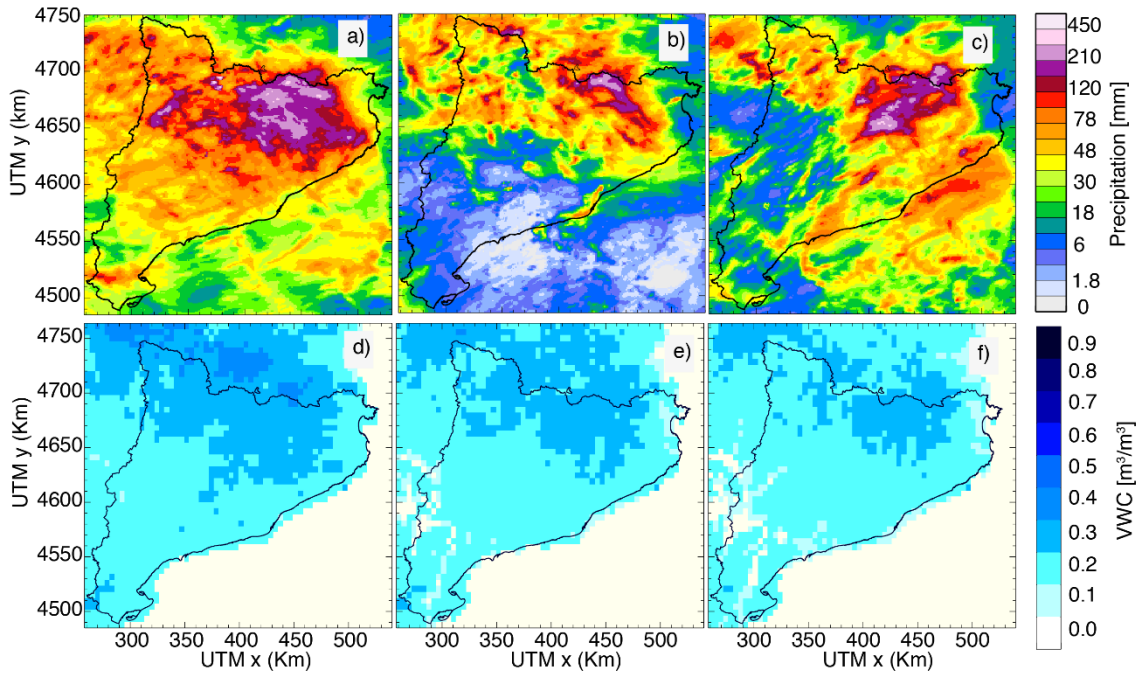
Figure 37. Rainfall accumulations during (a) June, (b) July, and (c) August 2020. Monthly mean volumetric water content conditions during the months of (d) June, (e) July, and (f) August 2020.

4.5.2. Performance at specific locations

Because of limitations in inventory, the performance of the two LEWS configurations has been quantitatively analysed only at the location of the nine rainfall triggered landslides of the ICGC impact inventory (see Section 0 and Figure 30). To account for the spatial uncertainty of the landslide reports, a neighbouring window of 250 m around each landslide observation has been used to search for the warnings.

The number of reported landslides at the nine specific sites has been compared with the number of days that achieved a moderate or high warning level within the neighbouring window (Table 11). The LEWS performance has been assessed by counting the number of hits, misses and false alarms. Hits are defined as the number of rainfall events during which a landslide was reported, and within its neighbouring window, the LEWS issued a moderate or high warning. Misses are defined as the number of rainfall events during which a landslide was included in the inventory, but no moderate or high warning was issued within its neighbouring window. Finally, false alarms are rainfall events during which the LEWS issued a moderate or high warning within the neighbouring window of a landslide reported at a different time.

Table 11 Comparison of the LEWS performance at the locations of the nine landslides of the ICGC impact inventory used for the performance demonstration.

		I-D set-up			Hydrometeorological Set-up		
Landslide ID	Susceptibility Class	Hits	False alarms	Misses	Hits	False alarms	Misses
A	High	1	2	0	1	1	0
B	High	0	6	1	0	2	1
C	Moderate	0	0	1	0	0	1
D	High	1	4	0	1	2	0
E	High	1	7	0	1	6	0
F	High	1	1	0	1	1	0
G	High	1	1	0	1	0	0
H	Moderate	1	3	0	1	1	0
I	High	1	4	0	1	4	0

Generally, both the configurations using rainfall-only and hydrometeorological thresholds issued the same number of hits and misses (Table 11 and Figure 38). The main difference between the two configurations is the number of false alarms. Generally, when running the LEWS with the I-D thresholds, the number of false alarms is higher than the number of false alarms issued employing the hydrometeorological thresholds.

Figure 38 shows the rainfall, VWC, and daily warning level time-series at two of the nine sites, site A and site B. In both cases, high susceptibility areas were located within the neighbouring window of the landslide location (Table 11). At site A, the LEWS was able to issue a moderate warning at the time of the landslide report using the two types of thresholds.
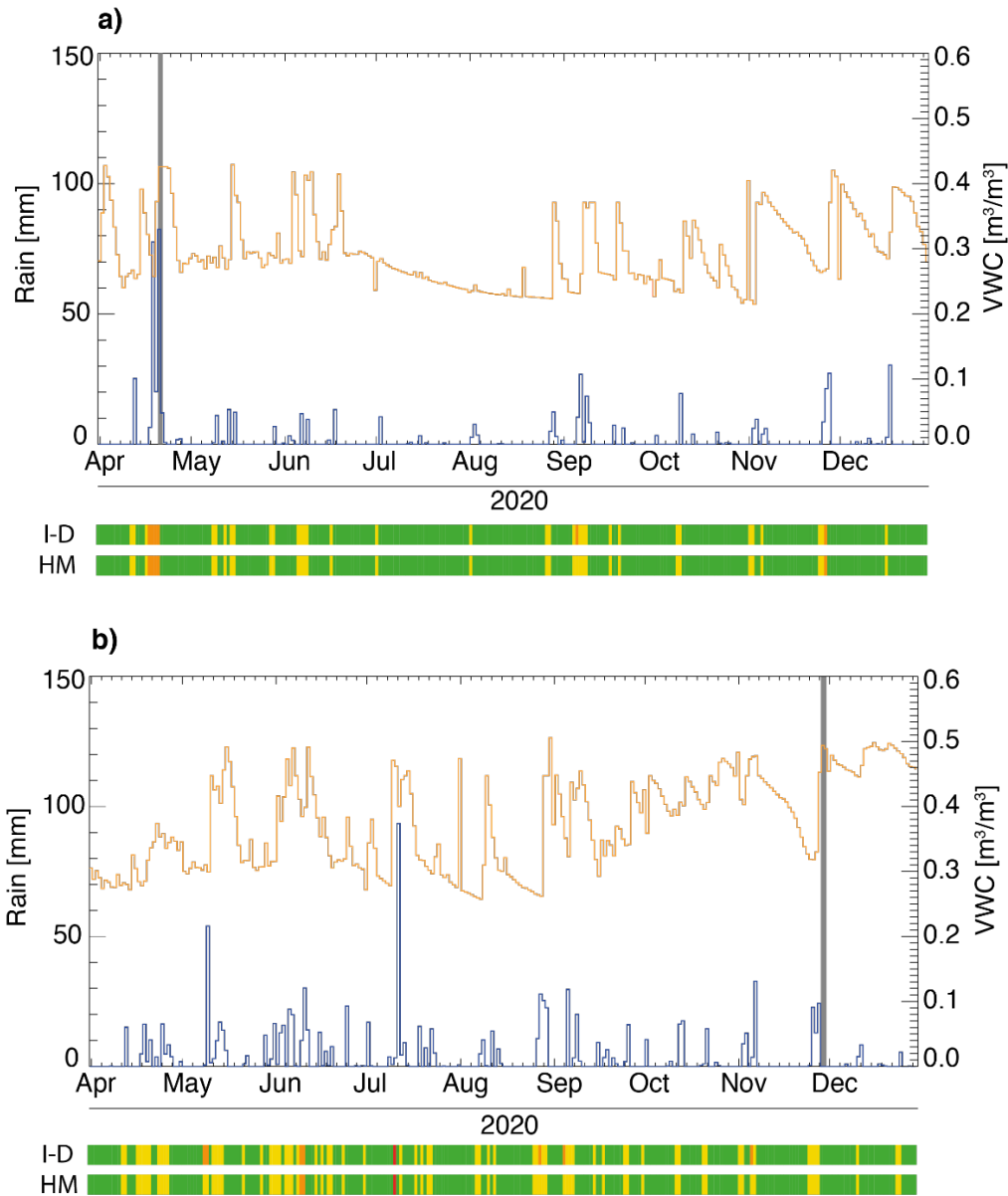
Figure 38. 24-h rainfall accumulation (blue line)-volumetric water content (orange line) time series at site A (a), and B (b). The colour bars represent the daily warning level time-series for the I-D set-up and the hydrometeorological set-up (HM). The grey strips represent the time when the landslide happened.

At site A, a landslide was reported during a significant rainfall event in April 2020. Within its neighbouring window, the LEWS was able to issue a moderate warning at the time of the landslide report using the two types of thresholds (Figure 38 a). At site B, one landslide was reported in December 2020. However, the recorded rainfall intensities were rather low, and any of the two LEWS configurations could issue a warning within the neighbouring window of site B (Figure 38 b).

At both sites, the LEWS issued a larger number of false positives when applying the I-D thresholds (Figure 38 a and b). The analysis of the VWC timeseries (Figure 38 a and b)

shows that generally warnings were issued exclusively by the rainfall-only configuration when the VWC was below 0.3 m3/m3. For such VWC conditions, the hydrometeorological thresholds are higher than the rainfall-only thresholds (Figure 34).

4.6. Conclusions

This study explores the potential of using soil moisture information obtained from a Pan-European hydrological model to increase the performance of the LEWS for the region of Catalonia. The objective is that the combination of the hydrometeorological thresholds and susceptibility allow an improved classification between landslide events and no-events.

We have analysed the hydrometeorological conditions at the time of 603 landslide events that occurred in the period April-December 2018, October 2019 and April-December 2020. The majority of the reported landslides were triggered when the volumetric water content conditions ranged between 0.3 m^3/m^3 and 0.45 m^3/m^3 and the 30-min equivalent intensity of the triggering rainfall was higher than 40 mm/h.

Based on this data, three empirical hydrometeorological thresholds have been determined for its application in the LEWS. Each threshold allows distinguishing the equivalent intensity and volumetric water content conditions that can lead to landslides at areas with a specific susceptibility. Although the skill of the hydrometeorological thresholds is very similar to the skill of rainfall-only thresholds, it is slightly better. The methodology that has been used in this work to obtain the hydrometeorological thresholds is heuristic. Accurate landslide inventories, covering longer periods, and containing a larger number of entries are required to derive more objective statistical hydrometeorological thresholds for Catalonia.

The LEWS has been run for nine months in 2020 using the rainfall-only thresholds and the new hydrometeorological thresholds. The evaluation of the LEWS performance has been challenging because of the limitations of the landslide inventory. Thus, we have evaluated the performance qualitatively over the entire domain, and quantitatively at specific locations where landslides have been registered. The analyses of the LEWS performance shows that landslide warnings are generally located in susceptible areas affected by significant rainfalls. From a qualitative point of view, the number of days

during which moderate or high warnings have been issued is much smaller when applying the hydrometeorological thresholds than when using the rainfall-only thresholds. The results at the locations where landslides were reported show that generally the number of true positives and false negatives is the same for both LEWS configurations. However, fewer false positives were issued using the hydrometeorological thresholds set up.

These results suggest that hydrometeorological thresholds can positively contribute to improving the performance of the LEWS over Catalonia, mainly by reducing the number of false alarms. Having many false alarms or misses can undermine the trust in a LEWS (Wilson 2012). Thus, reducing the number of false alarms is very beneficial since it helps gain credibility to the LEWS. However, a more exhaustive evaluation over longer periods of time and with a larger number of inventory reports would be required to make these results more conclusive.

Chapter 5

CONCLUSIONS AND FUTURE RESEARCH

5.1. General Conclusions

The main contribution of this thesis is the implementation of a regional-scale landslide early warning system in Catalonia. The system is currently running in real-time at the university servers for testing purposes.

The warning system proposed in this study combines susceptibility and high-resolution rainfall information. Rainfall intensity-duration thresholds are used to characterise if a given rainfall event has the potential to trigger landslides. A limitation of this methodology is the lack of well-established rainfall thresholds in Catalonia. We have overcome this shortcoming by adapting the existing IDF curves established by the time series of a meteorological station.

For the first time a susceptibility map covering the entire Catalonia region is proposed. The susceptibility map of Catalonia has been obtained, combining slope angle and land cover information with a simple fuzzy logic approach. The susceptibility map covers Catalonia with a resolution of 30 m and classifies the terrain into four susceptibility classes "Very Low", "Low", "Moderate", and "High". Generally, high susceptibility areas are located in mountainous regions like the Pyrenees. Low susceptibility areas span over flatlands like the Ebro Basin.

The suitability of the mapping units used to compute and visualise the warnings has been analysed. The results show that 30-m grid-cells offer a compromise between resolution, performance and computational cost. Thus, 30-m grid-cells have been selected as the most suitable mapping unit for warning calculation. However, to simplify the

visualization at a regional scale, subbasins have been proposed to summarize the 30 m resolution warnings.

One of the main constraints for the analysis of the LEWS performance is the availability of systematic inventory data, including the time and location of landslide events. Within the framework of this thesis, the #Esllavicat inventory has been created to collect landslide inventory data from social network posts on Twitter. This collaborative initiative began in 2018, and since then, 336 landslides have been compiled. The inventory analysis shows that landslide data is biased towards linear infrastructures and areas with a high population density. Additionally, it has been seen that some of the entries have significant spatial and temporal uncertainties.

To deal with the effect of these shortcomings, a fuzzy verification method has been applied to evaluate the LEWS performance. Our results indicate that fuzzy verification methods are a useful tool to analyse the performance of high-resolution landslide warning models at a regional scale. Their main advantage over traditional verification methods is that they allow some flexibility to match the warnings and the landslide observations. Fuzzy verification methods have long been used to assess the performance of mesoscale high-resolution precipitation forecasts (Ebert 2008). Still, their application in the field of LEWS is a novelty.

The analysis of landslide inventories showed that the significant rainfall of the Gloria storm triggered multiple-occurrence regional landslide events in Catalonia. This event gave us an opportunity for the performance evaluation of the LEWS over the region. Results from the evaluation show that generally, the LEWS has been able to issue warnings in the areas where landslides were reported. The outcomes of the fuzzy verification confirm that subbasins are a suitable mapping unit to summarise the warnings. Furthermore, the results suggest that the LEWS effective resolution is around 1 km. In other words, if a warning is issued, we will probably be able to find a landslide within a surrounding area of 1 km^2.

Finally, soil moisture has been introduced in the assessment of the magnitude of the rainfall event. Empirical equivalent intensity-volumetric water content hydrometeorological thresholds have been obtained and applied in the LEWS.

The outputs of the LEWS using the intensity-duration and using the equivalent intensity-volumetric water content thresholds have been compared. Due to the lack of an exhaustive inventory, it has been difficult to assess the LEWS performance. Only a qualitative performance analysis has been possible. The results from this analysis suggest that using hydrometeorological thresholds can positively contribute to improving the Catalonia region LEWS performance by reducing the number of false positives.

Summarising, in this thesis the components of a real-time warning system for the region of Catalonia have been developed. The model has been running in real time for about two years and it has proved to be useful to detect the occurrence of past landslide events over the region. One of the advantages of the proposed methodology is its modularity, that enables the different LEWS components to be easily changed. This allows a simple upgrade of the LEWS components, and also an easy implementation of the LEWS in other regions.

5.2. Lines for future research

The present study supposes a great contribution to regional scale landslide emergency management and risk mitigation in Catalonia. However, there are still many questions that remain unsolved and components that could be improved and should be addressed in future research.

The warning model is currently run using real-time rainfall observations. However, shallow slides and debris flows are rapid phenomena that happen during or just after the triggering rainfall. Warnings are issued without enough lead-time to enhance population preparedness. Thus, LEWS can only be used as a tool to manage the situation once the landslide has already happened. To issue effective early warnings, the presented methodology should be implemented employing rainfall forecasts (Alfieri et al. 2012).

Having reliable inventory data is essential to evaluate the performance of the LEWS and improve its components. Landslide reports from media sources provide valuable information but are often limited to landslides that have caused impacts. The analysis of remote sensing data or the use of seismic networks to detect non-earthquake triggered landslides could contribute to completing the landslide inventory. The gathering of data and the evaluation of the system performance is a task that should be continued in future.

The uncertainties of the input susceptibility, rainfall, and volumetric water content data are sources of uncertainty of the LEWS. Further research is required in order to quantify these uncertainties, and determine in which extent the three factors might influence the final warnings.

Due to the inventory limitations, in this thesis, we have developed empirical hydrometeorological thresholds. As the landslide inventory grows, we will probably be able to characterise the landslides triggering rainfall and soil moisture conditions more accurately. Thus, the hydrometeorological thresholds could be improved in the future.

It has been seen that most of the landslides included in the inventories were reported in road cuts. However, road cuts are small and generally are not well represented in the current version of the susceptibility map. Improving the susceptibility resolution along roads and railways would possibly help improving the performance of the LEWS.

Research could be conducted to develop tools to translate from landslide warnings to the expected socio-economic impacts. This approach, would help the authorities in charge to manage the landslide risk to make more objective and rapid decisions.

Finally, this thesis has focused on the development of components of a warning model. The design of effective communication and dissemination strategies is out of the scope of this thesis and is a topic for future work.

REFERENCES

Abancó C, Hürlimann M, Moya J, Berenguer M (2016) Critical rainfall conditions for the initiation of torrential flows. Results from the Rebaixader catchment (Central Pyrenees). J Hydrol 541:218–229. https://doi.org/10.1016/j.jhydrol.2016.01.019

Abancó C, Bennett GL, Matthews AJ, et al (2021) The role of geomorphology, rainfall and soil moisture in the occurrence of landslides triggered by 2018 Typhoon Mangkhut in the Philippines. Nat Hazards Earth Syst Sci 21:1531–1550. https://doi.org/10.5194/nhess-21-1531-2021

Alcántara-Ayala I, Murray V, Daniels P, McBean G (2017) International Council for Science (ICSU)-On the future challanges for the integration of science into international policy developement for landlide disaster risk reduction. Adv Cult Living with Landslides 5:1–557. https://doi.org/10.1007/978-3-319-53483-1

Aleotti P (2004) A warning system for rainfall-induced shallow failures. Eng Geol 73:247–265. https://doi.org/10.1016/j.enggeo.2004.01.007

Alfieri L, Salamon P, Pappenberger F, et al (2012) Operational early warning systems for water-related hazards in Europe. Environ Sci Policy 21:35–49. https://doi.org/10.1016/j.envsci.2012.01.008

Alvioli M, Guzzetti F, Rossi M (2014) Scaling properties of rainfall induced landslides predicted by a physically based model. Geomorphology 213:38–47. https://doi.org/10.1016/j.geomorph.2013.12.039

Ardizzone F, Cardinali M, Carrara A, et al (2002) Impact of mapping errors on the reliability of landslide hazard maps. Nat Hazards Earth Syst Sci 2:3–14. https://doi.org/10.5194/nhess-2-3-2002

Atger F (2001) Verification of intense precipitation forecasts from single models and ensemble prediction systems. Nonlinear Process Geophys 8:401–417. https://doi.org/10.5194/npg-8-401-2001

Ayala F (1995) Probabilidad y vulnerabilidad en movimientos de ladera. In: Reducción de riesgos geológicos en España. ITGE, Madrid, Spain, pp 95–113

Ayala F, Olcina J, Vilaplana JM (2004) Impacto social de los riesgos naturales en España en el periodo 1990-2000 (II). Gerenci de riesgos XXI:17–29

Badoux A, Graf C, Rhyner J, et al (2009) A debris-flow alarm system for the Alpine Illgraben catchment: design and performance. Nat Hazards 517–539. https://doi.org/10.1007/s11069-008-9303-x

Baum RL, Godt JW (2010) Early warning of rainfall-induced shallow landslides and debris flows in the USA. Landslides 7:259–272. https://doi.org/10.1007/s10346-009-0177-0

Bazin S (2012) Guidelines for landslide monitoring and early warning systems in Europe - Design and required technology. In: Project SafeLand "Living With Landslide Risk in Europe: Assesment, Effects of Global Change, and Risk Management Strategies". Derivable 4.8. pp 1–153

Bee E, Pennington C, Dashwood C, Lee K (2017) A User Guide for the GeoSure Extra: Debris Flow Susceptibility Model for Great Britain (version 6.0)

Bee E, Pennington C, Dashwood C, Lee K (2018) Creating a national scale debris flow susceptibility model for Great Britain. Geophys Res Abstr 20:7939

Beldring S, Engeland K, Roald LA, et al (2003) Estimation of parameters in a distributed precipitation-runoff model for Norway. Hydrol Earth Syst Sci 7:304–316. https://doi.org/10.5194/hess-7-304-2003

Berastegui X, Casas JM, Liesa M, et al (2010) Històtria geològica de Catalunya. Atles geològic de Catalunya 68–77

Berenguer M, Sempere-Torres D, Pegram GGS (2011) SBMcast - An ensemble nowcasting technique to assess the uncertainty in rainfall forecasts by Lagrangian extrapolation. J Hydrol 404:226–240. https://doi.org/10.1016/j.jhydrol.2011.04.033

Berenguer M, Sempere-Torres D, Hürlimann M (2015) Debris-flow forecasting at regional scale by combining susceptibility mapping and radar rainfall. Nat Hazards Earth Syst Sci 15:587–602. https://doi.org/10.5194/nhess-15-587-2015

Berti M, Martina MLV, Franceschini S, et al (2015) Implementation of a probabilistic model of landslide occurrence on a civil protection alert system at regional scale. In: Engineering Geology for Society and Territory - Volume 2: Landslide Processes. pp 659–662. https://doi.org/10.1007/978-3-319-09057-3_110

Biagio E Di, Kjekstad O (2007) Early Warning, Instrumentation and Monitoring Landslides. In: 2nd in Regional Training Course, Reclaim II. Phuket, Thailand, pp 18–21

Bogaard T, Greco R (2016) Landslide hydrology: from hydrology to pore pressure. WIREs Water 3:439–459. https://doi.org/10.1002/wat2.1126

Bogaard T, Greco R (2018) Invited perspectives: Hydrological perspectives on precipitation intensity-duration thresholds for landslide initiation: proposing hydro-meteorological thresholds. Nat Hazards Earth Syst Sci 18:31–39. https://doi.org/10.5194/nhess-18-31-2018

Boje S, Øyehaug GB, Colleuille H (2018) Improvement of the temporal resolution of thresholds used by the Norwegian landslide warning service; future steps. Geophys Res Abstr 20:18920

Borga M, Stoffel M, Marchi L, et al (2014) Hydrogeomorphic response to extreme rainfall in headwater systems: Flash floods and debris flows. J Hydrol 518:194–205. https://doi.org/10.1016/j.jhydrol.2014.05.022

Brand EW, Premchitt J, Phillipson HB (1984) Relationship between rainfall and landslides in Hong Kong. In: 4th International Symposium on Landslides. Toronto, Canada, pp 276–284

Bregoli F, Medina V, Chevalier G, et al (2015) Debris-flow susceptibility assessment at regional scale: Validation on an alpine environment. Landslides 12:437–454. https://doi.org/10.1007/s10346-014-0493-x

Brigandì G, Aronica GT, Bonaccorso B, et al (2017) Flood and landslide warning based on rainfall thresholds and soil moisture indexes: the HEWS (Hydrohazards Early Warning System) for Sicily. Adv Geosci 44:79–88. https://doi.org/10.5194/adgeo-44-79-2017

Brocca L, Melone F, Moramarco T (2008) On the estimation of antecedent wetness conditions in rainfall–runoff modelling. Hydrol Process 22:629–642. https://doi.org/10.1002/hyp.6629

Brooks HE, Kay M, Hart J. (1998) Objective limits on forecasting skill of rare events. In: 19th Conf. Severe Local Storms. American Meteorological Society, Minneapolis, MN, USA, pp 552–555

Brunetti M, Peruccacci S, Rossi M, et al (2010) Rainfall thresholds for the possible occurrence of landslides in Italy. Nat Hazards Earth Syst Sci 10:447–458. https://doi.org/10.5194/nhess-10-447-2010

Brunetti M, Melillo M, Peruccacci S, et al (2018) How far are we from the use of satellite rainfall products in landslide forecasting? Remote Sens Environ 210:65–75. https://doi.org/10.1016/j.rse.2018.03.016

Burek P, Van Der Knijff J, De Roo A (2013) LISFLOOD - Distributed Water Balance and Flood Simulation Model - Revised User Manual 2013. Publications Office of the European Union, Luxembourg

Buxó P, Palau J (2020) Projecció del risc associat a les esllavissades a Catalunya i eines per a la seva prevenció. In: Canals M, Miranda J (eds) Sobre el temporal Gloria (19-23.01.20), els seus efectes sobre el país i el que se'n deriva. institut d'Estudis Catalans. Secció de Ciències i tecnologia, Barcelona, Spain, pp 131–142

Caine N (1980) The rainfall intensity-duration control of shallow landslides and debris flows. Geogr Ann 62A:23–27

Calvello M, Cascini L, Mastroianni S (2013) Landslide zoning over large areas from a sample inventory by means of scale-dependent terrain units. Geomorphology 182:33–48. https://doi.org/10.1016/j.geomorph.2012.10.026

Calvello M, D'Orsi RN, Piciullo L, et al (2015a) The Community-Based Alert and Alarm System for Rainfall Induced Landslides in Rio de Janeiro, Brazil. In: Engineering Geology for Society and Territory - Volume 2. Springer International Publishing, Cham, pp 653–657. https://doi.org/10.1007/978-3-319-09057-3_109

Calvello M, D'Orsi RN, Piciullo L, et al (2015b) The Rio de Janeiro early warning system for rainfall-induced landslides: Analysis of performance for the years 2010–2013. Int J Disaster Risk Reduct 12:3–15. https://doi.org/10.1016/j.ijdrr.2014.10.005

Calvello M, Papa MN, Pratschke J, Nacchia Crescenzo M (2016) Landslide risk perception: a case study in Southern Italy. Landslides 13:349–360. https://doi.org/10.1007/s10346-015-0572-7

Calvello M, Piciullo L (2016) Assessing the performance of regional landslide early warning models: the EDuMaP method. Nat Hazards Earth Syst Sci 16:103–122. https://doi.org/10.5194/nhess-16-103-2016

Calvello M (2017) Early warning strategies to cope with landslide risk. Riv Ital di Geotec 51:63–91. https://doi.org/10.19199/2017.2.0557-1405.063

Calvello M, Pecoraro G (2019) A Probabilistic Approach for Identifying Correlations between Landslides and Rainfall at Regional Scale. In: Proceedings of the 7th International Symposium on Geotechnical Safety and Risk (ISGSR 2019). Research Publishing Services, Singapore, pp 727–732

Campbell RH (1975) Soil Slips, Debris Flows, and Rainstorms in the Santa Monica Mountains and Vicinity, Southern California. US Geol Surv Prof Pap 851 51 pages

Canals M, Miranda J (2020) Sobre el temporal Gloria (19-23.01.20), els seus efectes sobre el país i el que se'n deriva: Report de Resposta Rapida (R3), 1a edició. institut d'Estudis Catalans. Secció de Ciències i tecnologia, Barcelona

Cannon SH, Ellen S (1985) Rainfall conditions for abundant debris avalanches, San Francisco Bay region. Calif Geol 38:267–272

Cannon SH, Gartner JE, Wilson RC, et al (2008) Storm rainfall conditions for floods and debris flows from recently burned areas in southwestern Colorado and southern California. Geomorphology 96:250–269. https://doi.org/10.1016/j.geomorph.2007.03.019

Carrara A, Crosta G, Frattini P (2007) Comparing models of debris-flow susceptibility in the alpine environment. Geomorphology 94:353–378. https://doi.org/10.1016/j.geomorph.2006.10.033

Casas MC, Codina B, Redano A, Lorente J (2004) A methodology to classify extreme rainfall events in the western mediterranean area. Theor Appl Climatol 77:139–150. https://doi.org/10.1007/s00704-003-0003-x

Cassiraga E, Gómez-Hernández JJ, Berenguer M, et al (2020) Spatiotemporal Precipitation Estimation from Rain Gauges and Meteorological Radar Using Geostatistics. Math Geosci. https://doi.org/10.1007/s11004-020-09882-1

Chan CHW, Ting SM, Wong ACW (2012) Development of natural terrain landslip alert criteria. Geotechnical Engineering Office, Hong Kong 68p

Chen C, Lin LL, Yu F, et al (2007) Improving debris flow monitoring in Taiwan by using high-resolution rainfall products from QPESUMS. Nat Hazards 447–461. https://doi.org/10.1007/s11069-006-9004-2

Cheung SPY, Wong MCC, Yeung LHY, et al (2006) Application of Rainstorm Nowcast to Real-time Warning of Landslide Hazards in Hong Kong. In: WMO PWS Workshop on Warnings of Real-Time Hazards by Using Nowcasting Technology. Sydney, Australia, p 21

Chevalier GG (2013) Assessing debris-flow hazard focusing on statistical morpho-fluvial susceptibility models and magnitude-frequency relationships : application to the central-eastern Pyrenees. TDX (Tesis Dr en Xarxa)

Chevalier GG, Medina V, Hürlimann M, Bateman A (2013) Debris-flow susceptibility analysis using fluvio-morphological parameters and data mining: application to the Central-Eastern Pyrenees. Nat Hazards 67:213–238. https://doi.org/10.1007/s11069-013-0568-3

Chitu Z, Bogaard T, Busuioc A, et al (2017) Identifying hydrological pre-conditions and rainfall triggers of slope failures at catchment scale for 2014 storm events in the Ialomita Subcarpathians, Romania. Landslides 14:419–434. https://doi.org/10.1007/s10346-016-0740-4

Choi KY, Cheung RWM (2013) Landslide disaster prevention and mitigation through works in Hong Kong. J Rock Mech Geotech Eng 5:354–365. https://doi.org/10.1016/j.jrmge.2013.07.007

Ciarapica L, Todini E (2002) TOPKAPI: a model for the representation of the rainfall-runoff process at different scales. Hydrol Process 16:207–229. https://doi.org/10.1002/hyp.342

Ciavolella M, Bogaard T, Gargano R, Greco R (2016) Is there Predictive Power in Hydrological Catchment Information for Regional Landslide Hazard Assessment? Procedia Earth Planet Sci 16:195–203. https://doi.org/10.1016/j.proeps.2016.10.021

Ciurleo M, Calvello M, Cascini L (2016) Susceptibility zoning of shallow landslides in fine grained soils by statistical methods. Catena 139:250–264. https://doi.org/10.1016/j.catena.2015.12.017

Clavero P, Martín-Vide J, Raso-Nadal J (1996) Atles Climàtic de Catalunya. Termopluviometria i RadiacióSolar; Barcelona, Spain, Spain

Cloke H, Pappenberger F, Thielen J, Thiemig V (2013) Operational European Flood Forecasting. In: Environmental Modelling. John Wiley & Sons, Ltd, Chichester, UK, pp 415–434. https://doi.org/10.1002/9781118351475.ch25

Corominas J, Alonso E (1990) Geomorphological effects of extreme floods (November 1982) in the southern Pyrenees. In: Hydrology in Mountainous regions. II - Artificial Reservoirs; Water and Slopes. IAHS no. 194, Lausanne, Switzerland, pp 295–302

Corominas J (2000) Landslides and climate. 8th Int Symp Landslides 1–33

Corominas J, Moya J, Hürlimann M (2002) Landslide rainfall triggers in the Spanish Eastern Pyrenees. In: 4th EGS Plinius Conference "Mediterranean Storms." Editrice, Mallorca, Spain, pp 1–4

Corominas J, van Westen C, Frattini P, et al (2014) Recommendations for the quantitative analysis of landslide risk. Bull Eng Geol Environ 73:209–263. https://doi.org/10.1007/s10064-013-0538-8

Corominas J, Mateos RM, Remondo J (2015) Review of landslide occurrence in Spain and its relation to climate. In: Ken H, Lacasse S, Picarelli L (eds) Slope Safety Preparedness for Impact of Climate Change. "Workshop on Slope Safety Preparedness for Effects of Climate Change. Taylor & Francis, Napoli, Italy, pp 1–28378

Corral C, Velasco D, Forcadell D, et al (2009) Advances in radar-based flood warning systems . The EHIMI system and the experience in the Besòs flash-flood pilot basin. Flood Risk Manag Res Pract Ext Abstr Vol 332 Pages Full Pap CDROM 1772 Pages 1295–1303

CREAF (2009) Mapa de Cobertes del Sòl de Catalunya (MSC-4), V4 edn.

Cremonini R, Tiranti D (2018) The Weather Radar Observations Applied to Shallow Landslides Prediction: A Case Study From North-Western Italy. Front Earth Sci 6:. https://doi.org/10.3389/feart.2018.00134

Crosta GB, Frattini P (2003) Distributed modelling of shallow landslides triggered by intense rainfall. Nat Hazards Earth Syst Sci 3:81–93. https://doi.org/10.5194/nhess-3-81-2003

Crozier MJ (1999) Prediction of rainfall-triggered landslides: a test of the Antecedent Water Status Model. Earth Surf Process Landforms 24:825–833. https://doi.org/10.1002/(SICI)1096-9837(199908)24:9<825::AID-ESP14>3.0.CO;2-M

Crozier MJ (2005) Multiple-occurrence regional landslide events in New Zealand: Hazard management issues. Landslides 2:247–256. https://doi.org/10.1007/s10346-005-0019-7

Cruden DM (1991) A simple definition of a landslide. Bull Int Assoc Eng Geol 43:27–29. https://doi.org/10.1007/BF02590167

Cruden DM, Varnes DJ (1996) Landslide types and processes. In: Turner AK, Schuster RL (eds) Landslides: investigation and mitigation. Transportation Research Board, Washington DC, pp 36–75

Damrath U (2004) Verification against precipitation observations of a high density network – what did we learn? In: International Verification Methods Workshop. Montreal, Canada

Destro E, Marra F, Nikolopoulos EI, et al (2017) Spatial estimation of debris flows-triggering rainfall and its dependence on rainfall return period. Geomorphology 278:269–279. https://doi.org/10.1016/j.geomorph.2016.11.019

Devoli G, Tiranti D, Cremonini R, et al (2018) Comparison of landslide forecasting services in Piedmont (Italy) and Norway, illustrated by events in late spring 2013. Nat Hazards Earth Syst Sci 18:1351–1372. https://doi.org/10.5194/nhess-18-1351-2018

DGMT DG d'Infraestructures de MT (2019) Graf d'Infraestructures Vectorial de la DGIMT. Barcelona

Easterling DR (2000) Climate Extremes: Observations, Modeling, and Impacts. Science (80-) 289:2068–2074. https://doi.org/10.1126/science.289.5487.2068

Ebert EE (2008) Fuzzy verification of high-resolution gridded forecasts: a review and proposed framework. Meteorol Appl 15:51–64. https://doi.org/10.1002/met.25

Ebert EE (2009) Neighborhood Verification: A Strategy for Rewarding Close Forecasts. Weather Forecast 24:1498–1510. https://doi.org/10.1175/2009WAF2222251.1

EEA (1990) CORINE land cover - contents. CORINE L Cover 1–163

Ekker R, Kværne K, Os A, Humstad T (2013) regObs - public database for submitting and sharing observations. In: International Snow Science Workshop. Grenoble, Chamonix Mont-Blanc, p 5pp

Emberger L (1952) Sur le quotient pluviothermique. C.R. Acade´mie Science: Paris; 2508–2510. Comptes Rendus l'Academie des Sci 234:2508–2510

Fawcett T (2006) An introduction to ROC analysis. Pattern Recognit Lett 27:861–874. https://doi.org/10.1016/j.patrec.2005.10.010

Fell R, Ho KKS, Lacasse S, Leroi E (2005) A framework for landslide risk assessment and management. Int Conf Landslide Risk Manag Vancouver, Canada 3–25

Fell R, Corominas J, Bonnard C, et al (2008) Guidelines for landslide susceptibility, hazard and risk zoning for land use planning. Eng Geol 102:85–98. https://doi.org/10.1016/j.enggeo.2008.03.022

Ferrer M (1995) Los movimientos de ladera en España. In: Reducción de Riesgos Geológicos en España. Instituto Tecnológico Geominero de España, Madrid, pp 69–82

Frattini P, Crosta G, Sosio R (2009) Approaches for defining thresholds and return periods for rainfall-triggered shallow landslides. Hydrol Process 23:1444–1460. https://doi.org/10.1002/hyp.7269

Froude MJ, Petley DN (2018) Global fatal landslide occurrence from 2004 to 2016. Nat Hazards Earth Syst Sci 18:2161–2181. https://doi.org/10.5194/nhess-18-2161-2018

Gallart F, Clotet N (1988) Some aspects of the geomorphic processes triggered by an extreme rainfall event: the November 1982 flood in Eastern Pyrenees. Catena Suppl 79–95

Galli M, Ardizzone F, Cardinali M, et al (2008) Comparing landslide inventory maps. Geomorphology 94:268–289. https://doi.org/10.1016/j.geomorph.2006.09.023

Gariano SL, Brunetti M, Iovine G, et al (2015) Calibration and validation of rainfall thresholds for shallow landslide forecasting in Sicily, southern Italy. Geomorphology 228:653–665. https://doi.org/10.1016/j.geomorph.2014.10.019

Gariano SL, Guzzetti F (2016) Landslides in a changing climate. Earth-Science Rev 162:227–252. https://doi.org/10.1016/j.earscirev.2016.08.011

Gariano SL, Petrucci O, Rianna G, et al (2018) Impacts of past and future land changes on landslides in southern Italy. Reg Environ Chang 18:437–449. https://doi.org/10.1007/s10113-017-1210-9

Glade T, Crozier M, Smith P (2000) Applying probability determination to refine landslide-triggering rainfall thresholds using an empirical "Antecedent Daily Rainfall Model." Pure Appl Geophys 157:1059–1079. https://doi.org/10.1007/s000240050017

Godt JW, Baum RL, Lu N (2009) Landsliding in partially saturated materials. Geophys Res Lett 36:n/a-n/a. https://doi.org/10.1029/2008GL035996

González M, Pinyol J, Ramisa J, et al (2017) La base de datos de movimientos del terreno de Cataluña (LLISCAT): una herramienta para la gestión de los riesgos geológicos. In: IX Simposio Nacional sobre Taludes y Laderas Inestables. Santander, pp 651–662

González M, Pinyol J, Micheo MJ, et al (2020) El temporal Gloria (19-23/01/2020): Els efectes dels procesos geológics sobre el territori. Institut Cartogràfic i Geològic de Catalunya, Barcelona

Guzzetti F, Cardinali M, Reichenbach P (1994) The AVI project: A bibliographical and archive inventory of landslides and floods in Italy. Environ Manage 18:623–633. https://doi.org/10.1007/BF02400865

Guzzetti F, Carrara A, Cardinali M, Reichenbach P (1999) Landslide hazard evaluation: A review of current techniques and their application in a multi-scale study, Central Italy. In: Geomorphology. pp 181–216. https://doi.org/10.1016/S0169-555X(99)00078-1

Guzzetti F, Peruccacci S, Rossi M, Stark CP (2007) Rainfall thresholds for the initiation of landslides in central and southern Europe. Meteorol Atmos Phys 98:239–267. https://doi.org/10.1007/s00703-007-0262-7

Guzzetti F, Peruccacci S, Rossi M, Stark CP (2008) The rainfall intensity–duration control of shallow landslides and debris flows: an update. Landslides 5:3–17. https://doi.org/10.1007/s10346-007-0112-1

Guzzetti F, Mondini AC, Cardinali M, et al (2012) Landslide inventory maps: New tools for an old problem. Earth-Science Rev 112:42–66. https://doi.org/10.1016/j.earscirev.2012.02.001

Guzzetti F, Gariano SL, Peruccacci S, et al (2020) Geographical landslide early warning systems. Earth-Science Rev 200:102973. https://doi.org/10.1016/j.earscirev.2019.102973

Hansen MJ (1984) Strategies for classification of landslides. In: Brunsden D (ed) Slope Instability. John Wiley, Chichester, pp 1–25

Hidayat R, Sutanto SJ, Hidayah A, et al (2019) Development of a Landslide Early Warning System in Indonesia. Geosciences 9:451. https://doi.org/10.3390/geosciences9100451

Hong Y, Alder R, Huffman G (2006) Evaluation of the potential of NASA multi-satellite precipitation analysis in global landslide hazard assessment. Geophys Res Lett 33:. https://doi.org/10.1029/2006GL028010

Hong Y, Adler R, Huffman G (2007) Use of satellite remote sensing data in the mapping of global landslide susceptibility. Nat Hazards 43:245–256. https://doi.org/10.1007/s11069-006-9104-z

Huat LT, Ali F, Osman AR, Rahman NA (2012) Web Based Real Time Monitoring System Along North-South Expressway, Malaysia. Electron J Geothechnical Eng 17:623–632

Hungr O, Evans SG, Bovis MJ, Hutchinson JN (2001) A review of the classification of landslides of the flow type. Environ Eng Geosci 7:221–238. https://doi.org/10.2113/gseegeosci.7.3.221

Hungr O, Leroueil S, Picarelli L (2014) The Varnes classification of landslide types, an update. Landslides 11:167–194. https://doi.org/10.1007/s10346-013-0436-y

Hürlimann M, Abancó C, Moya J, Vilajosana I (2014) Results and experiences gathered at the Rebaixader debris-flow monitoring site, Central Pyrenees, Spain. Landslides 11:939–953. https://doi.org/10.1007/s10346-013-0452-y

Hürlimann M, Lantada N, Gonzalez M, Pinyol J (2016) Susceptibility assessment of rainfall-triggered flows and slides in the Central-Eastern Pyrenees. In: Aversa S, Cascini L, Picarelli L, Scavia C (eds) XII Int. Symposium on Landslides and Engineered Slopes. CRC Press, Naples, pp 1129–1136

Hürlimann M, Palau RM, Berenguer M, Pinyol J (2017) Analysis of the rainfall conditions inducing torrential activity in the Portainé catchment (Eastern Pyrenees, Spain). Geophys Res Abstr 19:12494

Hurlimann M, Medina V, Lloret A, Vaunat, J, Puig-Polo C, Moya J (2021) Effect of land cover and climate changes on rainfall-induced landslides: regional-scale modelling in the Val d'Aran (Pyrenees, Spain). In: International Symposium on Landslides. International Society for Soil Mechanics and Geotechnical Engineering (ISSMGE), pp 1–8

Hutchinson JN (1988) General report: Morphological and geotechnical parameters of landslides in relation to geology and hydrogeology. In: Bonnard C (ed) 5th Internation Symposium on Landslides. Balkema, Lausanne, pp 3–35

ICGC (2013) Model d'Elevacions del Terreny de Catalunya 5x5metres v1.0 (MET-5 v1.0). ICGC

IEC-Generalitat de Catalunya (2016) Tercer informe sobre el canvi climàtic a Catalunya (Coord. J.Martín-Vide). Barcelona

Intrieri E, Gigli G, Casagli N, Nadim F (2013) Brief communication "Landslide Early Warning System: toolbox and general concepts." Nat Hazards Earth Syst Sci 13:85–90. https://doi.org/10.5194/nhess-13-85-2013

Iverson RM (2000) Landslide triggering by rain infiltration. Water Resour Res 36:1897–1910. https://doi.org/10.1029/2000WR900090

Jacobs K, Garfin G, Lenart M (2005) More than Just Talk: Connecting Science and Decisionmaking. Environ Sci Policy Sustain Dev 47:6–21. https://doi.org/10.3200/ENVT.47.9.6-21

Jakob M, Hungr O (2005) Debris flow Hazards and Related Phenomena. Springer, Berlin

Jakob M, Owen T, Simpson T (2012) A regional real-time debris-flow warning system for the District of North Vancouver, Canada. Landslides 9:165–178. https://doi.org/10.1007/s10346-011-0282-8

Janeras M, Gili JA, Guinau M, et al (2018) Lessons learned from Degotalls rock wall monitoring in the Montserrat Massif (Catalonia, NE Spain). In: 4th RSS Rock Slope Stability Symposium (RSS-2018). Chambèri, France, p 3

Janeras M, Marturià J, Jara JA, Buxó P (2017) Revista Catalana de Geografia. Rev Catalana Geogr XXII:1–7

Juang CS, Stanley TA, Kirschbaum DB (2019) Using citizen science to expand the global map of landslides: Introducing the Cooperative Open Online Landslide Repository (COOLR). PLoS One 14:e0218657. https://doi.org/10.1371/journal.pone.0218657

Kang S, Lee S-R, Vasu NN, et al (2017) Development of an initiation criterion for debris flows based on local topographic properties and applicability assessment at a regional scale. Eng Geol 230:64–76. https://doi.org/10.1016/j.enggeo.2017.09.017

Kanjanakul C, Chub-uppakarn T, Chalermyanont T (2016) Rainfall thresholds for landslide early warning system in Nakhon Si Thammarat. Arab J Geosci 9:. https://doi.org/10.1007/s12517-016-2614-4

Keefer DK, Wilson RC, Mark RK, Brabb BB, Ellen SD, Harp EL, Wieczorek, GF, Alger CS (1987) Real-Time Landslide Warning During Heavy Rainfall. Science (80-) 238:921–925. https://doi.org/10.1126/science.238.4829.921

Kirschbaum DB, Adler R, Hong Y, Lerner-Lam A (2009) Evaluation of a preliminary satellite-based landslide hazard algorithm using global landslide inventories. Nat Hazards Earth Syst Sci 9:673–686. https://doi.org/10.5194/nhess-9-673-2009

Kirschbaum DB, Adler R, Hong Y, Hill S, Lerner-Lam A (2010) A global landslide catalog for hazard applications: method, results, and limitations. Nat Hazards 52:561–575. https://doi.org/10.1007/s11069-009-9401-4

Kirschbaum DB, Adler R, Hong Y, Peters-Lidad C, Huffman G (2012) Advances in landslide nowcasting: evaluation of a global and regional modeling approach. Environ Earth Sci 66:1683–1696. https://doi.org/10.1007/s12665-011-0990-3

Kirschbaum DB, Stanley T, Yatheendradas S (2016) Modeling landslide susceptibility over large regions with fuzzy overlay. Landslides 13:485–496. https://doi.org/10.1007/s10346-015-0577-2

Kirschbaum DB, Stanley T (2018) Satellite-Based Assessment of Rainfall-Triggered Landslide Hazard for Situational Awareness. Earth's Futur 6:505–523. https://doi.org/10.1002/2017EF000715

Kong VWW, Kwan JSH, Pun WK (2020) Hong Kong's landslip warning system—40 years of progress. Landslides 17:1453–1463. https://doi.org/10.1007/s10346-020-01379-6

Krøgli IK, Devoli G, Colleuille H, Boje S, Sund M, Engen IK (2018) The Norwegian forecasting and warning service for rainfall- and snowmelt-induced landslides. Nat Hazards Earth Syst Sci 18:1427–1450. https://doi.org/10.5194/nhess-18-1427-2018

Lacasse S, Nadim F, Kalsnes B (2010) Living with Landslide Risk. Geotech Eng J SEAGS AGSSEA 41.

Lagomarsino D, Segoni S, Fanti R, Catani F (2013) Updating and tuning a regional-scale landslide early warning system. Landslides 10:91–97. https://doi.org/10.1007/s10346-012-0376-y

Lee ML, Ng KY, Huang YF, Li WC (2014) Rainfall-induced landslides in Hulu Kelang area, Malaysia. Nat Hazards 70:353–375. https://doi.org/10.1007/s11069-013-0814-8

Lee S, Won JS, Jeon SW, et al (2015) Spatial Landslide Hazard Prediction Using Rainfall Probability and a Logistic Regression Model. Math Geosci 47:565–589. https://doi.org/10.1007/s11004-014-9560-z

Leopold P, Heiss G, Petschko H, et al (2013) Susceptibility maps for landslides using different modelling approaches. Landslide Sci Pract Landslide Invent Susceptibility Hazard Zo 1:353–356. https://doi.org/10.1007/978-3-642-31325-7-46

Liao Z, Hong Y, Wang J, et al (2010) Prototyping an experimental early warning system for rainfall-induced landslides in Indonesia using satellite remote sensing and geospatial datasets. Landslides 7:317–324. https://doi.org/10.1007/s10346-010-0219-7

Liu C, Li W, Wu H, et al (2013) Susceptibility evaluation and mapping of China's landslides based on multi-source data. Nat Hazards 69:1477–1495. https://doi.org/10.1007/s11069-013-0759-y

Lloyd DM, Wilkinson PL, A. M O, M. G. Anderson (2001) Predicting landslides: Assessment of an automated rainfall based landslide warning system. In: KKS H, KS L (eds) 14th South East Asia Geothecnical Conference. Balkema, Hong Kong, pp 135–139

Lombardo L, Opitz T, Huser R (2018) Point process-based modeling of multiple debris flow landslides using INLA: an application to the 2009 Messina disaster. Stoch Environ Res Risk Assess 32:2179–2198. https://doi.org/10.1007/s00477-018-1518-0

Longobardi A, Villani P, Grayson R., Western AW (2003) On The Relationship Between Runoff Coefficient And Catchment Initial Conditions. In: MODSIM 2003 Int. Congress on Modelling and Simulation. Modelling and Simulation Society of Australia andNew Zealand Inc, Townsville, Australia, pp 867–872

Ma T, Li C, Lu Z, Wang B (2014) An effective antecedent precipitation model derived from the power-law relationship between landslide occurrence and rainfall level. Geomorphology 216:187–192. https://doi.org/10.1016/j.geomorph.2014.03.033

Malone AW (1988) The role of Government in landslide disaster prevention in Hong Kong and Indonesia. Geotech Eng 2:227–252

Marino P, Peres DJ, Cancelliere A, et al (2020) Soil moisture information can improve shallow landslide forecasting using the hydrometeorological threshold approach. Landslides 17:2041–2054. https://doi.org/10.1007/s10346-020-01420-8

Marra F, Nikolopoulos EI, Creutin JD, Borga M (2014) Radar rainfall estimation for the identification of debris-flow occurrence thresholds. J Hydrol 519:1607–1619. https://doi.org/10.1016/j.jhydrol.2014.09.039

Marra F, Nikolopoulos EI, Creutin JD, Borga M (2016) Space–time organization of debris flows-triggering rainfall and its effect on the identification of the rainfall threshold relationship. J Hydrol 541:246–255. https://doi.org/10.1016/j.jhydrol.2015.10.010

Marra F, Destro E, Nikolopoulos EI, et al (2017) Impact of rainfall spatial aggregation on the identification of debris flow occurrence thresholds. Hydrol Earth Syst Sci 21:4525–4532. https://doi.org/10.5194/hess-21-4525-2017

Martelloni G, Segoni S, Fanti R, Catani F (2012) Rainfall thresholds for the forecasting of landslide occurrence at regional scale. Landslides 9:485–495. https://doi.org/10.1007/s10346-011-0308-2

Martelloni G, Segoni S, Lagomarsino D, et al (2013) Snow accumulation/melting model (SAMM) for integrated use in regional scale landslide early warning systems. Hydrol Earth Syst Sci 17:1229–1240. https://doi.org/10.5194/hess-17-1229-2013

Martín Vide F, Olcina Cantos J (2001) Climas y tiempos de España. Alianza Editorial

Marturià J, Ripoll J, Concha A, Barberà M (2010) Monitoring techniques for analysing subsidence: a basis for implementing an Early Warning System. In: Land Subsidence, Associated hazards and the role of natural resources development. Proceedings of EISOLS. IAHS Publ. 339, Queretaro, Mexico, pp 264–267

Melillo M, Brunetti MT, Peruccacci S, et al (2015) An algorithm for the objective reconstruction of rainfall events responsible for landslides. Landslides 12:311–320. https://doi.org/10.1007/s10346-014-0471-3

Mendel JM (1995) Fuzzy Logic Systems for Engineering : A tutorial. Proc IEEE 83:345–377. https://doi.org/10.1109/5.364485

Michoud C, Bazin S, Blikra LH, et al (2013) Experiences from site-specific landslide early warning systems. Nat Hazards Earth Syst Sci 13:2659–2673. https://doi.org/10.5194/nhess-13-2659-2013

Mirus B, Becker RE, Baum RL, Smith JB (2018a) Integrating real-time subsurface hydrologic monitoring with empirical rainfall thresholds to improve landslide early warning. Landslides 15:1909–1919. https://doi.org/10.1007/s10346-018-0995-z

Mirus B, Morphew M, Smith J (2018b) Developing Hydro-Meteorological Thresholds for Shallow Landslide Initiation and Early Warning. Water 10:1274. https://doi.org/10.3390/w10091274

Morss RE, Wilhelmi O V., Meehl GA, Dilling L (2011) Improving Societal Outcomes of Extreme Weather in a Changing Climate: An Integrated Perspective. Annu Rev Environ Resour 36:1–25. https://doi.org/10.1146/annurev-environ-060809-100145

Nadim F, Kjekstad O, Peduzzi P, et al (2006) Global landslide and avalanche hotspots. Landslides 3:159–173. https://doi.org/10.1007/s10346-006-0036-1

Nicolet P, Foresti L, Caspar O, Jaboyedoff M (2013) Shallow landslide's stochastic risk modelling based on the precipitation event of August 2005 in Switzerland: Results and implications. Nat Hazards Earth Syst Sci 13:3169–3184. https://doi.org/10.5194/nhess-13-3169-2013

Nikolopoulos EI, Crema S, Marchi L, et al (2014) Impact of uncertainty in rainfall estimation on the identification of rainfall thresholds for debris flow occurrence. Geomorphology 221:286–297. https://doi.org/10.1016/j.geomorph.2014.06.015

NOAA-USGS Debris Flow Task Force (2005) NOAA-USGS Debris-Flow Warning System - Final Report

OCCC (2020) L'impacte de la tempesta Gloria. Informe intern. Barcelona

Oller P, Barberà M, González M, et al (2009) El mapa de prevenció de riscos geològics de Catalunya 1:25.000. 'El mapa de prevención de riesgos geológicos de Cataluña.' In: VII Simposio Nacional sobre Taludes y Laderas Inestables. Barcelona, pp 817–828

Oorthuis R, Hurlimann M, Moya J, Vaunat J (2017) In-situ monitoring of slope mass-wasting: examples from the Pyrenees. JTC1 Work Adv Landslide Underst 105–108

Oorthuis R, Hürlimann M, Vaunat J, et al (2021) Relationship between triggering rainfalls, hydrological state and initiation of torrential flows. Monitoring data from of the Rebaixader catchment (Central Pyrenees, Spain) (in prep). Landslides

Ortigao B, Justi MG (2004) Rio-Watch: the Rio de Janeiro Landslide Alarm System. Geotech News 22:28–31

Osanai N, Shimizu T, Kuramoto K, et al (2010) Japanese early-warning for debris flows and slope failures using rainfall indices with Radial Basis Function Network. Landslides 7:325–338. https://doi.org/10.1007/s10346-010-0229-5

Palau RM, Hürlimann M, Pinyol J, et al (2017) Recent debris flows in the Portainé catchment (Eastern Pyrenees, Spain): analysis of monitoring and field data focussing on the 2015 event. Landslides 14:1161–1170. https://doi.org/10.1007/s10346-017-0832-9

Palau RM, Hürlimann M, Berenguer M, Sempere-Torres D (2020) Influence of the mapping unit for regional landslide early warning systems: comparison between pixels and polygons in Catalonia (NE Spain). Landslides 17:2067–2083. https://doi.org/10.1007/s10346-020-01425-3

Palau RM, Berenguer M, Hürlimann M, Sempere-Torres D (2021) Evaluation of a regional-scale landslide early warning system during the January 2020 Gloria storm in Catalonia (NE Spain). (under review). Landslides

Palau RM, Berenguer M, Hürlimann M, Sempere-Torres D Implementation of hydrometeorological thresholds for regional landslide warning in Catalonia (NE Spain). (in prep.)

Pan HL, Jiang YJ, Wang J, Ou GQ (2018) Rainfall threshold calculation for debris flow early warning in areas with scarcity of data. Nat Hazards Earth Syst Sci 18:1395–1409. https://doi.org/10.5194/nhess-18-1395-2018

Papa MN, Medina V, Ciervo F, Bateman A (2013) Derivation of critical rainfall thresholds for shallow landslides as a tool for debris flow early warning systems. Hydrol Earth Syst Sci 17:4095–4107. https://doi.org/10.5194/hess-17-4095-2013

Park J-Y, Lee S-R, Lee D-H, et al (2019) A regional-scale landslide early warning methodology applying statistical and physically based approaches in sequence. Eng Geol 260:105193. https://doi.org/10.1016/j.enggeo.2019.105193

Park J-Y, Lee S-R, Kim Y-T, et al (2020) A Regional-Scale Landslide Early Warning System Based on the Sequential Evaluation Method: Development and Performance Analysis. Appl Sci 10:5788. https://doi.org/10.3390/app10175788

Pecoraro G, Calvello M, Piciullo L (2018) Monitoring strategies for local landslide early warning systems. Landslides. https://doi.org/10.1007/s10346-018-1068-z

Pecoraro G, Calvello M (2021) Integrating local pore water pressure monitoring in territorial early warning systems for weather-induced landslides. Landslides 18:1191–1207. https://doi.org/10.1007/s10346-020-01599-w

Peduto D, Oricchio L, Nicodemo G, et al (2021) Investigating the kinematics of the unstable slope of Barberà de la Conca (Catalonia, Spain) and the effects on the exposed facilities by GBSAR and multi-source conventional monitoring. Landslides 18:457–469. https://doi.org/10.1007/s10346-020-01500-9

Peres DJ, Cancelliere A, Greco R, Bogaard TA (2018) Influence of uncertain identification of triggering rainfall on the assessment of landslide early warning thresholds. Nat Hazards Earth Syst Sci 18:633–646. https://doi.org/10.5194/nhess-18-633-2018

Persichillo MG, Bordoni M, Meisina C (2017) The role of land use changes in the distribution of shallow landslides. Sci Total Environ 574:924–937. https://doi.org/10.1016/j.scitotenv.2016.09.125

Peruccacci S, Brunetti MT, Luciani S, et al (2012) Lithological and seasonal control on rainfall thresholds for the possible initiation of landslides in central Italy. Geomorphology 139–140:79–90. https://doi.org/10.1016/j.geomorph.2011.10.005

Peruccacci S, Brunetti MT, Gariano SL, et al (2017) Rainfall thresholds for possible landslide occurrence in Italy. Geomorphology 290:39–57. https://doi.org/10.1016/j.geomorph.2017.03.031

Petley D (2012) Global patterns of loss of life from landslides. Geology 40:927–930. https://doi.org/10.1130/G33217.1

Piciullo L, Dahl M-P, Devoli G, et al (2017a) Adapting the EDuMaP method to test the performance of the Norwegian early warning system for weather-induced landslides. Nat Hazards Earth Syst Sci 17:817–831. https://doi.org/10.5194/nhess-17-817-2017

Piciullo L, Gariano SL, Melillo M, et al (2017b) Definition and performance of a threshold-based regional early warning model for rainfall-induced landslides. Landslides 14:995–1008. https://doi.org/10.1007/s10346-016-0750-2

Piciullo L, Calvello M, Cepeda JM (2018) Territorial early warning systems for rainfall-induced landslides. Earth-Science Rev 179:228–247. https://doi.org/https://doi.org/10.1016/j.earscirev.2018.02.013

Piciullo L, Tiranti D, Pecoraro G, et al (2020) Standards for the performance assessment of territorial landslide early warning systems. Landslides 17:2533–2546. https://doi.org/10.1007/s10346-020-01486-4

Pisano L, Zumpano V, Malek, et al (2017) Variations in the susceptibility to landslides, as a consequence of land cover changes: A look to the past, and another towards the future. Sci Total Environ 601–602:1147–1159. https://doi.org/10.1016/j.scitotenv.2017.05.231

Ponziani F, Pandolfo C, Stelluti M, et al (2012) Assessment of rainfall thresholds and soil moisture modeling for operational hydrogeological risk prevention in the Umbria region (central Italy). Landslides 9:229–237. https://doi.org/10.1007/s10346-011-0287-3

Ponziani F, Berni N, Stelluti M, et al (2013) Landwarn: An Operative Early Warning System for Landslides Forecasting Based on Rainfall Thresholds and Soil Moisture. In: Landslide Science and Practice. Springer Berlin Heidelberg, Berlin, Heidelberg, pp 627–634. https://doi.org/10.1007/978-3-642-31445-2_82

Portilla M, Chevalier G, Hürlimann M (2010) Description and analysis of major mass movements occurred during 2008 in the Eastern Pyrenees. Nat Hazards Earth Syst Sci 10:1635–1645. https://doi.org/10.5194/nhess-10-1635-2010

Portilla M (2014) Reconstrucción y análisis de ocurrencias regionales de múltiples eventos de movimientos en masa generados por lluvias históricas en los Pirineos. In: TDX (Tesis Doctorals en Xarxa). Universitat Politècnica de Catalunya

Posner AJ, Georgakakos KP (2015) Soil moisture and precipitation thresholds for real-time landslide prediction in El Salvador. Landslides 12:1179–1196. https://doi.org/10.1007/s10346-015-0618-x

Raïmat Quintana C (2018) Dinámica y peligrosidad de las corrientes de derrubios : aplicación en el barranco de Erill, Pirineo catalán. TDX (Tesis Dr en Xarxa)

RISKCAT (2008) RISKCAT Els riscos naturals a Catalunya. Informe executiu

Roberts NM, Lean HW (2008) Scale-selective verification of rainfall accumulations from high-resolution forecasts of convective events. Mon Weather Rev. https://doi.org/10.1175/2007MWR2123.1

Rossi M, Peruccacci S, Brunetti M, et al (2012) SANF: National warning system for rainfall-induced landslides in Italy. In: Eberhardt E, Froese C, Turner AK, Leroueil S (eds) 11th International and 2nd North American Symposium on Landslides and Engineered Slopes. CRC Press/Balkema, Banff, Canada, pp 1895–1899

Rossi M, Luciani S, Valigi D, et al (2017) Statistical approaches for the definition of landslide rainfall thresholds and their uncertainty using rain gauge and satellite data. Geomorphology 285:16–27. https://doi.org/10.1016/j.geomorph.2017.02.001

Sánchez-Diezma R, Sempere-Torres D, Creutin J-D, et al (2001) Factors Affecting the Precision of Radar Measurements of Rain An Assessment From an Hydrological Perspective. In: Asociation AM (ed) 30th Conference on Radar Meteorology. American Meteorological Society, Munich, Germany, pp 573–575

Santacana N, Baeza B, Corominas J, et al (2003) A GIS-Based Multivariate Statistical Analysis for Shallow Landslide Susceptibility Mapping in La Pobla de Lillet Area (Eastern Pyrenees, Spain). Nat Hazards 30:281–295. https://doi.org/10.1023/B:NHAZ.0000007169.28860.80

Sassa K (2017) The ISDR-ICL Sendai Partnerships 2015–2025: Background and Content BT - Advancing Culture of Living with Landslides. In: Sassa K, Mikoš M, Yin Y (eds). Springer International Publishing, Cham, pp 3–21. https://doi.org/10.1007/978-3-319-59469-9_1

Sassa K (2020) Thematic issue: Sendai Landslide Partnerships 2015–2025. Landslides 17:2249–2252. https://doi.org/10.1007/s10346-020-01493-5

Schmidt KM, Roering JJ, Stock JD, et al (2002) The variability of root cohesion as an influence on shallow landslide susceptibility in the Oregon Coast Range. Can Geotech J 38:995–1024. https://doi.org/10.1139/cgj-38-5-995

Schwarz M, Preti F, Giadrossich F, et al (2010) Quantifying the role of vegetation in slope stability: a case study in Tuscany (Italy). Ecol Eng 36:285–291. https://doi.org/10.1016/j.ecoleng.2009.06.014

Segoni S, Rossi G, Rosi A, Catani F (2014) Landslides triggered by rainfall: A semi-automated procedure to define consistent intensity-duration thresholds. Comput Geosci 63:123–131. https://doi.org/10.1016/j.cageo.2013.10.009

Segoni S, Battistini A, Rossi G, et al (2015) Technical Note: An operational landslide early warning system at regional scale based on space–time-variable rainfall thresholds. Nat Hazards Earth Syst Sci 15:853–861. https://doi.org/10.5194/nhess-15-853-2015

Segoni S, Rosi A, Fanti R, et al (2018a) A Regional-Scale Landslide Warning System Based on 20 Years of Operational Experience. Water 10:1297. https://doi.org/10.3390/w10101297

Segoni S, Rosi A, Lagomarsino D, et al (2018b) Brief communication: Using averaged soil moisture estimates to improve the performances of a regional-scale landslide early warning system. Nat Hazards Earth Syst Sci 18:807–812. https://doi.org/10.5194/nhess-18-807-2018

Servei Meteorològic de Catalunya S (2020a) Nota de Premsa. Balanç d'una llevantada històrica a Catalunya. Barcelona, Spain

Servei Meteorològic de Catalunya S (2020b) Butlletí climàtic mensual. gener del 2020. Barcelona, Spain

Shu H, Hürlimann M, Molowny-Horas R, et al (2019) Relation between land cover and landslide susceptibility in Val d'Aran, Pyrenees (Spain): Historical aspects, present situation and forward prediction. Sci Total Environ 693:133557. https://doi.org/10.1016/j.scitotenv.2019.07.363

Stanley T, Kirschbaum DB (2017) A heuristic approach to global landslide susceptibility mapping. Nat Hazards 87:145–164. https://doi.org/10.1007/s11069-017-2757-y

Stini J (1941) Unsere Täler wachsen zu. Geol Bauwes 13:71–79

Strahler AN (1957) Quantitative Analysis of Watershed Geomorphology. EOS, Trans - Am Geophys Union 38:913–920. https://doi.org/10.1029/tr038i006p00913

Terzaghi K (1943) Theoretical Soil Mechanics. John Wiley & Sons, Inc., Hoboken, NJ, USA

Thiebes B, Glade T, Bell R (2012) Landslide analysis and integrative early warning — local and regional case studies. 1915–1921. https://doi.org/10.13140/RG.2.1.1229.7844

Thielen J, Bartholmes J, Ramos M-H, de Roo A (2009) The European Flood Alert System – Part 1: Concept and development. Hydrol Earth Syst Sci 13:125–140. https://doi.org/10.5194/hess-13-125-2009

Thomas MA, Collins BD, Mirus BB (2019) Assessing the Feasibility of Satellite-Based Thresholds for Hydrologically Driven Landsliding. Water Resour Res 55:9006–9023. https://doi.org/10.1029/2019WR025577

Tien Bui D, Pradhan B, Lofman O, et al (2013) Regional prediction of landslide hazard using probability analysis of intense rainfall in the Hoa Binh province, Vietnam. Nat Hazards 66:707–730. https://doi.org/10.1007/s11069-012-0510-0

Tiranti D, Rabuffetti D (2010) Estimation of rainfall thresholds triggering shallow landslides for an operational warning system implementation. Landslides 7:471–481. https://doi.org/10.1007/s10346-010-0198-8

Tiranti D, Rabuffetti D, Salandin A, Tararbra M (2013) Development of a new translational and rotational slides prediction model in Langhe hills (north-western Italy) and its application to the 2011 March landslide event. Landslides 10:121–138. https://doi.org/10.1007/s10346-012-0319-7

Tiranti D, Cremonini R, Marco F, et al (2014) The DEFENSE (debris Flows triggEred by storms – nowcasting system): An early warning system for torrential processes by radar storm tracking using a Geographic Information System (GIS). Comput Geosci 70:96–109. https://doi.org/10.1016/j.cageo.2014.05.004

Tofani V, Bicocchi G, Rossi G, et al (2017) Soil characterization for shallow landslides modeling: a case study in the Northern Apennines (Central Italy). Landslides 14:755–770. https://doi.org/10.1007/s10346-017-0809-8

UNISDR - United Nations International Strategy for Disaster Reduction (2006) Global Survey of Early Warning Systems: An assessment of capacities, gaps and opportunities towards building a comprehensive global early warning system for all natural hazards

UNISDR - United Nations International Strategy for Disaster Reduction (2009) Terminology on disaster risk reduction. https://www.unisdr.org/files/7817_UNISDRTerminologyEnglish.pdf

UNISDR - United Nations International Strategy for Disaster Reduction (2015) Sendai Framework for Disaster Risk Reduction 2015-2030.

Van Den Eeckhaut M, Hervás J (2012) State of the art of national landslide databases in Europe and their potential for assessing landslide susceptibility, hazard and risk. Geomorphology 139–140:545–558. https://doi.org/10.1016/j.geomorph.2011.12.006

Van Der Knijff JM, Younis J, De Roo APJ (2010) LISFLOOD: a GIS-based distributed model for river basin scale water balance and flood simulation. Int J Geogr Inf Sci 24:189–212. https://doi.org/10.1080/13658810802549154

Varnes DJ (1958) Landslide types and processes. In: Eckel EB (ed) Landslides in Engineering Practice. Highway Research Board, pp 20–47

Varnes DJ (1978) Slope movements types and processes. Landslides analysis and control transportation research board. Natl Acad Sci Spec Rep 176:11–33

Velasco-Forero CA, Sempere-Torres D, Cassiraga EF, Jaime Gómez-Hernández J (2009) A non-parametric automatic blending methodology to estimate rainfall fields from rain gauge and radar data. Adv Water Resour 32:986–1002. https://doi.org/10.1016/j.advwatres.2008.10.004

Whittaker KA, McShane D (2012) Comparison of slope instability screening tools following a large storm event and application to forest management and policy. Geomorphology 145–146:115–122. https://doi.org/10.1016/j.geomorph.2012.01.001

Wicki A, Jansson P-E, Lehmann P, et al (2021) Simulated or measured soil moisture: Which one is adding more value to regional landslide early warning? Hydrol Earth Syst Sci Discuss. [: https://doi.org/10.5194/hess-2021-133

Wicki A, Lehmann P, Hauck C, et al (2020) Assessing the potential of soil moisture measurements for regional landslide early warning. Landslides. https://doi.org/10.1007/s10346-020-01400-y

Wieczorek GF (1996) Landslide triggering mechanisms. In: Schuster AK, Turner RL (eds) Landslides: investigation and mitigation. TRB Special Report, 247. National Academy Press, Washington, pp 76–90

Wieczorek GF (1987) Effect of rainfall intensity and duration on debris flows in central Santa Cruz Mountains, California. In: Costa JE, Wieczorek GF (eds) Debris flows/avalanches: process, recognition, and mitigation. Geological Society of America, pp 93–104

Wilde M, Günther A, Reichenbach P, et al (2018) Pan-European landslide susceptibility mapping: ELSUS Version 2. J Maps 14:97–104. https://doi.org/10.1080/17445647.2018.1432511

Wilson RC (2012) The Rise and Fall of a Debris-Flow Warning System for the San Francisco Bay Region, California. In: Glade T, Anderson M, Crozier MJ (eds) Landslide Hazard and Risk. John Wiley & Sons, Ltd, Chichester, West Sussex, England, pp 493–516. https://doi.org/10.1002/9780470012659.ch17

Wong ACW, Ting SM, Shiu YK, Ho KKS (2014) Latest Developments of Hong Kong's Landslip Warning System. In: Landslide Science for a Safer Geoenvironment. Springer International Publishing, Cham, pp 613–618. https://doi.org/10.1007/978-3-319-05050-8_95

Yang H, Yang T, Zhang S, et al (2020) Rainfall-induced landslides and debris flows in Mengdong Town, Yunnan Province, China. Landslides 17:931–941. https://doi.org/10.1007/s10346-019-01336-y

Yeung H. (2012) Recent developments and applications of the SWIRLS nowcasting system in Hong Kong. In: 3rd WMO International Symposium on Nowcasting and Very Short-Range Forecasting (WSN12). Rio de Janeiro, pp 6–10

Yin H-Y, Lee C-Y, Jan C-D (2015) A Web-Based Decision Support System for Debris Flow Disaster Management in Taiwan. In: Engineering Geology for Society and Territory - Volume 3. Springer International Publishing, Cham, pp 109–113. https://doi.org/10.1007/978-3-319-09054-2_21

Yin K, Chen L, Zhang G (2008) Regional Landslide Hazard Warning and Risk Assessment. Earth Sci Front 14:85–93. https://doi.org/10.1016/s1872-5791(08)60005-6

Yu F-C, Chen T-C, Lin M-L, et al (2006) Landslides and Rainfall Characteristics Analysis in Taipei City during the Typhoon Nari Event. Nat Hazards 37:153–167. https://doi.org/10.1007/s11069-005-4661-0

Yu YF (2004) Correlations Between Rainfall, Landslide Frequency and Slope Information for Registered Man-made Slopes. Hong Kong. Geo Report No. 144. 109p

Zawadzki I (1984) Factors Affecting the Precision of Radar Measurements of Rain. In: 22nd Conference on Radar Meteorology. American Meteorological Society, Zurich (Switzerland), pp 251–256

Zhao B, Dai Q, Han D, et al (2019) Probabilistic thresholds for landslides warning by integrating soil moisture conditions with rainfall thresholds. J Hydrol 574:276–287. https://doi.org/10.1016/j.jhydrol.2019.04.062

APPENDIX A: LIST OF PUBLICATIONS

Papers in indexed journals

Palau RM, Berenguer M, Hürlimann M, Sempere-Torres D (in prep.) Implementation of hydrometeorological thresholds for regional landslide warning in Catalonia (NE Spain)

Palau RM, Berenguer M, Hürlimann M, Sempere-Torres D (2021) Evaluation of a regional-scale landslide early warning system during the January 2020 Gloria storm in Catalonia (NE Spain). (Under review). Landslides

Palau RM, Hürlimann M, Berenguer M, Sempere-Torres D (2020) Influence of the mapping unit for regional landslide early warning systems: comparison between pixels and polygons in Catalonia (NE Spain). Landslides 17:2067–2083. https://doi.org/10.1007/s10346-020-01425-3

Furdada G, Victoriano A, Díez-Herrero A, et al (2020) Flood consequences of land-use changes at a ski resort: Overcoming a geomorphological threshold (Portainé, Eastern Pyrenees, Iberian Peninsula). Water (Switzerland) 12:. https://doi.org/10.3390/w12020368

Conference Publications

Hürlimann M, Berenguer M, Sempere-torres D (2021) Towards the use of hydrometeorological thresholds for the regional- scale LEWS of Catalonia (NE Spain). 8221. vPICO presentation In: EGU General Assembly 2020. Vienna https://doi.org/10.5194/egusphere-egu21-8221

Berenguer M, Hürlimann M, Sempere-torres D, et al (2020) An early warning system for rainfall-triggered shallow slides and debris flows . Application in Catalonia , Spain and Canton of Bern , Switzerland. In: EGU General Assembly 2020. Vienna https://doi.org/10.5194/egusphere-egu2020-479

Palau RM, Hurlimann M, Berenguer M, Sempere-Torres D (2019) Debris-flow early warning system at regional scale using weather radar and susceptibility mapping. In: 7th International Conference on Debris-Flow Hazards Mitigation. Association of Environmental & Engineering Geologists (AEG), Golden, Colorado, pp 184–191

Palau RM, Berenguer M, Hürlimann M, Sempere-torres D (2019) Which is the best mapping unit for a regional scale landslide early warning system? Comparison between pixel and polygons for Catalonia. Poseter presentation. Geophys Res Abstr 21:2019

Palau RM, Berenguer M, Hürlimann M, Sempere-torres D (2018) A prototype regional early warning system for shallow landslides and debris flows. Oral presentation. Geophys Res Abstr 20:2018